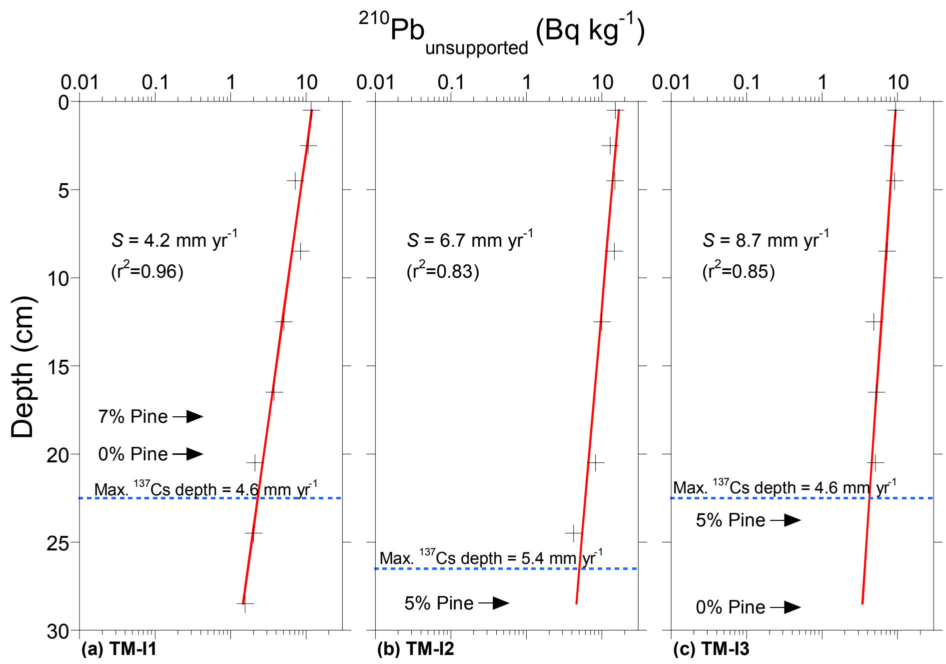

Figure 3.65: Te Matuku intertidal cores. Unsupported ^{210}Pb profiles plotted on a log scale, with linear regression fits used to calculate sedimentation rates (*S*). Also shown is the maximum depth of ^{137}Cs and average SAR.

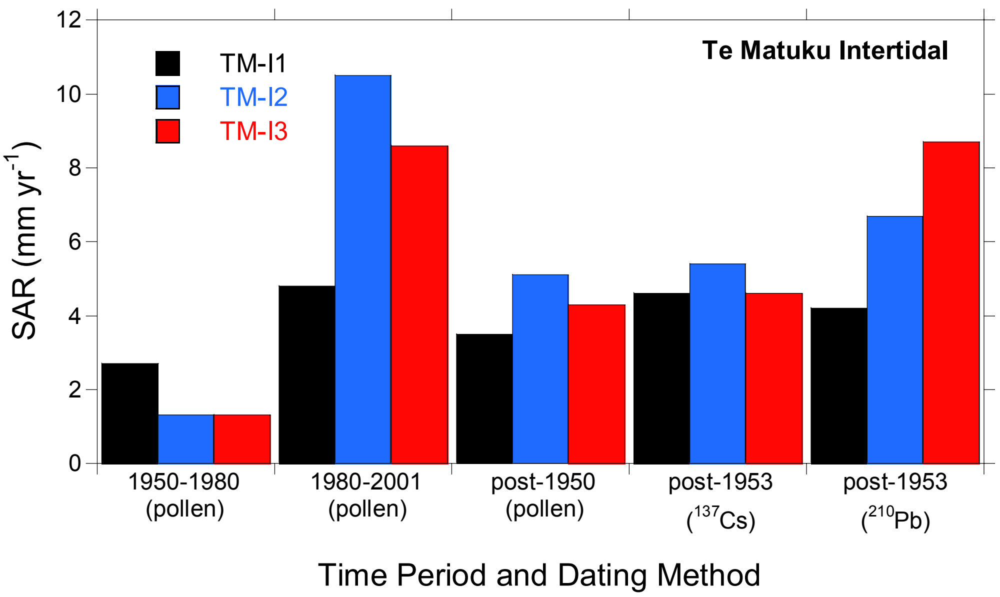

Figure 3.66: Te Matuku intertidal cores, post-1950/1953 SAR estimated from pollen, ^{137}Cs and ^{210}Pb dating of sediment cores.

The good linear-regression fits to the ^{210}Pb data and close agreement between the dating methods in cores TM-I1 and TM-I2 in the Te Matuku intertidal cores enable detailed sedimentation histories to be developed for the last ~150 years using the constrained ^{210}Pb CRS dating model (Figs. 3.67–3.69). We calculated depth-age, age-mass sedimentation (g cm^{-2} yr^{-1}) and age-SAR (mm yr^{-1}) curves for three depth increments. This accounts for the uncertainty in the maximum depth of ^{137}Cs ($^{137}Cs_{max}$), which results from the 4-cm depth interval between samples.

For core TM-I1, results are only available for the $^{137}Cs_{max}$=20.5-cm case because there is insufficient unsupported ^{210}Pb in the profile below that depth to satisfy Equation 4. There is close agreement between the CRS and CIC model depth-age curves for sediments <100 years old (Fig. 3.67a). The age-mass sedimentation curves show a two-fold increase from ~0.2 g cm^{-2} yr^{-1} 150 years ago to ~0.4 g cm^{-2} yr^{-1} today (Fig. 3.67b). Similarly, the age-SAR curves indicate that net sedimentation rates have increased from pre-deforestation values of ~1 mm yr^{-1} to ~4 mm yr^{-1} today (Fig. 3.67c).

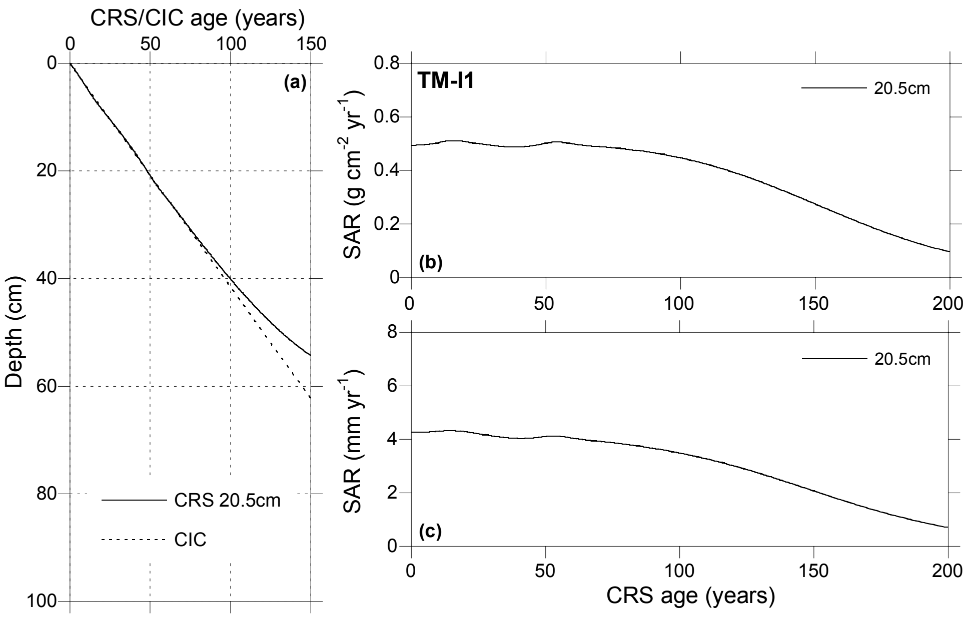

Figure 3.67: Core TM-I1 sedimentation chronology (a) depth-age curves for CRS and CIC ^{210}Pb models, (b) age-mass (g cm^{-2} yr^{-1}) accumulation curves and (c) age-SAR (mm yr^{-1}) curves based on the constrained CRS model.

Table 3.7 summarises the constrained ^{210}Pb CRS modelling results for core TM-I1. The mean supply rates (*P*) of 0.0061 Bq cm^{-2} yr^{-1} is very similar to the measured atmospheric flux (0.0059 Bq cm^{-2} yr^{-1}), although the age-SAR profile (Fig. 3.67c) is unusual in that sedimentation rates ~150 years ago (2 mm yr^{-1}) are higher than expected.

Table 3.7: Summary of constrained ^{210}Pb CRS modelling results for core TM-I1: linear regression fit to natural-log transformed ^{210}Pb data; depth for integration of ^{210}Pb profile; total unsupported ^{210}Pb in the profile ($A(o)$) and mean annual flux (P).

	$^{137}Cs_{max}$ = 20.5 cm
^{210}Pb profile fit (r^2)	0.96
^{210}Pb profile depth (cm)	63.5
***A*(*o*)** (Bq cm^{-2})	0.1967
P (Bq cm^{-2} yr^{-1})	0.0061

The depth-age curves for core TM-I2 show good agreement between the CRS and CIC dating models for sediments <50 years old (Fig. 3.68a). The age-mass sedimentation curves show a six-fold increase from ~0.1 g cm^{-2} yr^{-1} 150 years ago to ~0.6 g cm^{-2} yr^{-1} to the present today (Fig. 3.68b). The age-SAR curves indicate that SAR increased from pre-deforestation values of <0.5 mm yr^{-1} to ~6.5 mm yr^{-1} today (Fig. 3.68c).

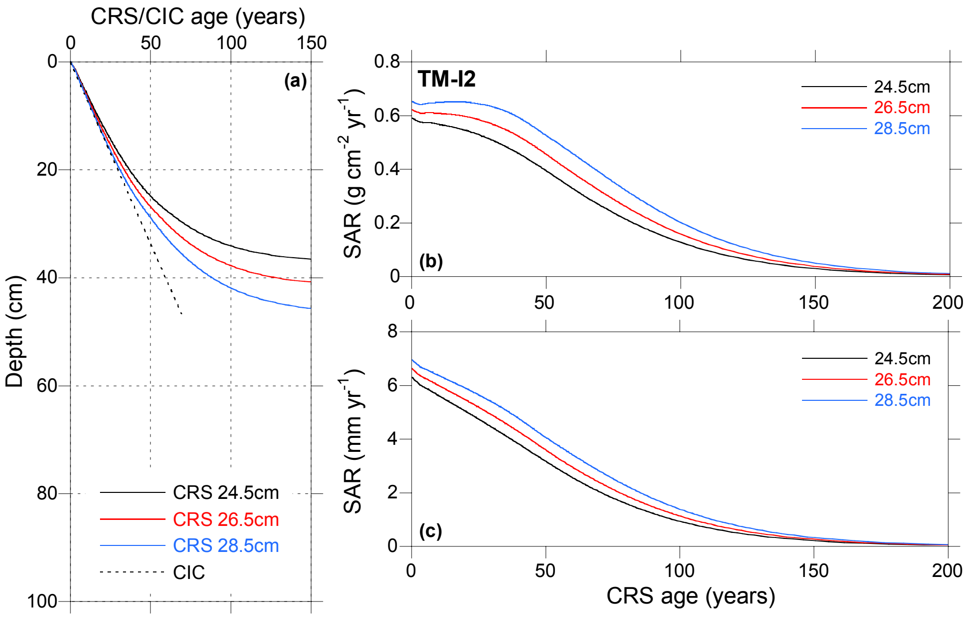

Figure 3.68: Core TM-I2 sedimentation chronology (a) depth-age curves for CRS and CIC ^{210}Pb models, (b) age-mass (g cm^{-2} yr^{-1}) accumulation curves and (c) age-SAR (mm yr^{-1}) curves based on the constrained CRS model.

Table 3.8 summarises the constrained ^{210}Pb CRS modelling results for core TM-I2. The range of mean supply rates (*P*) of 0.0102–0.0112 Bq cm^{-2} yr^{-1} is ~70% higher than the 0.0061 Bq cm^{-2} yr^{-1} obtained for TM-I1 and the measured atmospheric flux (0.0059 Bq cm^{-2} yr^{-1}).

Table 3.8: Summary of constrained ^{210}Pb CRS modelling results for core TM-I2: linear regression fit to natural-log transformed ^{210}Pb data; depth for integration of ^{210}Pb profile; total unsupported ^{210}Pb in the profile (*A*(*o*)) and mean annual flux (*P*).

	$^{137}Cs_{max}$ = 24.5 cm	$^{137}Cs_{max}$ = 26.5 cm	$^{137}Cs_{max}$ = 28.5 cm
^{210}Pb profile fit (r^2)	0.83	–	–
^{210}Pb profile depth (cm)	37.3	41.7	46.8
***A*(*o*)** (Bq cm^{-2})	0.3267	0.3440	0.3607
P (Bq cm^{-2} yr^{-1})	0.0102	0.0107	0.0112

The depth-age curves for core TM-I3 show poor agreement between the CRS and CIC dating models for sediments, which is indicative of substantial increases in SAR during the last 150 years (Fig. 3.69a). The age-mass sedimentation curves show a ten-fold increase from ~0.05 g cm^{-2} yr^{-1} 150 years ago to ~0.7 g cm^{-2} yr^{-1} today (Fig. 3.69b). The age-SAR curves indicate that SAR increased from pre-deforestation values of <0.2 mm yr^{-1} to ~6.5 mm yr^{-1} today (Fig. 3.69c).

Table 3.9 summarises the constrained ^{210}Pb CRS modelling results for core TM-I3. The range of mean supply rates (*P*) of 0.0064–0.0072 Bq cm^{-2} yr^{-1} is similar to the 0.0061 Bq cm^{-2} yr^{-1} obtained for TM-I1 and the measured atmospheric flux (0.0059 Bq cm^{-2} yr^{-1}). The range of *P* values obtained for core TM-I2 are substantially higher than for cores TM-I1 or TM-I3 and more than the ±30% (2 standard deviations) inter-annual variability observed in direct measurements of atmospheric ^{210}Pb deposition (section 2.2.2). The *P* values obtained for core TM-I2 may relate to the fact that the dry bulk density profile for this core differs from the profiles for the other two cores (Appendix IV). In particular, the slope of the linear regression relation fitted to the bulk density data for TM-I2 is higher, so that below 30 cm depth the apparent ^{210}Pb activity (Bq cm^{-2}) and therefore *A*(*o*) and *P* is also higher than calculated for cores TM-I1 and TM-I3.

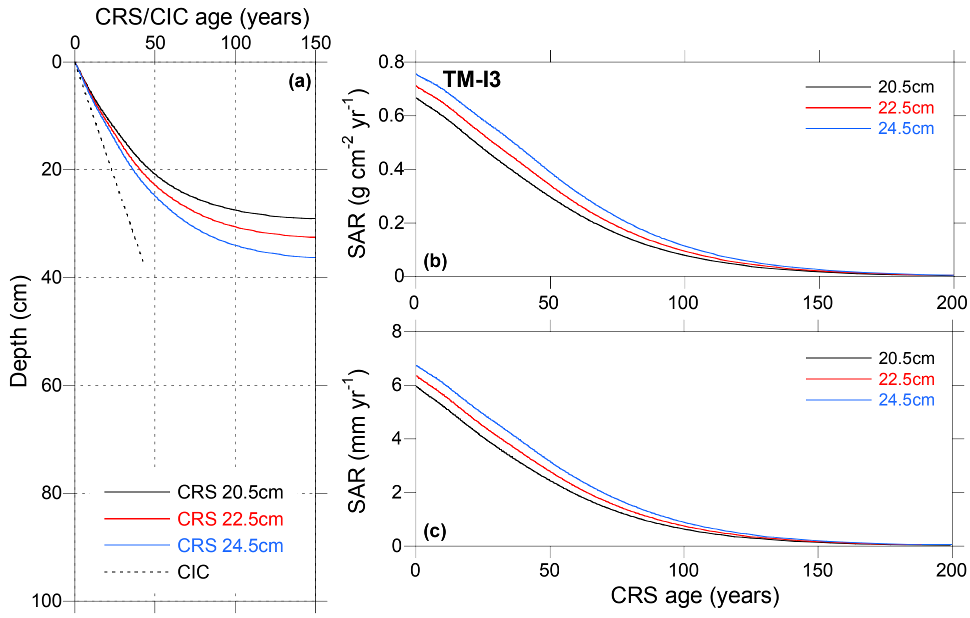

Figure 3.69: Core TM-I3 sedimentation chronology (a) depth-age curves for CRS and CIC ^{210}Pb models, (b) age-mass (g cm^{-2} yr^{-1}) accumulation curves and (c) age-SAR (mm yr^{-1}) curves based on the constrained CRS model.

Table 3.9: Summary of constrained ^{210}Pb CRS modelling results for core TM-I3: linear regression fit to natural-log transformed ^{210}Pb data; depth for integration of ^{210}Pb profile; total unsupported ^{210}Pb in the profile (*A*(*o*)) and mean annual flux (*P*).

	^{137}Cs$_{max}$ = 20.5 cm	^{137}Cs$_{max}$ = 22.5 cm	^{137}Cs$_{max}$ = 24.5 cm
^{210}Pb profile fit (r^2)	0.85	–	–
^{210}Pb profile depth (cm)	29.6	33.1	37.0
***A*(*o*)** (Bq cm^{-2})	0.2043	0.2179	0.2313
P (Bq cm^{-2} yr^{-1})	0.0064	0.0068	0.0072

4. Recent sedimentation in Auckland estuaries

4.1 Comments on physical indicators

In this study, a standard suite of physical parameters or indicators have been used to reconstruct a regional snapshot of the present physical condition and recent sedimentation history of a representative cross-section of Auckland estuaries. In this section we comment on each of these parameters and discuss their utility as indicators of physical changes in estuaries.

Particle size

Profiles of average and median particle diameter and mud content (volume %) show that the recent estuarine sediments we sampled have similar particle size characteristics. Typically, the upper 30-cm of the sediment column is composed of muddy fine-sands with fine silt (~20 μm diameter) and very fine sand (100–150 μm diameter) making up the bulk of the sediments. These data show that differences occur in particle size characteristics between sites and between intertidal and sub-tidal flat sub-environments (e.g., Mahurangi and Wairoa estuaries). The sediment mud content appears to be a more sensitive indicator of differences between sub-environments rather than median particle diameter. However, we found no clear evidence of changes in particle size in the sediment cores that could unequivocally be attributed to human activities in catchments. For example, at Whitford the subtidal cores display an overall trend of increasing mud content from the bottom to the top of the cores, which matches gradual increases in sediment Zn concentrations. These particle-size changes could be attributed to urban stormwater runoff, although most of the Whitford catchment is undeveloped. Alternatively, the observed "fining" of Whitford sub-tidal sediments could reflect changes in the depositional environment, such as shifts in tidal channel positions (Swales et al. 1997).

At Okura, the sediment cores, and in particular OK-I1, show a clear reduction in median particle size and increasing mud content in the top 3-cm of the sediment column. Pollen dating indicates that the upper 10-cm of sediment has been deposited after 1980. Given an average sedimentation rate of ~5 mm yr^{-1}, deposition of these increasingly muddy sediments has likely occurred within the last 5 years. Although construction of the Okura section of the Albany-Puhoi highway in 1998 coincides with this period, we have no evidence to link the increasing mud content of surface sediments to a particular catchment activity.

In interpreting particle size data from the present study it is important to bear in mind that these short cores, in most cases, represent a small fraction of the estuary sedimentation history. For example, long cores collected from the Mahurangi estuary by Swales et al. (1997) and geophysical surveys (Trotter, 1990) show that as much as 15 m of sediment has been deposited in this drowned-valley estuary during the last 7300 years or so. Throughout most of the estuary, a relatively thin veneer (average depth 0.3 m, range 0.11–0.9 m) of muddy fine sand caps 4–15 m of the distinctive, clay-rich, green-grey Mahurangi mud (Swales et al. 1997). At 2.3–2.8 m depth the average particle diameter is of clay size (i.e., <3 μm) and in the upper one metre of the sediment column the sand content increases from 5 to 30% (by volume). Swales et al. (1997) concluded that the ubiquitous coarsening of estuary sediments in the last 150 years was a result of catchment deforestation and subsequent deeper erosion of less weathered soils. The original pollen dating of these cores by McGlone (1994) indicated that the top 15–25 cm of the sediment column have been deposited since 1900 A.D. In the present study, more detailed dating of these sediments using complimentary pollen and ^{137}Cs shows that the upper 23–29 cm of the sediment column has been deposited since the early 1950's.

Changes in sediment particle size must be interpreted with caution. The value of particle-size data as an indicator of the effects of catchment sediment runoff on an estuary largely depend on the availability of complimentary indicators and, most importantly, reliable dating. Clearly, the conclusions drawn from a particular coring study will also be influenced by the relative time-scales of catchment changes and the time period sampled by cores.

Zn concentration

Previous sedimentation studies in Auckland estuaries have demonstrated the value of heavy metal measurements, and in particular Zn, in dating the onset of catchment urbanisation in estuarine sediments (e.g., Williamson and Morrisey, 2000; Craggs et al. 2001; Swales et al. 2002). Our results show that Zn concentrations (particle diameter <2000 μm, silt and sand fraction) in sub-tidal and intertidal surficial sediments deposited in the Mahurangi, Puhoi, Okura and Te Matuku estuaries are ≤30 μg g^{-1} and within the "background" range of pre-urban values. Thus, there is presently no indication of Zn contamination of sediments in these estuaries due to human activities. This may reflect the relative absence of urban development from these estuaries catchments or alternatively dilution of Zn concentrations in estuarine sediments by uncontaminated catchment subsoil derived from earthworks. Present day (i.e., surface) Zn concentrations in Wairoa estuary intertidal and sub-tidal sediments slightly exceed the upper limit of the background range and in most cases Zn concentrations are within the estimated ±5 $\mu g\ g^{-1}$ uncertainty of the acid-extraction method.

In Whitford embayment, Zn concentrations in the top 10-cm of the sub-tidal cores have reached 35–42 $\mu g\ g^{-1}$ and marginally exceed the background range of Zn concentrations in Auckland estuaries. The ^{210}Pb profiles for cores WH-S1 and WH-S2 show surface mixed layers of ~5cm and ~13-cm respectively (Fig. 3.44). Thus, surface Zn concentrations are likely to be less than they would otherwise be in the absence of sediment mixing because recent, more contaminated, sediment is mixed with previously deposited, older and less contaminated sediment.

Nearby, surface Zn concentrations in muddy sediments deposited in mangroves at the mouth of the Waikopua estuary, are substantially higher than in the Whitford subtidal cores, and range between 35–60 $\mu g\ g^{-1}$ (Craggs et al. 2001). The likely source of this Zn is stormwater discharged from Howick sub-catchments draining to the bay, where large-scale urban development began in the early 1960's. In the Waikopua cores there is generally good agreement between the depth of the 1953 (^{137}Cs) sedimentation layer and the depth of the 1960 sedimentation layer identified by a rapid increase in Zn concentrations above 30 $\mu g\ g^{-1}$. These results indicate that the mangrove stands fringing the catchment outlets to Whitford Bay act as sinks for mud and heavy metals bound to fine particles. In the Whitford sub-tidal muds, early signs of the effects of urbanisation of nearby catchments are just starting to be detected albeit with a reduced Zn loading.

In the middle Waitemata Harbour, Zn contamination of estuarine sediments due to human activities is unambiguous. Surface Zn concentrations in the Henderson intertidal (83–100 $\mu g\ g^{-1}$) and Te Atatu subtidal (95–105 $\mu g\ g^{-1}$) cores substantially exceed the range of background values typical of Auckland estuaries. At both sites, the initial increase in Zn concentrations pre-dates the early-1950's and is consistent with the fact that many catchments fringing the southern shore of the middle harbour were already urbanised by the early-1900's. Our results are consistent with Zn concentrations in surface sediments (<500 μm fraction) measured in the Henderson and Whau estuaries (~175 $\mu g\ g^{-1}$) and ~250 $\mu g\ g^{-1}$ at the heads of many urbanised tidal creeks (Mathieson et al. 2002). These data indicate that urbanised catchments are major sources of Zn accumulating in middle-harbour sediments. Dating of long-cores from the Pakuranga creek by Swales et al. (2002) indicates that Zn concentrations typical of present-day (i.e., surficial) middle-harbour sediments were exceeded as early as the mid-1970's. Interim sediment quality guidelines (ISQG) proposed by ANZECC (2000) suggest that Zn concentrations in the Henderson and Te Atatu cores do not yet exceed the trigger value (ISQG-Low) for Zn (200 $\mu g\ kg^{-1}$), where adverse biological effects may occur.

Where corroborating dating of sediments is available, Zn concentration profiles are a reliable physical indicator to identify the onset of catchment urbanisation in estuarine sediments.

Pollen dating

Our study demonstrates the critical importance of using complimentary and independent methods to date estuarine sediments. Comparison of the pollen, ^{137}Cs and ^{210}Pb profiles generally showed excellent agreement for post-1950/1953 SAR.

A prerequisite for the successful application of pollen as a dating tool is the availability of an accurate and detailed catchment history. The primary source of uncertainty in pollen dating, however, relates to (1) estimating the time-lag between initial plant introduction and the production of sufficient pollen and/or spores to be reliably detected in the stratigraphic record, (2) sediment accumulation rate and (3) sampling interval (e.g., Vallette-Silver, 1993; Swales et al. 2002).

In Auckland estuaries, we found that *P. radiata* pollen is an excellent dating tool for recent estuarine sediments because the history of large-scale pine planting in the Auckland region is well known and also because pine pollen has been widely dispersed in large quantities and is ubiquitous. Furthermore, the ±10–15 yr time-lag in pollen production, after initial planting, is well established. The general increase in grass pollen in estuarine sediments may represent an Auckland-wide trend towards more pure grass cover, as a result of suppression of previous rough tall weed and scrub.

Pollen is not an absolute dating method, unlike radioisotopes (e.g., ^{210}Pb), which decay at a constant rate and which in turn provides a quantitative basis for dating. However, the assemblage of many different pollen types (e.g., bracken, native trees, pine, exotic grasses and trees) provides a snap-shot of plant species that were present in the catchment at the time of sedimentation. The pollen record is selective in that those plant species that produce large quantities of widely dispersed pollen are most likely to be represented in the stratigraphic record. Thus, many different strands of evidence are used to assign an age to a particular sediment layer. Another advantage is that only a relatively small quantity of sediment (~ 3 cm^3) is required for dating. Also, because pollen grains are detected by eye, the presence of sufficient numbers of a particular pollen type is enough to confirm at least the presence or absence of a plant species in a sample. However, the effects of sediment mixing need to be considered when assigning a boundary between historical landcover periods. By comparison, the uncertainty in determining radioisotope concentrations reduces with increasing sample size.

The temporal resolution of any dating method, including pollen, depends on sedimentation rate and sampling interval. For example, we sampled 1-cm sediment slices at 4-cm increments down the cores. Given an average sedimentation rate of 5 mm yr^{-1} each 1-cm slice represents (on average) two years sedimentation and the interval between slices represents (on average) six years sedimentation. Increasing or reducing either the sedimentation rate or sampling interval affects the temporal resolution accordingly.

The differentiation of the 1950–1980 and 1980–2001 time periods in the sediment cores is largely based on the rapid increase in pine pollen abundance following forest planting in the mid-1970's. However, unlike the 1950/1953 sedimentation layer we have no independent dating to corroborate the depth of the 1980 (pollen) layer, thus we have no means to confirm the accuracy of the 1980 sedimentation layer assigned to each core.

To conclude, pollen is a reliable, although imprecise (i.e., no absolute aging), dating tool that can be applied in both estuarine muds and sands. The method is simple and the key assumption that must be made relates to the time-lag for a pollen type to appear in the stratigraphic record. Furthermore, pollen, and ^{14}C have been used to reconstruct the sedimentation histories (i.e., 6500 yr B.P. to present-day) of many estuarine systems (Hume et al. 2002).

^{137}Cs dating

Swales et al. (2002) showed that ^{137}Cs profiles measured in Pakuranga estuary sediments preserve a record of catchment soil erosion rather than direct atmospheric deposition, which is the usual basis for dating. In the present study the initial appearance of ^{137}Cs in sediment cores is assumed to date the initial introduction of the radioisotope to the environment (i.e., 1953) resulting from atmospheric nuclear weapons tests. Although there is likely to have been an initial delay for ^{137}Cs-labelled soil to be deposited in these estuaries, this time lag is likely to be small because eroded soil is delivered with flood runoff. We assigned the 1953 deposition layer to the mid-depth between the last occurrence of ^{137}Cs and the next sample down the core. Thus, the main source of uncertainty is that ^{137}Cs may occur deeper in the core at concentrations below the minimum detectable concentration (MDC). The MDC is not a fixed quantity and depends on the sample mass and counting time. We minimised this uncertainty by increasing the nominal sample mass to ~60 g, in comparison to the ~15 g samples analysed at Waikopua (Craggs et al. 2001) and by counting each sample for 24 hours. Like pollen, the temporal resolution of ^{137}Cs dating will vary with sedimentation rate and sampling interval. The good agreement between the 1950 pollen and 1953 ^{137}Cs sedimentation layers indicates that our method is reliable.

^{210}Pb dating

Hume et al. (2002) noted that (1) ^{210}Pb had not been widely applied in New Zealand estuaries and (2) recommended that ^{210}Pb dating method should be tested in a variety of estuarine environments to assess its value for sedimentation studies in Auckland estuaries. In our study, ^{210}Pb dating has been applied to replicate cores collected from intertidal and subtidal sedimentary environments in drowned valley, coastal lagoon and embayment type estuaries. As such, this likely represents the most comprehensive test in New Zealand of ^{210}Pb dating of estuarine sediments. The ^{210}Pb profiles have been used to derive average SAR (S) for the last 50–100 years and to identify surface mixed layers (SML) which are the result of biological and/or physical processes. Where SML occur, we have estimated the particle residence time (R) in the SML before removal by burial, using S. Thus, the shape of the ^{210}Pb profiles can provide useful insights into sedimentation, early diagenetic processes and the mixing and burial of contaminants in these estuarine sediments.

An advantage of ^{210}Pb-derived SAR over ^{137}Cs dating is that the sedimentation rate is based on the entire ^{210}Pb profile rather than just the maximum depth of the tracer. Consequently, the uncertainty in the ^{137}Cs derived SAR relates to the depth interval between samples and the minimum detectable concentration of the analysis. Furthermore, if the pollen or ^{137}Cs tracer is present at the bottom of the core then the estimated SAR is only a minimum value. The uncertainty in the ^{210}Pb-derived SAR primarily relates to the fitting of the natural-log linear regression relation to the data (Equation 7). In turn the fitted slope is influenced by the uncertainty in the unsupported ^{210}Pb values (Equation 10) and the identification and exclusion of features such as surface mixed layers (SML), which may substantially alter the regression. We minimised the uncertainty in the unsupported ^{210}Pb data by analysing large sediment samples and took care to interpret the profiles before attempting to fit regression lines.

A key test of the validity of the ^{210}Pb chronology is to compare the mean annual atmospheric flux or supply rate of ^{210}Pb (*P*) estimated from cores and also with direct measurements from ^{210}Pb measured in rainfall. We found that cores collected several 100 m apart in the same estuary had similar *P* values which would be expected if direct atmospheric deposition, rather than eroded soil, is the primary ^{210}Pb supply pathway. The range of ^{210}Pb supply rates estimated for the Okura (0.0030–0.0034 Bq cm^{-2} yr^{-1}), Wairoa subtidal (0.0049–0.0078 Bq cm^{-2} yr^{-1}) and Te Matuku (0.0061–0.0107 Bq cm^{-2} yr^{-1}) cores also compared favourably with the measured atmospheric ^{210}Pb flux (0.0059 Bq cm^{-2} yr^{-1}, June 2002–June 2003), given the ±30% (2 standard deviations) interannual variation in *P* and the uncertainties involved in estimating this quantity from the cores.

When ^{210}Pb dating can be verified by these methods and by comparison with independent dating then reliable and detailed chronologies of recent sedimentation in estuaries can be reconstructed.

4.2 Comparison of pollen, ^{137}Cs and ^{210}Pb SAR

Figure 4.1 compares SAR calculated from the ^{210}Pb profiles with pollen and ^{137}Cs SAR for the post-1950/1953 period. There is reasonable agreement between SAR derived by the three dating methods, although most of the available data occupy a small range of values (i.e., SAR = 2–5 mm yr^{-1}). Although ^{210}Pb profiles for the Puhoi and Wairoa intertidal cores indicate SAR of as much as 35 mm yr^{-1}, they cannot be included here because ^{137}Cs was present at the base of these cores, so that calculated SAR are minimum values, and/or the pollen profiles lacked the tell-tale changes in pollen abundance of key species (e.g., pine) for dating post-1950 sediments to identify the 1950 depth horizon.

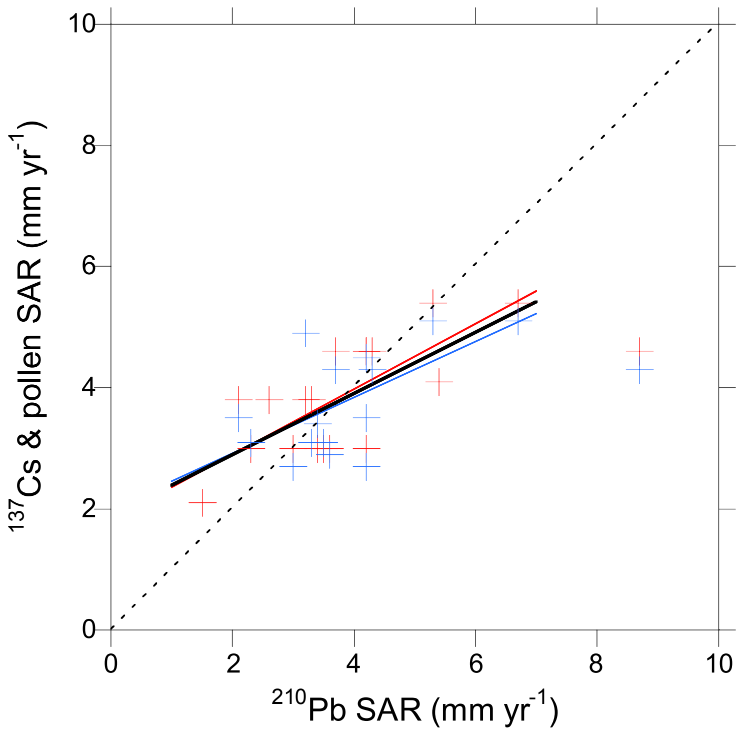

Figure 4.1 Comparison of SAR derived from ^{210}Pb profiles with ^{137}Cs (red) and pollen (blue) SAR for the post-1950/1953 period for cores with maximum ^{137}Cs depth <29 cm. Also shown are linear regression fits for ^{210}Pb with ^{137}Cs (red, r^2 =0.55), ^{210}Pb with pollen (blue, r^2 =0.36) and all data (black, r^2 =0.46).

4.3 Inter-core replication

The primary purpose of collecting (three) replicate cores from each intertidal and sub-tidal flat sampled in our study was to (1) provide confidence in the sedimentation histories reconstructed from the cores and (2) determine the spatial variability in sedimentation processes in the main body of estuaries and adjacent coastal waters.

Sediment particle size data show substantial variations between cores collected from the same intertidal or subtidal flat, which likely reflect between-core differences in environmental conditions (e.g., wave exposure, tidal current speed, distance from catchment outlet etc). By comparison, between-core differences in Zn concentrations were typically less than the combined uncertainty of the measurements (i.e., ±10 µg g^{-1}) and did not appear to vary with distance between cores or sedimentary environment. For example, sub-tidal cores collected at Whitford ~1.3-km apart showed no more variation in Zn concentration than the Te Matuku intertidal cores collected ~150-m apart.

Pollen and ^{137}Cs dating also showed that sedimentation outside the tidal creek environment, in the main body of estuaries, is a relatively homogenous process at decadal scales. Between-core differences in time-averages SAR (3–5 mm yr^{-1}), were <<1 mm yr^{-1} at most sites. By contrast, the ^{210}Pb profiles reveal substantial between-core differences in sedimentation rates and post-deposition sediment mixing at scales of 10–100's of metres that is masked by average SAR statistics. In some cases, the replicate cores displayed similar ^{210}Pb profiles with simple exponential decay of unsupported ^{210}Pb concentration from the surface (e.g., Wairoa subtidal). At other sites the ^{210}Pb profiles were more complex with surface-mixed layers of variable thickness overlaying exponential decay profiles (e.g., Whitford subtidal) and two-layer ^{210}Pb profiles with abrupt changes in slope indicating local changes in sedimentation and/or mixing processes (e.g., Mahurangi and Whitford).

Core replication highlights the potential dangers in generalising the sedimentation history of even a discrete intertidal or subtidal flat within an estuary and increases our confidence in the conclusions that we can reasonably draw about the recent sedimentation history of our study estuaries.

4.4 Comparison of SAR between estuary sub-environment

Table 4.1 summarises the average sedimentation rates and differences-of-means test (two-tailed) results (95% Confidence Interval) calculated for the intertidal and sub-tidal flat sub-environments by pollen, ^{137}Cs and ^{210}Pb dating. The Puhoi and Wairoa intertidal cores have been excluded from the comparison because these cores are younger than 1953 and therefore we cannot accurately calculate SAR.

Pollen, ^{137}Cs and ^{210}Pb dating shows that average SAR on the intertidal flats (4.3–4.7 mm yr^{-1}) are consistently higher than on the sub-tidal flats (2.9–3.9 mm yr^{-1}). On average, the intertidal flats sampled are accumulating sediment 0.8 mm yr^{-1} faster than the sub-tidal flats based on pollen and ^{137}Cs dating and 1.8 mm yr^{-1} faster based on ^{210}Pb dating. In fact, the difference between the two sub-environments is even larger because the post-1950/1953 sedimentation rates in the discarded Puhoi and Wairoa intertidal cores are substantially ≥5.9 mm yr^{-1}. The difference-of-means tests for the pollen and ^{137}Cs indicate that average SAR since the early-1950's have been significantly higher (95% Confidence Level) on the intertidal flats than on the sub-tidal flats sampled in our study. Because of the larger variability in the average ^{210}Pb SAR values we fail to reject the null hypothesis (i.e., no statistically significant difference in average SAR values between environments). However two of our three dating methods indicate a statistically significant difference in intertidal and subtidal SAR since 1950.

Table 4.1: Two-tailed difference-of-means test for post-1950/1953 average SAR (mm yr^{-1}) on intertidal and sub-tidal flat sub-environments, for pollen, ^{137}Cs and ^{210}Pb dating. Rejection region $|t| \geq [t, p=0.975, df = n_1+n_2-2]$.

Environment	Pollen SAR (mm yr^{-1})			^{137}Cs SAR (mm yr^{-1})			^{210}Pb SAR (mm yr^{-1})		
	Ave.	SD	(*n*)	Ave.	SD	(*n*)	Ave.	SD	(*n*)
Intertidal	**4.3**	0.9	9	**4.7**	1.1	12	**4.7**	1.8	12
Sub-tidal	**3.5**	0.8	10	**3.9**	0.7	12	**2.9**	1.1	10
Difference of Means Test $|t| \geq [t, p, df]^1$	$|2.57| \geq 2.09$, **reject Ho**			$|2.33| \geq 2.07$, **reject Ho**			$|1.72| < 2.09$, **fail to reject Ho**		

Note: (1) F-statistic ($p=0.975$, $df = (n_1-1), (n_2-1)$) used to test for equality of sample variances. For ^{137}Cs and ^{210}Pb used pooled variance estimate to calculate *t* and separate variance estimates for pollen.

From our understanding of sedimentation and sediment dynamics in estuaries, we can identify several factors, which potentially explain the significantly higher sedimentation rates measured on the intertidal flats. Firstly, the intertidal sites are closer to the catchment outlet. Studies in tidal creeks, such as the upper reaches of the Mahurangi estuary (Swales et al. 1997), Brighams Creek (Vant et al. 1993), Pakuranga estuary (Swales et al. 2002) and Mangemangeroa estuary (Oldman and Swales, 1999), show a clear gradient of rapidly reducing sedimentation with increasing distance from the catchment outlet. During floods, sediment is deposited on the intertidal flats and as levee under mangrove fringing the main tidal channel. The tidal creeks effectively act as sumps for flood sediments. Secondly, tidal current speeds typically decline with distance from the tidal channel and because the intertidal flats are submerged for ~50% of the tidal cycle the potential for sediment re-suspension is reduced. Thirdly, the sub-tidal flats that we sampled had fetches of 3–10 km and thus the potential for wave and combined wave-current sediment re-suspension is likely to be substantially higher than on the intertidal flats.

Swales et al. (1997) hypothesised that intertidal sedimentation will become self-limiting as estuaries continue to infill because of the increasing effectiveness of sediment resuspension by small, short-period waves in shallow water. This process is offset by reduced submergence time as infilling proceeds. The spatial pattern of intertidal sediment re-suspension by waves is complicated by tidal-cycle variations in water depth and fetch and wave penetration to the seabed (e.g., Green et al. 1997). Generally, waves will tend to preferentially winnow mud, which will either be flushed from the estuary or deposited elsewhere in the estuary in sub-environments less exposed to wave action (e.g., mangroves). The results of our study suggest that other factors, such as proximity to the catchment sediment source, offset the potential limiting effect of wave re-suspension on intertidal sedimentation.

4.5 Physical similarity of estuaries

To quantify the physical similarities of the study estuaries, principal components analysis (PCA) was undertaken using centred and standardised data.

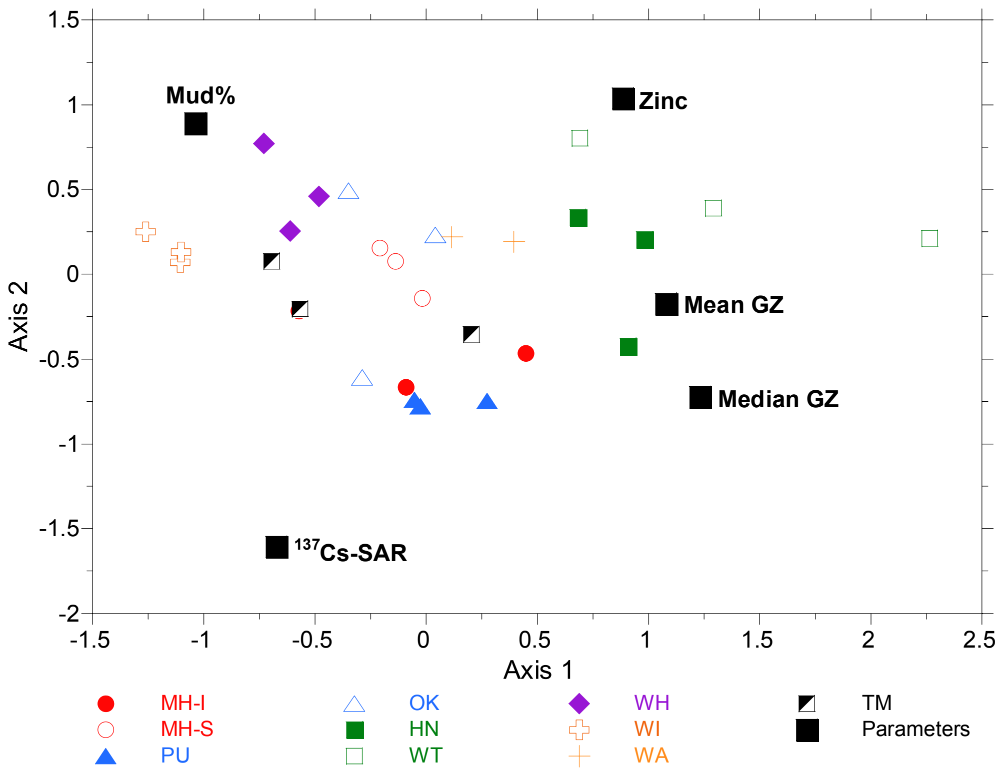

Figure 4.2: Principal components analysis (centred and standardised) of post-1953 core SAR, average Zn concentration, mud content (%), mean and median particle diameter (GZ) (µm). The post-1953 sediments in each core were identified by ^{137}Cs dating. Axes 1 and 2 account for 57% and 20% of the sample variance respectively. MH = Mahurangi, PU = Puhoi, OK = Okura, HN = Henderson, WT = Waitemata, WH = Whitford, WI = Wairoa Intertidal, WA = Wairoa Subtidal, TM = Te Matuku.

PCA was conducted for sediments deposited since 1953, so that we are comparing the physical characteristics of estuarine sediments deposited during the same time period. Post-1953 sediments were identified from ^{137}Cs dating. The physical factors analysed in each core were SAR (mm yr^{-1}), average Zn concentration, mud content (%), mean and median particle diameter (μm). The SAR used here are derived from ^{137}Cs dating although our results show that pollen and ^{210}Pb SAR are similar.

Figure 4.2 shows that there is generally a high degree of physical similarity between cores taken from each estuary (intertidal or sub-tidal flat). In particular, cores collected from Puhoi, Mahurangi (sub-tidal), Whitford, Wairoa (intertidal and subtidal) estuaries formed tight, distinctive clusters. Cores taken from the Waitemata Harbour at Henderson and Te Atatu (sub-tidal flats) were characterised by relatively high Zn concentrations and coarser sediments. The data also show increased sediment "muddiness" along a gradient moving from right to left. Post-1953 sediments deposited in the Wairoa (intertidal), Mahurangi (sub-tidal), Whitford and Te Matuku estuaries are particularly muddy.

Axes 1 (57%), 2 (20%) and 3(13%) accounted for 90% of the total sample variance. The large contribution of axis one to the total sample variance, which is largely driven by particle-size characteristics and to a lesser extent SAR, indicates that the study estuaries are primarily distinguished by sediment "muddiness" and sedimentation rate.

The PCA results also show that estuaries infilling with muddy sediments do not always coincide with the highest sedimentation rates, such as the Puhoi estuary. The Puhoi is a small estuary, close to the outlet of a steepland catchment and is infilling with relatively sand-rich sediments. By comparison, the Wairoa estuary is rapidly infilling with mud derived from a largely lowland pasture catchment. Outliers, such as Okura core OK-I2 indicate a rapid SAR, in comparison to its companion cores.

The large sub-tidal basins that we sampled in the Waitemata, Whitford and Wairoa estuaries also show differences in mud content. For example, the former two estuaries are infilling with mud whereas the Waitemata sediments are relatively sand-rich. The fact that large areas of the Whitford embayment and Tamaki Strait outside Wairoa estuary are rapidly infilling with mud is notable because: (1) all three sub-tidal basins are of similar size, depth and geometry, (2) have similar relative catchment to estuary areas (CER~5, Table 3.1, and Wairoa if sub-tidal area of Wairoa bay included) and (3) are likely to have similar wave exposure, as indicated by (1) above. Furthermore, Te Matuku Bay (Waiheke Island), which is located 11 km north of the Wairoa estuary, is also infilling rapidly with mud. This fact is difficult to reconcile in light of Te Matuku's relatively small (CER~6, Table 3.1) bush and pasture catchment. We hypothesise that sediment exported from the Wairoa catchment is not impacting the Tamaki Strait sub-tidal basin, but may also be impacting other nearby estuaries (refer to section 5.4).

5. How Auckland estuaries are impacted by catchment sediment loads

5.1 Estuary types and environments

There are a variety of estuary types in the Auckland region. Different types of estuaries are affected by catchment sediment loads in different ways because of differences in the relative importance of the various physical and biological processes in each estuary type.

Taking a fairly broad definition of estuaries into account, we identify five general types as being: (1) tidal creeks, (2) drowned valleys, (3) tidal lagoons, (4) tidal rivers and (5) coastal embayments. In reality there is a gradation between these types because all estuaries were formed by the drowning of a pre-existing landscape when the sea rose to its present level some 6,500 years ago. Today we see estuaries at different stages of maturity and, as they continue to infill, their form and physical processes and ecological characteristics change.

5.2 How estuaries infill with sediment and age

We can better understand how Auckland estuaries deal with their sediment loads today by examining how they have evolved and aged. This conceptual model of their physical processes is described below.

Estuaries have not always looked the same as they do today. These semi-enclosed coastal water bodies, where land drainage mixes with the sea, began life when climate warming caused sea level to rise some 150 m to reach its present level some 6,500 years ago. The sea level rise drowned an ancient and varied landscape. In the Auckland region, the seabed of the present-day Hauraki Gulf was once a broad alluvial plain with meandering river channels incised into it and the coast was out beyond Great Barrier Island. Today this landscape lies buried beneath marine sediments deposited in the estuaries and Hauraki Gulf.

Important factors controlling estuary evolution are (1) the shape and size of the flooded basin (which determines how much sediment and where it can accumulate) and (2) catchment sediment loads and (3) the interaction of stream/river processes, tidal exchange and waves. An important point is that estuaries infill with sediment derived from both the land and the sea. The variety of landscapes that were flooded by the sea and the many paths the aging process can take are the primary reasons we have so many different types of estuaries in New Zealand. Where the sea has drowned landscapes to only shallow depth and where there has been abundant soil runoff, then estuaries have aged rapidly.

In the Auckland region, drowned valley estuaries, such as the Mahurangi and Waitemata, have seen the accumulation of thick sequences of sediments, mostly derived from the land, in the incised river valleys and basins. Over time these have evolved into low-gradient intertidal flats drained by a network of channels. Coastal embayments are shallower bays that were flooded by the sea and infilled with catchment and marine sediments. Tidal creeks in the upper reaches of estuaries have infilled with many metres of mud. In tidal lagoons such as the Manukau, Okura, Orewa and Puhoi, river inputs are small relative to tidal flows that dominate the hydrodynamics. Sand driven along the open coast by waves is captured by the tidal flows at the entrance to build sand bodies outside the entrance (ebb tidal delta) and inside the bay (flood tidal delta). A quasi-equilibrium develops between sand being captured and stored in the shoals and sand being released back to the open coast. The middle parts of the lagoons contain a mixture of marine and catchment-derived material, the thickness of which depends on the topography of the original landscape that was drowned and subsequent sedimentation. Many of these landscapes were originally shallow embayments and today they have largely infilled so that when the tide goes out extensive areas of intertidal flats are exposed. Interestingly, sedimentation can slow down late in the infilling process because there is no opportunity for deposition when the tide is out and, particularly where the central areas are wide, wind-generated waves stir the seabed remobilising sediment which can then be transported out to sea. River mouth estuaries age differently. These systems, such as the Waikato River mouth, are short and narrow and have little accommodation space for sediment. It is perhaps surprising therefore, that given their large contributing catchments these estuaries age slowly. The reason for this is that floodwaters and suspended sediment are quickly jetted though the system to the sea, bypassing the estuary. Little sediment enters river mouth estuaries from the sea because the flows in the estuary are directed seawards for most of the time. Floodwaters also scour the bed, prolonging the life of river mouth estuaries.

Large estuaries are compound estuaries comprised of several component estuaries. The Manukau Harbour, for instance, is a combination of tidal creeks that drain to a large central tidal lagoon.

5.3 Factors that accelerate the aging process

The aging process can be dramatically accelerated by biological and anthropogenic factors. The colonisation of intertidal areas by fringing vegetation, such as mangroves or salt marsh rush (e.g., *Juncus*) and the introduced cord grass (*Spartina* spp.) accelerates infilling. Fringing vegetation reduces tidal flows and dampens waves that encourages sedimentation and also prevents resuspension of sediments. As a consequence, fine sediment accumulates on the intertidal flats, even in large wave-exposed estuaries such as the Whitford embayment (Craggs et al. 2001) and the Manukau harbour (Swales et al. in press) where this process would not otherwise occur in the absence of vegetation.

Human activities, in particular catchment deforestation in the last 150 years and rapid urbanisation in the last 50 years, have had a profound effect on the estuary aging process. Some effects are obvious. In places, the margins of estuaries have been infilled by reclamation for farmland or ports, or cut-off by causeways that form carriageways for roading and rail. Some anthropogenic effects are more subtle, such as increases in catchment runoff associated with land use change causing increased sediment infilling. Coring and dating estuarine sediments has revealed that increased runoff from catchment clearance associated with deforestation, agriculture and urban development has greatly increased sedimentation rates and infilling in estuaries.

5.4 Sedimentation in different types of estuaries

Sedimentation accumulation rates (SAR) measured in Auckland estuaries prior to catchment deforestation (1840–1900) and during several times periods since that time and up to the present day are summarised in Table 5.1. These data represent the most up to date and comprehensive summary of recent sedimentation in Auckland estuarine systems.

Table 5.1: Summary of annual average sediment accumulation rates (SAR, mm yr^{-1}) in Auckland estuaries prior to and following catchment deforestation (pre-1840), including their most recent (post 1950/1953) sedimentation history. SAR derived from dated (^{14}C, ^{210}Pb, ^{137}Cs and pollen) sediment cores collected during the present study and relevant earlier studies.

Estuary	Type[1]	Sedimentary Environment	Historical Time Period: Native Forest (pre-1840) (pollen & ^{14}C)	Post-European/ Deforestation 1840-1950 (pollen)	Post-1950 (pollen)	Post-1953 (^{137}Cs)	Post-1950 (^{210}Pb)	Source	Comments
Mahurangi	D.V.	Intertidal Flat Subtidal Flat Intertidal Flat Subtidal Flat Intertidal Flat and Channel	– – 0.3–0.8 – 0.4–0.8	– – 3.2–21.0 [a] 4.0 [a] 16.0 [a]	4.5–5.1 4.9 1.6–4.8 [b] 0.5 [b] 23.7 [b]	4.6–5.4 2.1–4.6	4.2–9.4 1.4–1.5	present study present study Swales et. al. (1997)	 (a) 1850–1900 (b) 1900–1993
Puhoi	T.L.	Intertidal Flat			–	5.4– >5.8	4.1–27.9	present study	
Okura		Intertidal Flat			2.9–3.4	3.0– >5.8	3.5–6.3	present study	
Henderson	D.V.	Intertidal Flat			4.9–11.4	3.8– >5.8	2.6–5.1	present study	
Waitemata/ Te Atatu	D.V.	Subtidal Flat			2.7–3.1	3.0	2.3–3.6	present study	
Brighams	T.C.	Intertidal Flat Subtidal	0.03–0.7 0.4–1.1	0.3–1.8	6.1–9.0/– 2.7			Vant et al. (1993)	
Lucas	T.C.	Intertidal Flat	1–1.50		3.0 [c]			Hume & McGlone (1986)	(c) post-1850
Hellyers	T.C.	Intertidal Flat			5.7–11.4 [d]			Hume (1983) Williamson & Morrisey (2000) & unpub. data	(d) post-1960
Pakuranga	T.C.	Mangrove/Intertidal Flat	0.2–0.5	0.1–1.6	1.7–32.6/1.4–26.4	19.0 [e] (^{137}Cs)	30.0[e] (^{137}Cs)	Swales et al. (2002)	(e) Fig. 6, Swales et al. (2002)
Whitford	C.E.	Subtidal Flat			3.5–4.3	3.8–4.6	0.6–5.7	present study	
Waikopua	C.E.	Mangrove Flat			–/2.6–4.4			Craggs et al. (2001)	
Mangemangeroa	T.C.	Intertidal Flat	0.04–0.14	1.9–5.2	–/1.1–23.4			Oldman & Swales (1999)	
Wairoa	D.V.	Intertidal Flat Subtidal Flat			– 2.7–4.3	>5.8 3.0–4.6	4.7–34.5 3.3–4.3	present study	
Te Matuku	C.E.	Intertidal Flat		0.6	3.5–5.1	4.6–5.4	4.2–8.7	present study	
Manukau	T.L.	Intertidal Flat	0.4–0.5		<5.7[f]			Murray-North (1988)	(f) pollen and ^{14}C
Drury	T.C.	Intertidal Flat		7.0	5. 0[g] /–			Hume et al. (1989)	(g) pollen and D.D.T.

NB: (1) Estuary types: D.V.=Drowned Valley, T.L.=Tidal Lagoon, T.C.=Tidal Creek, C.E.=Coastal Embayment.

Tidal Creeks

Table 5.1 shows large variations in sedimentation rates between estuary types. Tidal creeks have rapidly accumulated sediment during the last 150 years because of (1) increased catchment sediment loads following deforestation, conversion to pasture and, more recently urban development and (2) their close proximity to the catchment outlet. Tidal creeks are particularly susceptible to sedimentation because most sediment enters estuaries in the headwaters via the creeks where physical processes such as flocculation greatly enhance sedimentation. Furthermore, mud is cohesive, tidal currents are weak on the intertidal flats and in the mangroves, and there are no wind waves to resuspend sediment in this sheltered environment. While floods discharge sediment beyond the mouth so that some of the load bypasses the tidal creek, wind waves stir the tidal flats in the outer bodies of harbours and re-suspended mud is transport back into the tidal creeks with the flood tide.

Cores collected from the muddy intertidal flats, and particularly from areas where waves and currents are weak, show thick sequences of muds and complete stratigraphic records are commonly preserved. Sediment accumulation rates (derived from pollen and ^{137}Cs dating) over the last 50 years (post-1950/53) are high and of the order of 3–9 mm yr^{-1} and spectacularly high (c. 30 mm yr^{-1}) in creeks adjacent to urban development (e.g., Pakuranga) and steepland pasture catchments (e.g., Mangemangeroa). Tidal creeks can be likened to a sediment library preserving the history of catchment effects on estuarine systems as well as telling us a great deal about changes in terrestrial systems.

Tidal creeks were not included in our study because they have been relatively well studied in comparison to other estuary types and also because of their lower ecological sensitivity to fine sediment accumulation. Tidal creek sediments are typically utilised by a low diversity of fauna adapted to life in mud. The most diverse benthic macrofaunal communities are found in the main body of estuaries in more sandy substrates that are not exposed as frequently to large changes in water salinity, high suspended sediment concentrations and rapid sedimentation that characterise physical conditions in tidal creeks.

Drowned-valley estuaries

Our study included several drowned-valley estuaries. A drowned-valley estuary forms where the sea has drowned a pre-existing river valley. The larger drowned-valley systems are narrow, deep and river-like, or dendritic, in appearance and have rocky headlands on either shore of narrow inlets (e.g., Mahurangi and Waitemata Harbours). Freshwater enters the estuary at several points around the shore. Drowned valleys are generally deep and contain more subtidal habitat than other sorts of estuaries in the Auckland region.

An important feature of drowned valleys is that the tidal prism is much greater than the river discharge over the tidal cycle and so the hydrology is dominated by the tides, particularly in the middle and lower reaches of the estuary. Tides are important in the main channels, which are highways of sediment distribution. Suspended sediments 'slosh' back and forth in the upper and middle reaches for several tidal cycles before the sediment is deposited. During this time turbidity is elevated and clarity and light penetration are reduced. Preferential environments for sediment accumulation are where creeks meet with the main body of the estuary and on intertidal flats and current speeds reduce (e.g., Hamilton's Landing in the Mahurangi). The upper arms of the estuary are essentially tidal creeks. Here, tidal flushing is poor, and sedimentation rates are high on the intertidal flats in sheltered embayments, especially in mangrove stands where vegetation damps tides and waves. Because drowned-valley estuaries are narrow and valley-shaped there is little wind fetch and only small waves are generated, so wave resuspension processes are important only in wider outer water bodies. In the upper estuary, close to the stream inputs, stratification occurs, and during floods freshwater can displace seawater to the middle and lower reaches of the estuary for short periods. Sediments tend to be muddy in the upper and middle reaches where thick sequences of sediments accumulate in deep palaeo valleys (Hicks and Kibblewhite 1976; Hume and McGlone 1986; Heap and Nichol 1997; Trotter 1990). Because drowned valleys receive sediment mostly from the catchment, they are most susceptible to sedimentation in their headwaters.

In drowned valleys, sediment cores collected from the muddy intertidal and subtidal banks in the upper and middle reaches, where waves and currents are weak, show thick sequences of muds and a fairly complete stratigraphic record. In subtidal and intertidal environments in the Waitemata, Mahurangi and Wairoa sediment accumulation rates have been of the order of 2–7 mm yr^{-1} over the last 50 years (Table 5.1). Deep cores collected from the main body of the Mahurangi estuary revealed thick sequences (>10 m) of often featureless clay-rich "Mahurangi Mud" that was deposited in deep basins (former deep river valleys) in the later stages of sea level rise (e.g., at least 7,200 yr before present, Table 3.3. Swales et al. 1997). The muddy sand capping this thick mud sequence was deposited following catchment deforestation. Near the estuary mouth, cores contain sands and gravel (from channel lags) and generally reflect much more marine influence.

Present-day SAR (2–9 mm yr^{-1}) in our study estuaries are several times higher than before catchment deforestation, as indicated by the ^{210}Pb-CRS chronologies and previous studies (e.g., Hume and McGlone 1986, Vant et al. 1993, Swales et al. 1997, Oldman and Swales 1999, Swales et al. 2002). In the lower reaches of the Wairoa estuary, sedimentation rates of ~30 mm yr^{-1} are more typical of tidal creeks. Furthermore, detailed ^{210}Pb chronologies indicate that SAR have continued to increase over the last 50 years.

Tidal Lagoons

Tidal lagoons constitute one of the most common estuary types in New Zealand. They form where Holocene barriers have built across bays or the mouth of a drowned river valley to partially enclose a marine water body. Good examples in the Auckland region include the Whangateau, Orewa and Puhoi estuaries. Tidal lagoons are typically highly infilled and have extensive areas of intertidal sand flats cut by narrow drainage channels. Typically about 70% of the surface area is intertidal (Hume and Herdendorf 1992). As a consequence, flows in the main body of the estuary are dominated by the tides, and tidal pumping facilitates exchange and flushing between the estuary and the sea. Episodic floods deposit mud in the narrow creeks in the headwaters. Mud is transported to the main body of the estuary but its fate is dependent on the timing of the tides and flood event. At low tide, the tidal channels act as extensions to the fluvial system and can transport suspended sediment from the mouth of the estuary. Mud can completely bypass the estuary by this mechanism. If the flood coincides with a rising tide, then mud is likely to be deposited on the intertidal sand flats. Sediments tend to be sandy in the middle and lower reaches of the main estuary, where wind-generated waves work to winnow mud from the sands. Ebb and flood tide shoals are built at the entrance from marine sands. The water in tidal lagoons for most of the time has low turbidity because of the large exchange with the open sea each tide.

In the Puhoi estuary, we sampled a muddy intertidal flat adjacent to a channel meander. The morphology of the mud lobe, seaward of the meander indicates that these sediments have been deposited as the result of over-bank flow during catchment floods. The SAR that we derived from ^{210}Pb dating (4.1–27.9 mm yr^{-1}) cannot be confirmed by pollen or ^{137}Cs dating. These SAR may not be typical of the

Puhoi intertidal flats because mud deposition maybe locally increased by the proximity to a channel meander.

Compound estuaries

Large compound estuaries like the Manukau harbour are best thought of as a series of **tidal creeks** draining to a **tidal lagoon**. In the lagoon, the wind fetch is as much as 18 km (southwest –northeast), which generates sizeable waves, and wave orbital motion on the sand flats is important in sediment mixing, re-suspension and biological processes (e.g., Dolphin et al. 1995; Bell et al. 1997). The fine silts re-suspended by this process work their way into the channels where they are redistributed by tidal and wind generated currents to low energy environments like the tidal creeks fringing the harbour (Bell et al. 1997).

In general, cores from tidal lagoons are more sandy than those described for tidal creeks and drowned-valley estuaries. In the Manukau Harbour, SAR are low (0.5 mm yr^{-1}) and thin layers of sediment cap old shore platforms (Murray-North 1988).

Coastal embayments

A coastal embayment is an extension of the sea into a recess or indentation of the coast. A small embayment is referred to as a cove. Examples are Omaha Cove, Bon Accord Harbour on (Kawau Is) and Te Matuku (Waiheke Is). Whitford Bay is a compound estuary and is best thought of as **tidal creeks** draining to a **coastal embayment**. Coastal embayments fringe the open coast, and are common on offshore islands. Typically there is enough shelter from waves to form tidal flats in the upper reaches. Coastal embayments generally have little freshwater input and catchment sediment runoff is small. However, in situations where runoff is greater, such as at Whitford, where tidal creeks drain into an embayment, then catchment sediment runoff will result in greater sedimentation in the embayment. In our study, SAR in the Whitford and Te Matuku and embayments (2–9 mm yr^{-1}) were higher than we would have predicted for sites relatively distant from catchment outlets and exposed to waves and tidal currents.

5.5 Historical changes in estuary sedimentation.

Time-series of historical changes in annual sedimentation rates have been reconstructed for cores using the constrained CRS ^{210}Pb dating model when evidence of surface mixing was absent, with good linear-regression models fits to the natural-log transform ^{210}Pb profiles and good agreement with pollen and ^{137}Cs dating. This more detailed analysis of sedimentation chronology was attempted for cores collected in the Okura, Wairoa (subtidal) and Te Matuku estuaries. Figure 5.1 shows the time-series of SAR (mm yr^{-1}) for these cores normalised (NSAR) by the maximum SAR-value in the series so that the records from each site are dimensionless. This enables the sedimentation patterns from each site to be directly compared.

The overall pattern shown by Fig. 5.1 is an increase in NSAR 100–150 years ago (~1850–1900 AD), which coincides with European settlement and large-scale catchment deforestation. Sedimentation rates increased rapidly from ~100 years ago. The Okura and Wairoa cores indicate that sedimentation rates continued to increase until 20–40 years ago (~1960–1980 AD) and since that time have not increased further or have slightly reduced.

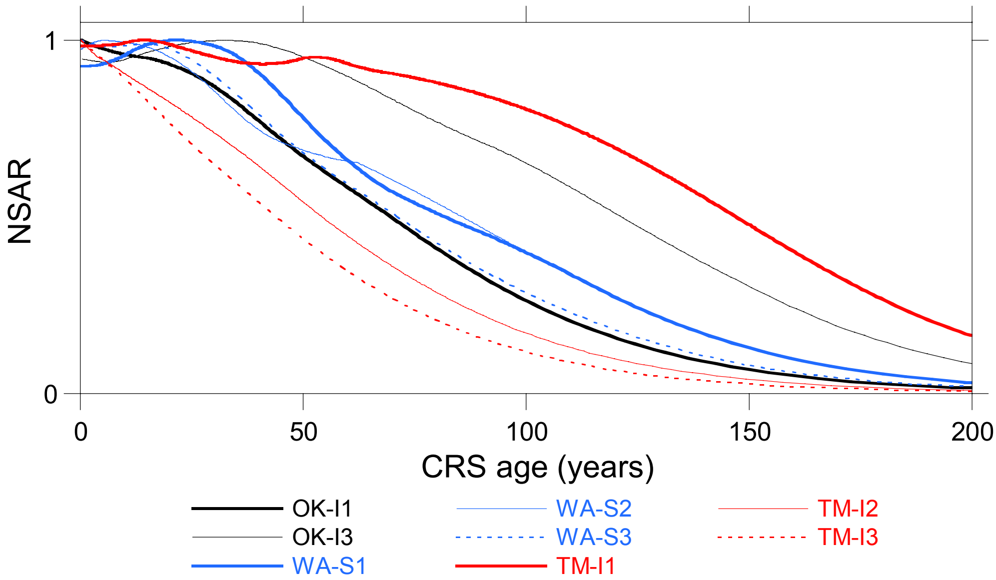

Figure 5.1 SAR normalised by maximum value in series (NSAR) for each core to enable direct comparison of sedimentation histories between sites. The mid-depth ^{137}Cs maximum depth case for the constrained ^{210}Pb CRS model is shown. OK = Okura, WA = Wairoa Subtidal, TM = Te Matuku.

The apparent plateaus in NSAR may relate to reductions in catchment sediment loads and/or estuary storage capacity. For example, in the Okura estuary, 300 ha of pine forest were planted in the early 1970's and this has probably reduced sediment loads from this former pasture sub-catchment. Alternatively, the Okura estuary infilled to such an extent that part of the catchment sediment load is now being exported from the estuary. At the core sites, this is exhibited as a 'levelling off' in sedimentation rates.

In the Wairoa subtidal cores, the plateau in SAR coincide with the construction of the Wairoa Dam (1972–1975) and the planting of a ~1600 ha *P. radiata* forest (1975–1986) in the Wairoa and Cosseys Dams sub-catchments. Alternatively, the observed plateaus in SAR for these subtidal cores may reflect changes in hydrodynamic conditions at the sites due to large-scale changes in seabed bathymetry, perhaps as a consequence of decades of accelerated sedimentation.

The time-series of NSAR for cores TM-I1 and OK-I3 are different to the other cores and shows an early increase in NSAR, which plateaus about 50–60 years ago to the present day. This pattern of initially higher NSAR values is likely explained by the fact that there is insufficient unsupported ^{210}Pb in the profile to provide a reliable time-series (section 3.9.3).

Te Matuku cores TM-I2 and TM-I3 show a different pattern to the Okura and Wairoa cores in that sedimentation rates have continued to increase to the present day. Prior to deforestation SAR were <0.5 mm yr^{-1} and began to rapidly increase ~120–140 years ago with the arrival of European settlers and subsequent land clearance. Over the last ~50 years SAR have increased at a steady rate so that today average SAR in the Te Matuku Bay cores are ~4–7 mm yr^{-1} (i.e., mid-range CRS-age SAR curves). The CRS-age–SAR curves for TM-I2 and TM-I3 show no indication of 'levelling off' or reduction in SAR in the near future and extrapolating these curves suggests future increases in SAR. This steady linear increase in SAR over the last ~50 years has occurred despite the fact that 50% of the Te Matuku catchment have reverted from pasture to kanuka/manuka scrub and, in recent decades, regenerating native forest since the 1940's. Furthermore, the catchment to estuary area ratio (CER) for Te Matuku is 6, which is similar to the CER values for the Mahurangi, Waitemata and Whitford estuaries (section 3.1). A distinguishing feature of these estuaries with CER<10 is that they remain substantially subtidal with a large accommodation volume remaining available for future sedimentation. In contrast, Te Matuku is rapidly infilling despite the fact that it has a relatively small catchment that has been reverting to native forest over the last 50 years. These observations suggest that the primary sediment source is other than the Te Matuku catchment. In section 3.8 we hypothesised that the Wairoa estuary is exporting a substantial quantity of its annual catchment sediment load to the open coast and some of this sediment is likely to be deposited in the Tamaki strait. This is indicated by:

- A large catchment to estuary area ratio (CER = 124).

- Steepland catchment dominated by pasture landcover (64%) supplying 70% of the estimated ~17,500 t yr^{-1} sediment load delivered to the estuary.

- Infilled estuary colonised by mangrove.

We estimate a spatially averaged sedimentation rate of 5.8 mm yr^{-1} from the estimated annual catchment sediment load (~17,500 t yr^{-1}) and estuary surface area (2.5 km) assuming (1) a typical wet bulk density of 1.2 t m^{-3} (McDowell and O'Connor 1977) and (2) all the sediment is deposited in the estuary. However we know that in mangrove-colonised estuaries sediment is deposited as levee, with maximum sedimentation occurring on the channel banks and rapidly declining across the intertidal flat with distance from the tidal channel (Craggs et al. 2001, Swales et al. 2002). Consequently, SAR will vary substantially with location and a proportion of the catchment sediment load will be discharged to the sea. ^{210}Pb (≤35 mm yr^{-1}) and ^{137}Cs-dating (>5.8 mm yr^{-1}) of cores indicates rapid sedimentation on the intertidal flats close to the main tidal channel during the last 50 years. In Wairoa Bay, our subtidal cores show the effects of accelerated sedimentation over the last 100 years with present day SAR of 3–6 mm yr^{-1} (Figs. 3.58–3.60) over at least the ~1.4 km^2 of seabed enclosed by our three core sites. We estimate present-day mass sedimentation of ~6600 t yr^{-1} in this small area of Wairoa Bay alone, assuming an average SAR of 3.9 mm yr^{-1} and a wet bulk density as above. These core data indicate substantial sedimentation in the Tamaki Strait.

Some ~340 catchments discharge stormwater to Auckland's east coast, however more than 90% of these catchments have areas ≤10 km^2. The Wairoa catchment, with an area of ~311 km^2, is by far the largest catchment draining to Auckland's east coast. The physical characteristics of this catchment, landcover history, its small infilled estuary as well as our core data indicate that (1) the Wairoa catchment is a major source of sediment delivered to the east coast and (2) a substantial proportion of this sediment load is exported to the enclosed waters of the Tamaki Strait. Given its close proximity, the Wairoa river is a likely source of the muddy sediment which is rapidly accumulating in Te Matuku Bay. This process of accelerated sedimentation may also be occurring in the numerous bays that fringe the south coast of Waiheke Island (e.g., Awaawaroa Bay) and the mainland.

Our data indicate that highly infilled estuaries in the latter stages of aging, such as the Wairoa, may pass a considerable proportion of their sediment load to the neighbouring coastal environment. Evidence for this was found in the surprisingly high sediment accumulation rates (2–6 mm yr^{-1}) measured in the Whitford and Wairoa subtidal cores, and in the Te Matuku cores (4–9 mm yr^{-1}). These estuaries fringe the

Tamaki Strait, a large semi-enclosed shallow body of water, which receives sediment runoff from a large catchment area. This coast is valued for its physical, ecological, economic values, recreational opportunities and includes several regional parks as well as the recently established marine reserve at Te Matuku. These high rates of sedimentation reflect a larger-scale region-wide pattern of accelerated sedimentation in all our study estuaries, including estuaries remote from large catchment sediment sources over the last 50 years.

5.6 What does the future hold ?

We can only make general predictions about future sedimentation in Auckland estuaries based on our coring studies, because of the complex variety of geological, catchment and oceanographic factors that determine estuary infilling and aging. Nevertheless, the consistent pattern of estuary sedimentation over the last 50 years or so that emerges from our study provides a high degree of confidence in our results.

Prediction of specific effects, albeit at short time-scales (e.g., minutes–days), is best made with numerical models backed up by field experiments. However, a key limitation of using models for predicting future outcomes has to do with accumulation of errors over long time periods (e.g., years–decades). There are a number of sources of error. These include the accuracy of equations describing real-world processes, the applicability of these equations to a particular situation, the model scale, numerical round-off and the accuracy of input data. In some applications, these types of errors can 'balloon' over long time periods such that the predictions are meaningless. As a general rule, the more steps in the modelling exercise, the more rapidly errors will accumulate. Many of these issues are the focus of on-going research. A key contribution of this study is that it provides robust estimates of sediment accumulation rates in Auckland estuaries that can be used to verify modelling hindcasts and predictions.

At decadal (management) time scales, we can use the sediment core data to make predictions with reasonable confidence. There is now overwhelming evidence that dramatic increases in sedimentation rates have accompanied changes in landuse and catchment clearance by the Polynesians and Europeans. Sedimentation rates today in intertidal and subtidal environments are as much as an order of magnitude higher than they were when the catchments were vegetated in their 'native' land cover. We cannot return to that situation and it is unrealistic to expect that improved land management practices will reduce catchment soil erosion and consequent sedimentation rates in Auckland estuaries to their pre-deforestation 'original' values. Furthermore, there is likely to be a time lag between changes in land management practices and potential reductions in soil loss because of sediment already stored in the stream system. The time lag will depend on factors including the catchment size, topography, flood frequency, sediment-size distribution and stream characteristics (e.g., vegetation). For example the time lag is likely to increase with catchment size because of the increasing capacity for in-stream storage and the transport distance. Flood frequency will increase the frequency of sediment transport but will also deliver more sediment to the stream network. Fine silts should be transported more rapidly than sand and gravel because of its substantially lower fall-speed, although cohesive clays may be more difficult to re-suspend. In the Mahurangi there is evidence that catchment deforestation has resulted in a permanent shift in the sedimentary regime of that system so that sediment loads today from the largely pasture catchment are not substantially less than during the height of catchment deforestation (Swales et al. 1997). In a relatively large catchment, such as the Wairoa, the time-lag for transport of sediment already stored in the stream system to the estuary and adjacent coastal marine environment is likely to be of the order of years–decades. Therefore, we must expect sedimentation to continue to infill Auckland estuaries more rapidly than before catchment deforestation and at a rate of several millimetres per year.

The detailed ^{210}Pb CRS sedimentation chronologies reconstructed for the Okura, Wairoa and Te Matuku estuaries suggest that at some sites sedimentation rates have "levelled off" although not reduced during the last 50 years. At other sites, SAR have continued to increase to the present day, which suggests further increases in SAR for the foreseeable future. There is no compelling evidence that sedimentation is yet slowing down in Auckland estuaries as they infill. The physical effects of catchment soil erosion will be greatest in the tidal creeks at catchment outlets, whereas the ecological effects of increased fine sediment loads will be more critical in the main body of estuaries.

We expect estuary infilling and aging to be partly offset by sea level rise associated with climate warming. At Auckland (Ports of Auckland tide gauge), the rate of sea level rise has averaged 1.3 mm yr^{-1} since 1904 (Hannah 1990) whereas SAR measured in Auckland estuaries are 2–9 mm yr^{-1}. Sea level rise will deepen estuaries and flood low lying margins which will evolve to marsh and then tidal flats. However, in the Auckland area this may not occur along urban shorelines, where engineering structures are likely to be used to prevent flooding and property loss. Thus, anthropogenic processes and climate change make the future for urban estuaries rather uncertain and human activities mean that some estuaries will not be able to grow old gracefully. In estuaries with deeper basins such as the Mahurangi and

Waitemata there is more accommodation space for sediments to infill and the main water bodies will remain much the same.

All estuaries follow similar evolutionary paths as they infill with sediment. Water areas and depths decrease over time and as a result hydrodynamic and sedimentological characteristics and biological communities change (Roy et al. 2001). The relative dominance of the fluvial system increases as estuaries mature and tidal volumes shrink. As estuaries age and infill, sedimentation rates may increase, even in the absence of catchment sediment load increases, because the available deposition areas reduce in size and will occur if the sediment trapping efficiency does not change. Thus, the longevity of an estuary depends on the original area and volume of the central mud basin (Roy et al. 2001), sediment supply rate and trapping efficiency. However, as Auckland estuaries age their trapping efficiency will decrease and consequently SAR will decline as more sediment is exported to adjacent coastal waters.

Auckland estuaries are at different points along this evolutionary cycle. Waitemata harbour retains substantial sediment accommodation space in its central mud basin, while the tidal creeks fringing it have largely infilled. In the Mahurangi estuary, the large tidal creek above Hamiltons Landing has largely infilled and sediment has now partially infilled the central mud basin, so that the subtidal volume of this system is shrinking. The Wairoa estuary represents the end-member of the evolutionary cycle and has reached 'old age' before most Auckland estuaries primarily because of its relatively large catchment (~311 km^2) and increased soil erosion following catchment deforestation. Our core data show that (1) post-1950 SAR in Wairoa Bay (3–6 mm yr^{-1}) and in Te Matuku Bay, Waiheke Island, (4–9 mm yr^{-1}) are as much as an order of magnitude higher than ~100 years ago and (2) suggest that the Wairoa estuary now exports sediment to the coastal environment, with the adverse impacts of fine catchment sediments transferred to neighbouring estuaries and inner Hauraki Gulf.

6. Acknowledgements

We gratefully acknowledge the assistance of Dominic McCarthy (ARC) in selecting core sites, Graeme Murdoch and Alastair Jamieson (ARC) for providing the Henderson historical landcover history and Helena Goj (ARC) for literature search. We thank Mr Craig Brebner of Point View Drive, Howick, for collection of monthly rainwater samples for ^{210}Pb analysis. We also acknowledge Dr Nikolaus Hermanspahn and Mary-Jane Oke (National Radiation Laboratory) for radioisotope analyses. Todd Williston (NIWA) provided landcover data and Vonda Cummings (NIWA) identified shells preserved in the sediment cores.

7. References

Abrahim, G. and Parker, R. (2002). Heavy-metal contaminants in Tamaki estuary: impacts of city development and growth, Auckland, New Zealand. *Environmental Geology*, *42*: 883–890.

Alexander, C.R.; Smith, R.G.; Calder, F.D.; Schropp, S.J.; Windom, H.L. (1993). The historical record of metal enrichment in two Florida estuaries. *Estuaries 16(3B)*: 627–637.

ANZECC (2000). Australian and New Zealand Guidelines for Fresh and Marine Water Quality 2000. Australian and New Zealand Environment and Conservation Council, Agriculture and Resource Management Council of Australia and New Zealand. ISBN 09578245 0 5 (set), ISSN 1038 7072.

Bell, R.G.; Hume, T.M.; Dolphin, T.J.; Green, M.O.; Walters, R.A. (1997). Characterisation of physical environmental factors on the intertidal sand flat, Manukau Harbour, New Zealand. *Journal of Experimental Marine Biology and Ecology 216*:11–31.

Bell, R.G.; Hume, T.M.; Hicks, D.M. (2001). Planning for climate change effects on coastal margins. Ministry for the Environment Report ME410 prepared for the NZ Climate Change Programme. September 2001, 73 p.

Benoit, G.; Rozan, T.F.; Patton, P.C.; Arnold, C.L. (1999). Trace metals and radionuclides reveal sediment sources and accumulation rates in Jordan Cove, Connecticut. *Estuaries 22(1)*: 65–80.

Blais, J.M.; Kalff, J.; Cornett, R.J.; Evans, R.D. (1995). Evaluation of ^{210}Pb dating in lake sediments using stable Pb, Ambrosia pollen and ^{137}Cs. *Journal of Paleolimnology 13*: 169–178.

Chagué-Goff, C.; Nichol, S.L.; Jenkinson, A.V.; Heijnis, H. (2000). Signatures of natural catastrophic events and anthropogenic impact in an estuarine environment, New Zealand. *Marine Geology 167*: 285–301.

Craggs, R.; Hofstra, D.; Ellis, J.; Schwarz, A.; Swales, A.; Nicholls, P.; Hewitt, J.; Ovenden, R.; Pickmere, S. (2001). Physiological responses of mangroves and saltmarsh to sedimentation. NIWA Client Report ARC01268/1, 78 p.

Denyer, K., Cutting, M., Campbell, G., Green, C., Hilton, M. (1993). Waitakere Ecological District: Survey Report No. 15 for the Protected Natural Areas Programme. Auckland Regional Council.

Dolphin, T.; Hume, T.M.; Parnell, K.E. (1995). Oceanographic processes and sediment mixing on a sand flat in an enclosed sea. *Marine Geology* 128: 169–181.

Douglas, I. (1985). Urban sedimentology. *Progress in Physical Geography 9(2):* 255–280.

Gibbs, M.; Thrush, S.; Sukias, J.; Berkenbusch, K.; Thompson, D.; Bury, S. (2001). Evaluation of terrestrial sediment spatial patterns throughout the Whitford embayment and its benthic food web using stable isotope techniques. NIWA Client Report ARC01270, 30 p.

Goldberg, E.D. (1963). Geochronology with ^{210}Pb. In: *Radioactive Dating*, 121–131. International Atomic Energy Agency, Vienna.

Goldberg, E.D. and Kiode M. (1962). Geochronological studies of deep sea sediments by the ionium/thorium method. *Geochimica et Cosmochimica Acta 26*: 417–450.

Green, M.O., Black, K.P.; Amos, C.L. (1997). Control of estuarine sediment dynamics by interactions between currents and waves at several scales. *Marine Geology 144*: 97–116.

Green, M.O. and Oldman, J.O. (1999). Deposition of flood-borne sediment in Okura estuary. NIWA Client Report ARC90242/2, 59 p.

Guinasso, N.L. Jr. and Schink, D.R. 1975. Quantitative estimates of biological mixing rates in abyssal sediments. *Journal of Geophysical Research 80*: 3032–3043.

Hannah, J. (1990). Analysis of mean sea level data from New Zealand for the period 1899–1988. *Journal of Geophysical Research 95(B8)*: 12,399–12,405.

Harris, T.F.W. (1993). The Mahurangi System. Environment and Planning Division, Auckland Regional Council.

Haworth, J. (1994). Faith and brotherhood. *New Zealand Geographic 21*: 73–88.

Heap, A.D. & Nichol, S.L. (1997). The influence of limited accommodation space on the stratigraphy of an incised-valley succession: Weiti River Estuary, New Zealand. *Marine Geology 144*: 229-252.

Hewitt, J.E.; Cummings, V.J.; Norkko, A. (1998). Monitoring of Okura Estuary for biological effects of road construction December 1997–July 1998. NIWA Client Report ARC80231.

Hicks, S.R.; Kibblewhite, A.C. (1976). Seismic reflection profiling in very shallow waters in the Upper Waitemata Harbour, New Zealand. *New Zealand Journal of Geology and Geophysics 19*:213-231.

Hume, T.M. (1983). Upper Waitemata Harbour sediments and the inferred impacts of future catchment and estuary use change (Specialist Report). Water Quality Centre Report No.3. Prepared for Auckland Regional Authority, 95 p.

Hume, T.M. and McGlone, M.S. (1986). Sedimentation patterns and catchment use changes recorded in the sediments of a shallow tidal creek, Lucas Creek, Upper Waitemata Harbour, New Zealand. *New Zealand Journal of Marine and Freshwater Research 20*: 677–687.

Hume, T.M.; Fox, M.E.; Wilcock, R.J. (1989). Use of organochlorine contaminants to measure sedimentation rates in estuaries: a case study from the Manukau Harbour. *Journal of the Royal Society of New Zealand 19*: 305–317.

Hume, T. and Herdendorf, C.E. (1992). Factors controlling tidal inlet characteristics on low-drift coasts. *Journal of Coastal Research 8(2)*: 355–375.

Hume, T.; Bryan, K.; Berkenbusch, K.; Swales, A. (2002). Evidence for the effects of catchment sediment runoff preserved in estuarine sediments. NIWA Client Report ARC01272, 57 p.

Johnston, R.M.S. (1984). Sediments and sedimentary processes in Mahurangi Harbour. M.Sc. thesis, Department of Earth Sciences, University of Waikato.

Lamb, H. (2001). Riverhead, and urban forest. *New Zealand Geographic 53*: 72–85.

Long, E. R.; Macdonald, D.D.; Smith, S.L.; Calder, F.D. (1995). Incidence of adverse biological effects within ranges of chemical concentrations in marine and estuarine sediments. *Environmental Management 19*: 81–97.

Luckman, P.G.; Hicks, D.L.; Jessen, M.R. (1999). Sediment sources in the Wairoa-Ness Valley Catchment. Landcare Research Contract Report LC9899/69.

Lundquist, C.; Vopel, K.; Thrush, S.F.; Swales, A. (2003). Evidence for the effects of catchment sediment runoff preserved in estuarine sediments: Phase III macrofaunal communities. NIWA Client Report HAM2003-051, 48 p.

Mathieson, T.J.; Olsen, G.M.; Hawken, J.L. (2002). Marine sediment monitoring programme – 2001 Results. NIWA Client Report ARC02282, 71 p.

Matthews, K.M. (1989). Radioactive fallout in the south pacific: a history. Part 1: Deposition in New Zealand. Report NRL1989/2, National Radiation Laboratory, Christchurch New Zealand.

McDowell, D.M. & B.A. O'Connor. (1977). Hydraulic behaviour of estuaries. The Macmillan Press Ltd, London, 292 p.

McGlone, M.S. (1994). Unpublished report on the pollen analysis of cores from the Mahurangi estuary. Landcare Research, Lincoln, 5p.

Monin, P. (1992). Waiheke Island: a history. The Dunmore Press, Palmerston North, 229 p.

Moore, P.D. & J.A. Webb. (1978). An illustrated guide to pollen analysis. Hodder and Stroughton.

Morrisey, D.J.; Hill, A.F.; Kemp, C.E.; Smith, R.K. (1999a). Changes in the abundance and distribution of coastal and estuarine vegetation in the Auckland region. NIWA Client Report ARC90232/1.

Morrisey, D.J.; DeWitt, T.H.; Roper, D.S.; Williamson, R.B. (1999b). Variation in the depth and morphology of burrows of the mud crab *Helice crassa* among different types of intertidal sediment in New Zealand. *Marine Ecology Progress Series* 182: 231–242.

Morrisey, D.J.; Williamson, R.B.; Van Dam, L.; Lee, D.J. (2000). Stormwater contamination of urban estuaries. 2. Testing a predictive model of the build-up of heavy metals in sediments. *Estuaries 23(1)*: 67–79.

Murdoch, G.J. (1988). Historical perspectives on the Southern Kaipara, Lower Waikato and Wairoa Valley, Part II: Lower Waikato and Wairoa Valley. ARA Future Bulk Water Supply Study Phase 4 background report No. 5.4.

Murray-North. (1988). Manukau Harbour Action Plan: Assessment of the recent sedimentation history of the Manukau Harbour. Prepared for Auckland Regional Council.

Norkko, A.; Talman, S.; Ellis, J.; Nicholls, P.; Thrush, S. (2001). Macrofaunal sensitivity to fine sediments in the Whitford embayment. NIWA Client Report ARC01266/2.

Oldfield, F.; Appleby, P.G. (1984). Empirical testing of ^{210}Pb-dating models for lake sediments. In: Lake sediments and environmental history, Haworth and Lund (eds): 93–124.

Oldman, J.O. & Swales, A. (1999). Maungamaungaroa Estuary numerical modelling and sedimentation. NIWA Client Report ARC70224.

Olsen, C.R.; Simpson, H.J.; Peng, T.-H.; Bopp, R.F.; Trier, R.M. (1981). Sediment mixing and accumulation rate effects on radionuclide depth profiles in Hudson Estuary sediments. *Journal of Geophysical Research 86 (C11)*: 11020–11028.

Ritchie, J.C. & McHenry, J.R. (1989). Application of radioactive fallout cesium-137 for measuring soil erosion and sediment accumulation rates and patterns: A review with bibliography. Hydrology Laboratory, Agriculture Research Service, U.S. Department of Agriculture, Maryland.

Robbins, J.A. (1978). Geochemical and geophysical applications of radioactive lead. In Biogeochemistry of Lead in the Environment, Nriagu, J.O. (ed.): 285–393.

Robbins, J.A. & Edgington, D.N. (1975). Determination of recent sedimentation rates in Lake Michigan using ^{210}Pb and ^{137}Cs. *Geochimica et Cosmochimica Acta 39*:285–304.

Roy, P.S.; Williams, R.J.; Jones, A.R.; Yassini, I.; Gibbs, P.J.; Coates, B.; West, R.J.; Scanes, P.R.; Hudson, J.P.; Nichol, S. (2001). Structure and function of south-east Australian estuaries. *Estuarine, Coastal and Shelf Science 53*: 351–384.

Schriven, J. (1981). History and prehistory of the Upper Waitemata Harbour. Unpublished working report No. 19. Upper Waitemata Harbour Catchment Study, Auckland Regional Authority, Auckland, 40 p.

Stroud, M.J.; Cooper, A.B.; Bottcher, A.B.; Hiscock, J.G.; Pickering, N.B. (1999). Sediment runoff from the catchment of Okura estuary. NIWA Client Report ARC90241/1, 37p.

Swales, A.; Hume, T.M.; Oldman, J.W.; Green, M.O. (1997). Sedimentation history and recent human impacts. NIWA Client Report ARC60201, 90p.

Swales, A.; Williamson, R.B.; Van Dam, L.; Stroud, M.J.; McGlone, M.S. (2002). Reconstruction of urban stormwater contamination of an estuary using catchment history and sediment profile dating. *Estuaries 25(1)*: 43–56.

Swales, A.; MacDonald, I.T.; Green, M.O. (2004). Influence of wave and sediment dynamics on cordgrass (*Spartina anglica*) growth and sediment accumulation on an exposed intertidal flat. *Estuaries 27(2)*: In press.

Thrush, S.; Cummings, V.; Norkko, A.; Hewitt, J.; Budd, R.; Swales, A.; Funnell, G. (1998). Response of horse mussels (*Atrina zelandica*) to sediment loading. NIWA Client Report ARC80230, 23p.

Tinker, R.A.; Pilvio, R. (2000). Environmental radioactivity in New Zealand and Rarotonga - annual report. National Radiation Laboratory Report NRL-F/80, 24 p.

Tonkin and Taylor Ltd. (1996). Watercare Services Ltd. Wairoa Catchment Consents. Sedimentation Study. Report 14048.

Trotter, S.A. (1990). Estuarine sedimentation and landcover history: The case of the Mahurangi. M.Sc. thesis, Departments of Geography and Environmental Science, University of Auckland.

Valette-Silver, N.J. (1993). The use of sediment cores to reconstruct historical trends in contamination of estuarine and coastal sediments. *Estuaries 16(3B)*: 577-588.

Vant, W.N.; Williamson, R.B.; Hume, T.M.; Dolphin, T.J. (1993). Effects of future urbanisation in the catchment of Upper Waitemata Harbour. NIWA Consultancy Report No. ARC220.

Williams, P.W. (1976). Impact of urbanisation on the hydrology of Wairau Creek, North Shore, Auckland. *Journal of Hydrology (N.Z.) 15*: 81–99.

Williamson, R.B.; Morrisey, D.J.; Swales, A. Mills, G.N. (1998). Distributions of contaminants in urbanised estuaries: Predictions and Observations. NIWA Client Report ARC60205.

Williamson, R.B. (1993). Urban runoff data book: a manual for the preliminary evaluation of urban stormwater impacts on water quality. Water Quality Centre Publication No. 20. Hamilton, NIWA.

Williamson, R.B.; Morrisey, D.J. (2000). Stormwater contamination of urban estuaries. 1. Predicting the build-up of heavy metals in sediments. *Estuaries 23(1)*: 56–66.

Wilmshurst, J.; Eden, D.N.; Froggatt, P.C. (1999). Late Holocene forest disturbance in Gisborne, New Zealand. *New Zealand Journal of Botany 37*: 523–540.

Wise, S. (1977). The use of radionuclides ^{210}Pb and ^{137}Cs in estimating denudation rates and in soil erosion measurement. Occasional Paper No. 7 University of London, King's College, Department of Geography, London.

8. Appendix I: Table of GPS Co-ordinates for sediment core locations

Estuary	Environment	Core	Water Depth (m C.D.)	Latitude	Longitude
Mahurangi	Intertidal	MH-I1		36°26.184'S	174°43.087'E
		MH-I2		36°26.423'S	174°43.078'E
		MH-I3		36°26.596'S	174°43.076'E
	Sub-tidal	MH-S1	-2.0	36°28.114'S	174°43.514'E
		MH-S2	-0.7	36°28.114'S	174°43.514'E
		MH-S3	-0.5	36°28.116'S	174°43.688'E
Puhoi	Intertidal	PU-I1		–	–
		PU-I2		36°31.528'S	174°41.351'E
		PU-I3		36°31.537'S	174°41.402'E
Okura	Intertidal	OK-I1		36°40.470'S	174°42.801'E
		OK-I2		36°40.473'S	174°42.860'E
		OK-I3		36°40.479'S	174°42.930'E
Henderson	Intertidal	HN-I1		36°48.665'S	174°39.432'E
		HN-I2		36°48.646'S	174°39.437'E
		HN-I3		36°48.617'S	174°39.515'E
Waitemata	Sub-tidal	WT-S1	-0.2	36°49.915'S	174°40.926'E
		WT-S2	-1.4	36°50.164'S	174°41.517'E
		WT-S3	-0.5	36°50.349'S	174°40.647'E
Whitford	Sub-tidal	WH-S1	-5.0	36°52.598'S	174°56.537'E
		WH-S2	-6.8	36°52.111'S	174°56.932'E
		WH-S3[1]	-5.0	36°52.630'S	174°57.390'E
Wairoa	Intertidal	WI-I1		36°56.810'S	175°05.207'E
		WI-I2		36°56.826'S	175°05.261'E
		WI-I3		36°56.837'S	175°05.319'E
	Sub-tidal	WA-S1	-2.4	36°54.824'S	175°06.969'E
		WA-S2	-3.5	36°53.919'S	175°07.189'E
		WA-S3	-2.8	36°54.602'S	175°08.105'E
Te Matuku	Intertidal	TM-I1		36°49.896'S	175°07.895'E
		TM-I2		36°49.939'S	175°07.846'E
		TM-I3		36°49.986'S	175°07.777'E

Note: (1) Actual position not recorded – the intended location is given.

9. Appendix II: Auckland estuaries cores: depth profiles of pollen and spore abundance by (1) major plant types and (2) detailed diagrams with scientific names to *Genus* or *species* level.

9.1 Mahurangi Estuary

Intertidal Cores

Core MH-I1

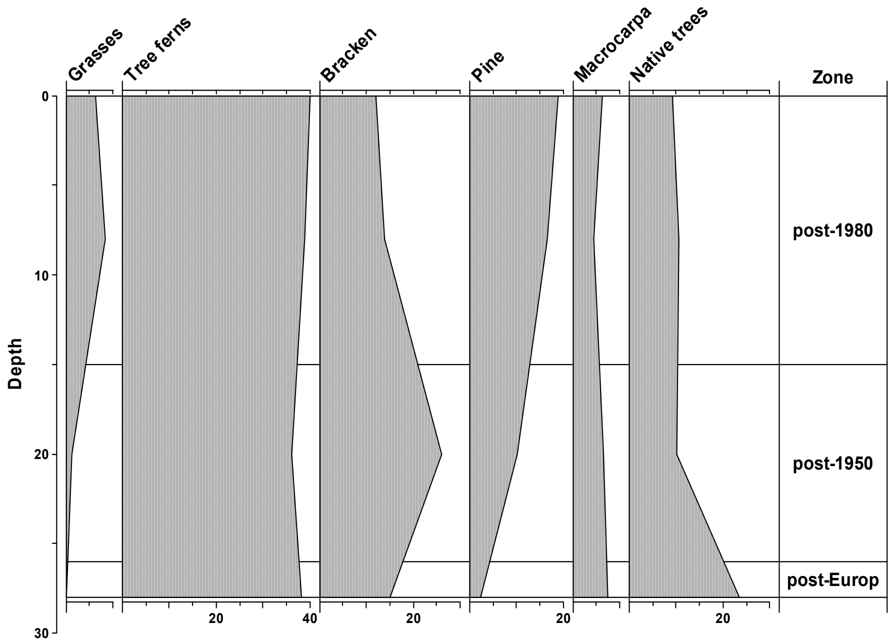
Grasses
Tree ferns
Bracken
Pine
Macrocarpa
Native trees
Zone
Depth
post-1980
post-1950
post-Europ
0
10
20
30
40

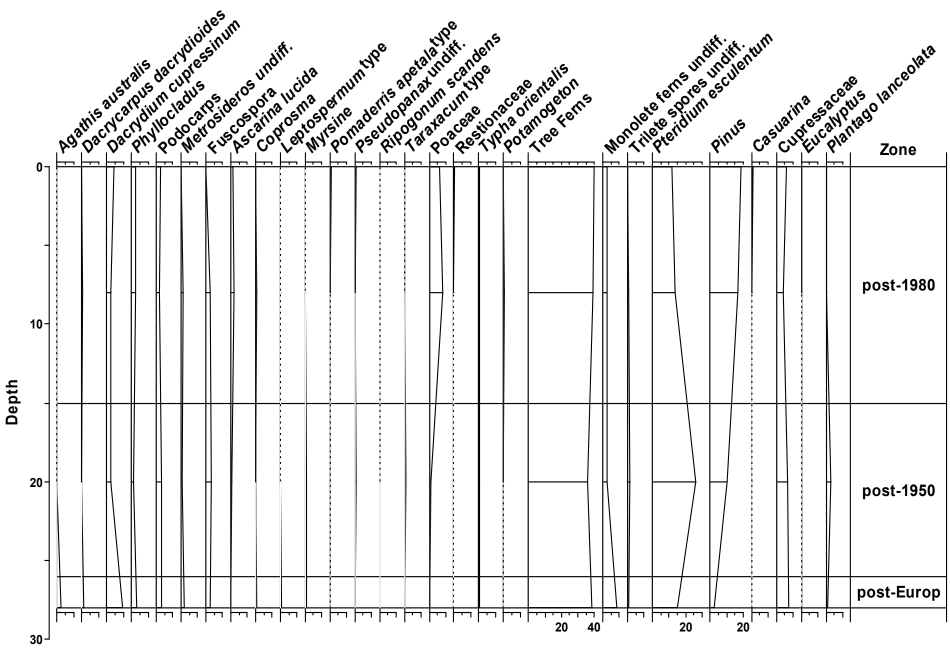
Agathis australis
Dacrycarpus dacrydioides
Dacrydium cupressinum
Phyllocladus
Podocarps
Metrosideros undiff.
Fuscospora
Ascarina lucida
Coprosma
Leptospermum type
Myrsine
Pomaderris apetala type
Pseudopanax undiff.
Ripogonum scandens
Taraxacum type
Poaceae
Restionaceae
Typha orientalis
Potamogeton
Tree Ferns
Monolete ferns undiff.
Trilete spores undiff.
Pteridium esculentum
Pinus
Casuarina
Cupressaceae
Eucalyptus
Plantago lanceolata
Zone
Depth
post-1980
post-1950
post-Europ
0
10
20
30
40

Core MH-I2

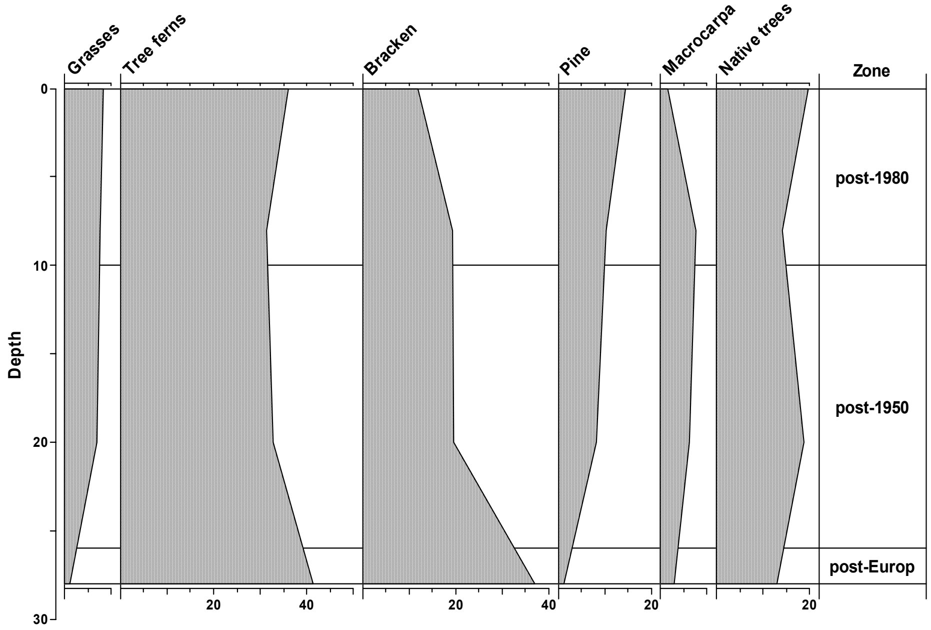

Grasses
Tree ferns
Bracken
Pine
Macrocarpa
Native trees
Zone
post-1980
post-1950
post-Europ
Depth
0
10
20
30
20
40
20
40
20
20

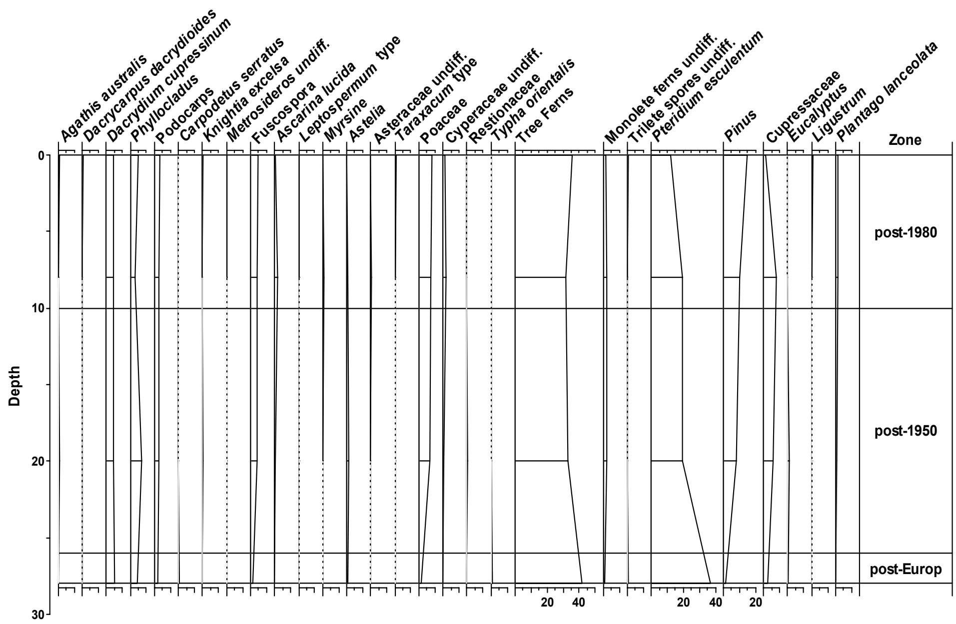

Agathis australis
Dacrycarpus dacrydioides
Dacrydium cupressinum
Phyllocladus
Podocarps
Carpodetus serratus
Knightia excelsa
Metrosideros undiff.
Fuscospora
Ascarina lucida
Leptospermum type
Myrsine
Astelia
Asteraceae undiff.
Taraxacum type
Poaceae
Cyperaceae undiff.
Restionaceae
Typha orientalis
Tree Ferns
Monolete ferns undiff.
Trilete spores undiff.
Pteridium esculentum
Pinus
Cupressaceae
Eucalyptus
Ligustrum
Plantago lanceolata
Zone
post-1980
post-1950
post-Europ
Depth
0
10
20
30
20
40
20
40
20

Core MH-I3

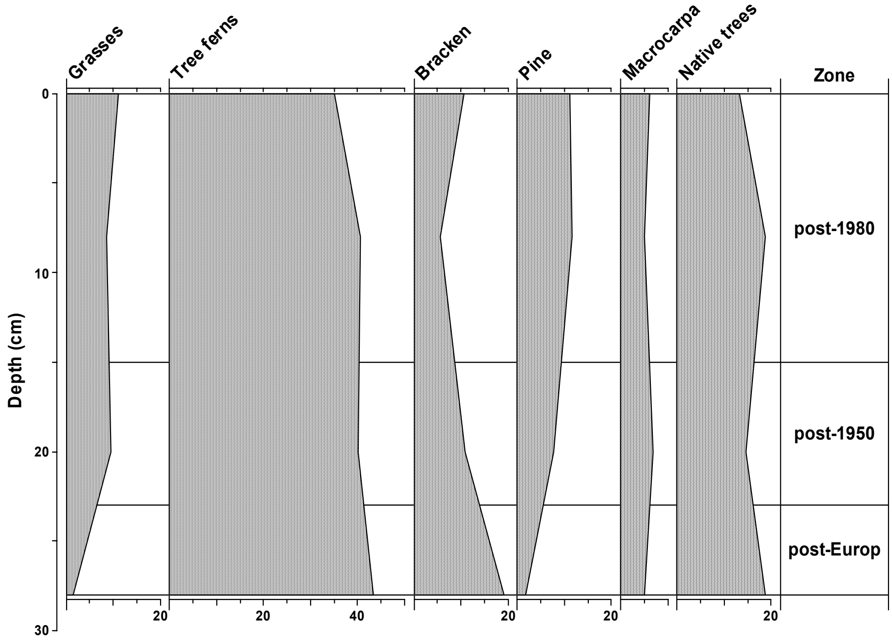
Grasses
Tree ferns
Bracken
Pine
Macrocarpa
Native trees
Zone
post-1980
post-1950
post-Europ
Depth (cm)
0
10
20
30
20
20
40
20
20
20

Sub-tidal Cores

Core MH-S1

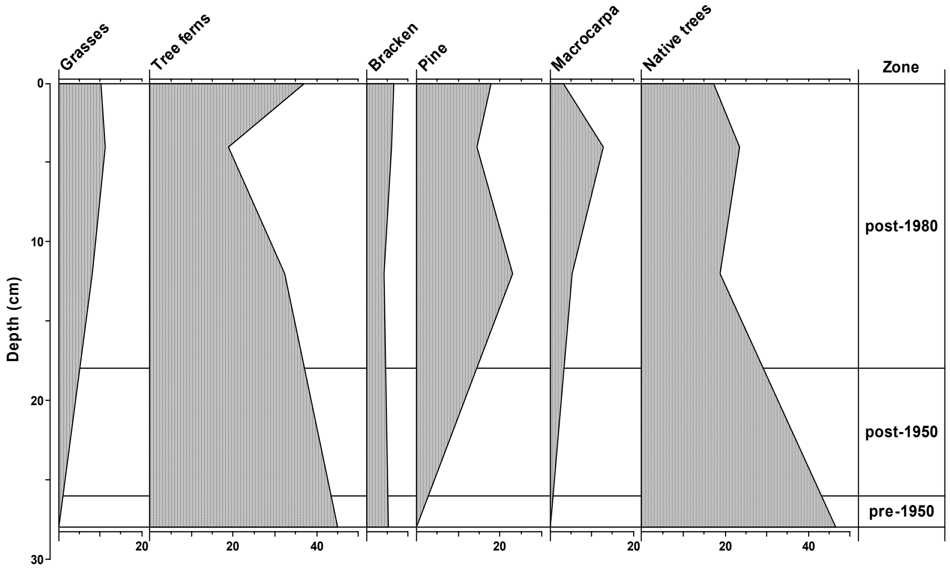

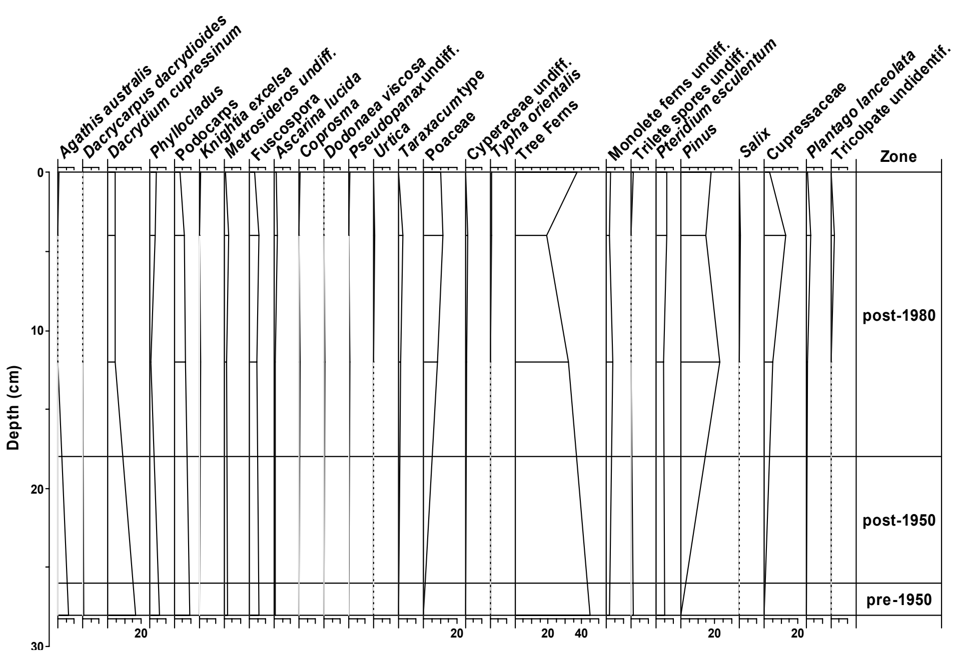

Core MH-S3

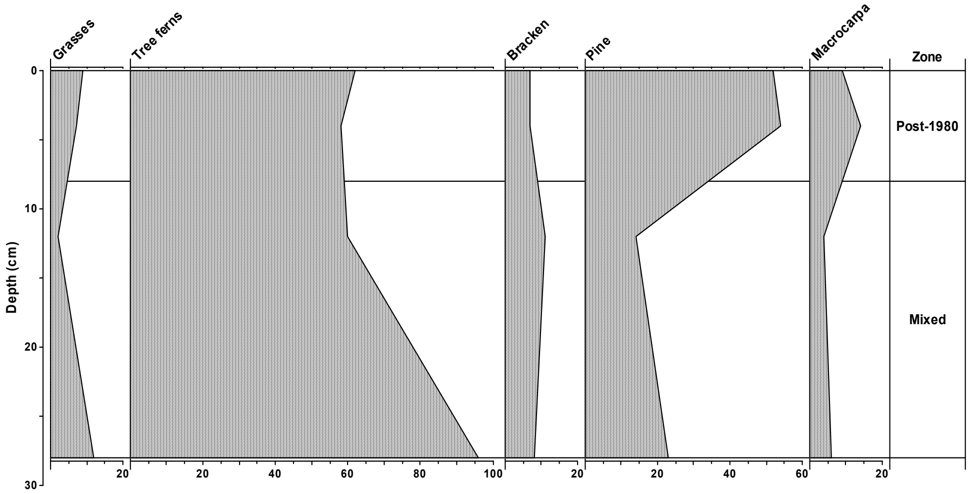
Grasses
Tree ferns
Bracken
Pine
Macrocarpa
Zone
Post-1980
Mixed
Depth (cm)
0
10
20
30
20
20
40
60
80
100
20
20
40
60
20

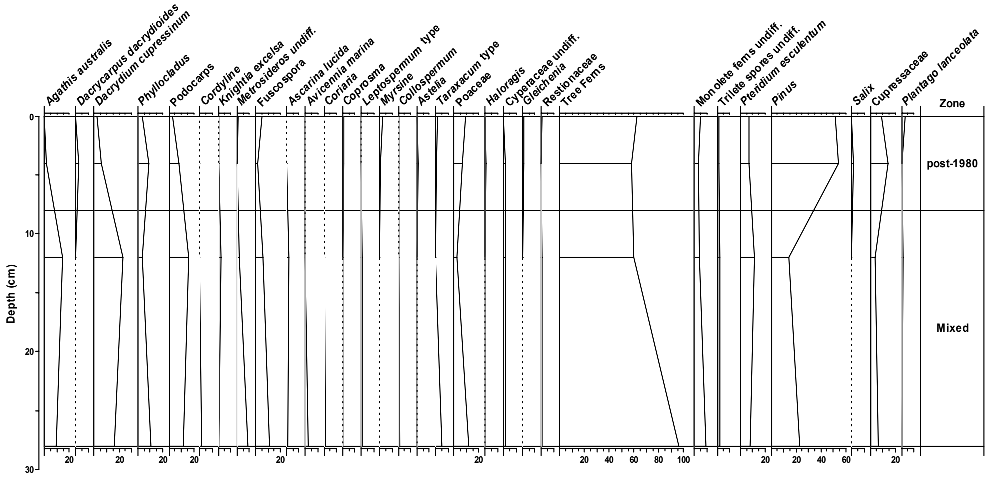
Agathis australis
Dacrycarpus dacrydioides
Dacrydium cupressinum
Phyllocladus
Podocarps
Cordyline
Knightia excelsa
Metrosideros undiff.
Fuscospora
Ascarina lucida
Avicennia marina
Coriaria
Coprosma
Leptospermum type
Myrsine
Collospermum
Astelia
Taraxacum type
Poaceae
Haloragis
Cyperaceae undiff.
Gleichenia
Restionaceae
Tree Ferns
Monolete ferns undiff.
Trilete spores undiff.
Pteridium esculentum
Pinus
Salix
Cupressaceae
Plantago lanceolata
Zone
post-1980
Mixed
Depth (cm)
0
10
20
30

9.2 Puhoi Estuary

Core PU-I1

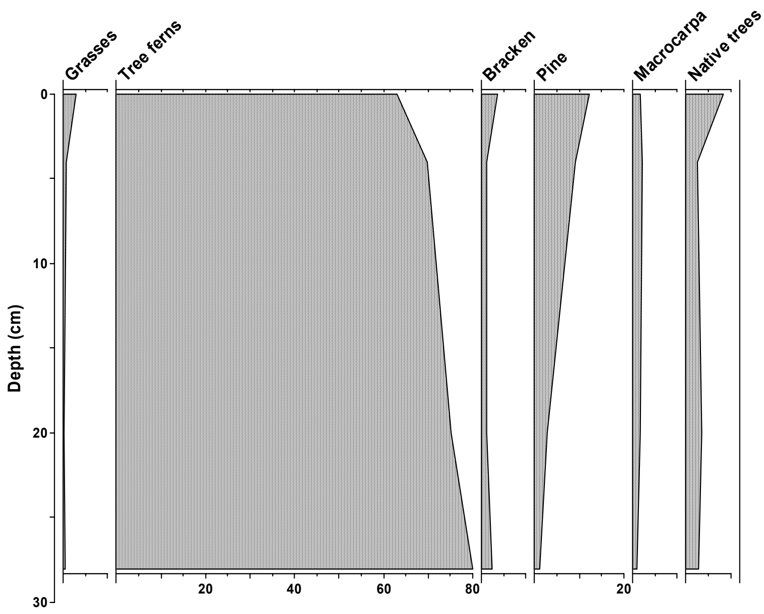

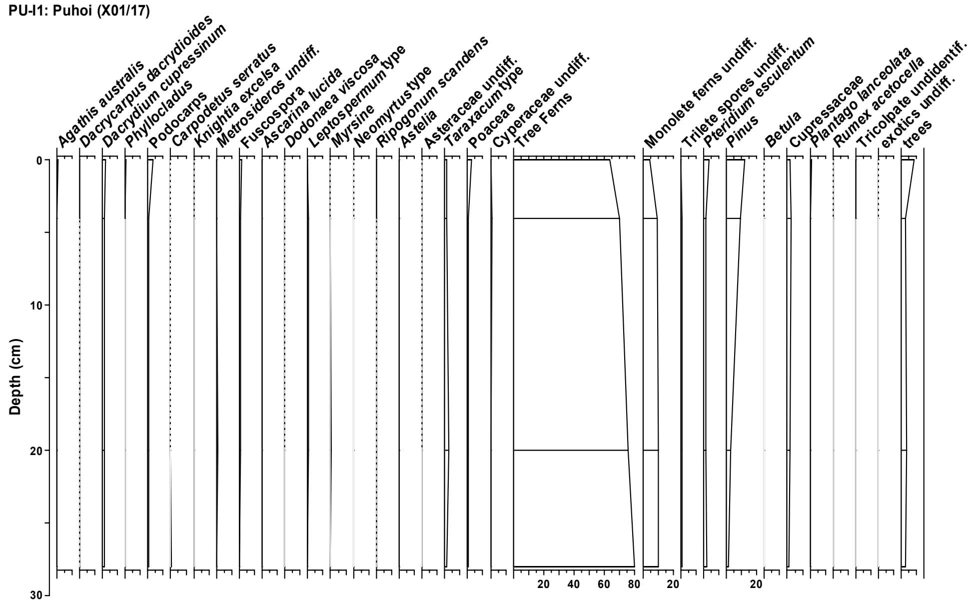

Core PU-I2

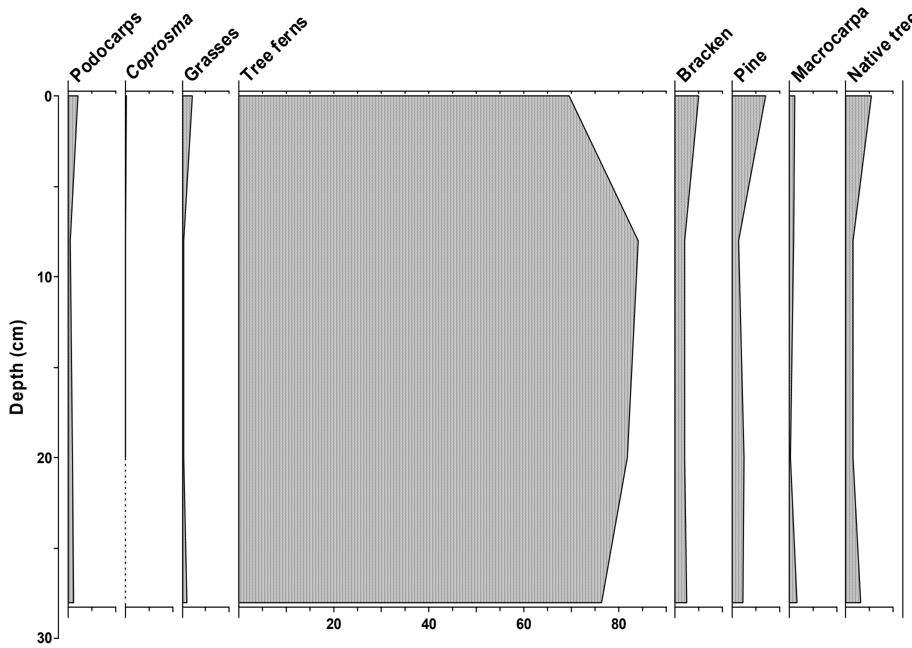
Podocarps
Coprosma
Grasses
Tree ferns
Bracken
Pine
Macrocarpa
Native trees
Depth (cm)
0
10
20
30
20
40
60
80

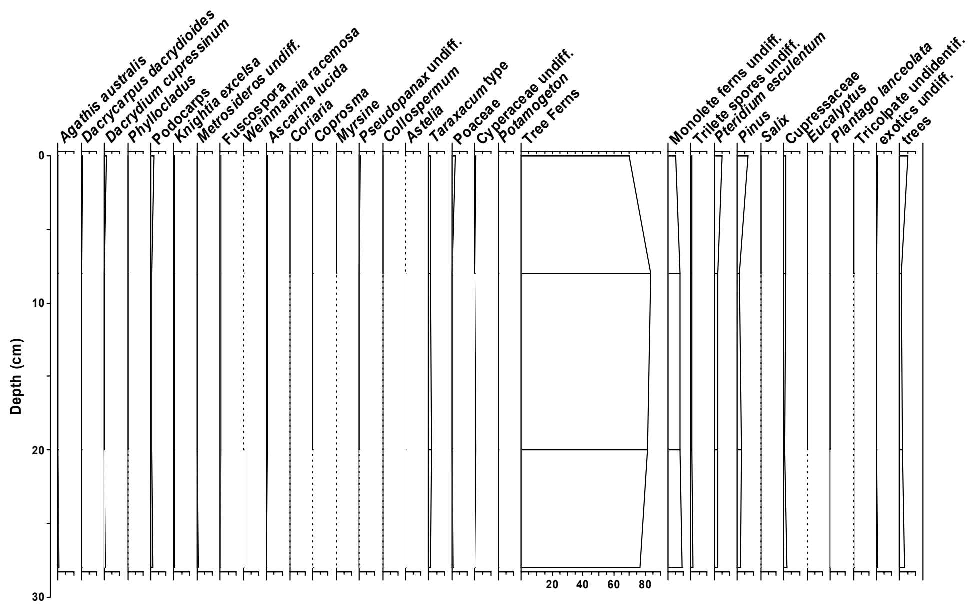
Agathis australis
Dacrycarpus dacrydioides
Dacrydium cupressinum
Phyllocladus
Podocarps
Knightia excelsa
Metrosideros undiff.
Fuscospora
Weinmannia racemosa
Ascarina lucida
Coriaria
Coprosma
Myrsine
Pseudopanax undiff.
Collospermum
Astelia
Taraxacum type
Poaceae
Cyperaceae undiff.
Potamogeton
Tree Ferns
Monolete ferns undiff.
Trilete spores undiff.
Pteridium esculentum
Pinus
Salix
Cupressaceae
Eucalyptus
Plantago lanceolata
Tricolpate undidentif.
exotics undiff.
trees
Depth (cm)
0
10
20
30
20
40
60
80

Core PU-I3

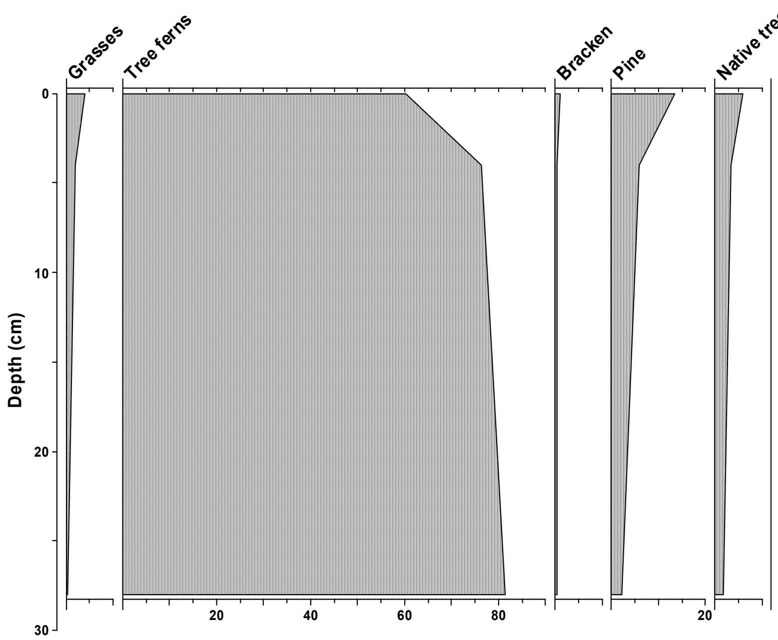
Grasses
Tree ferns
Bracken
Pine
Native trees
Depth (cm)
0
10
20
30
20
40
60
80
20

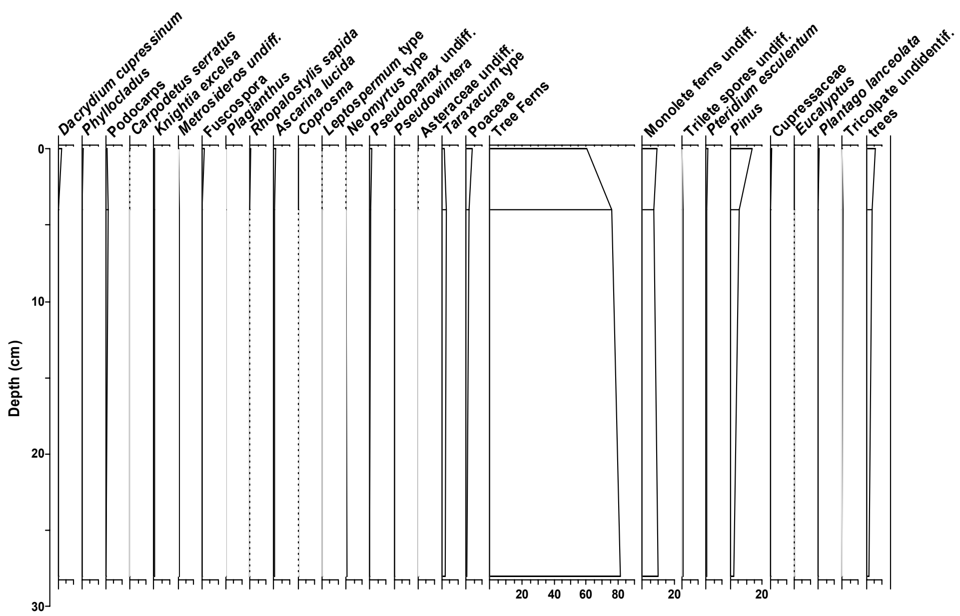
Dacrydium cupressinum
Phyllocladus
Podocarps
Carpodetus serratus
Knightia excelsa
Metrosideros undiff.
Fuscospora
Plagianthus
Rhopalostylis sapida
Ascarina lucida
Coprosma
Leptospermum type
Neomyrtus type
Pseudopanax undiff.
Pseudowintera
Asteraceae undiff.
Taraxacum type
Poaceae
Tree Ferns
Monolete ferns undiff.
Trilete spores undiff.
Pteridium esculentum
Pinus
Cupressaceae
Eucalyptus
Plantago lanceolata
Tricolpate unidentif.
trees
Depth (cm)
0
10
20
30
20
40
60
80
20
20

9.3 Okura Estuary

Core OK-I1

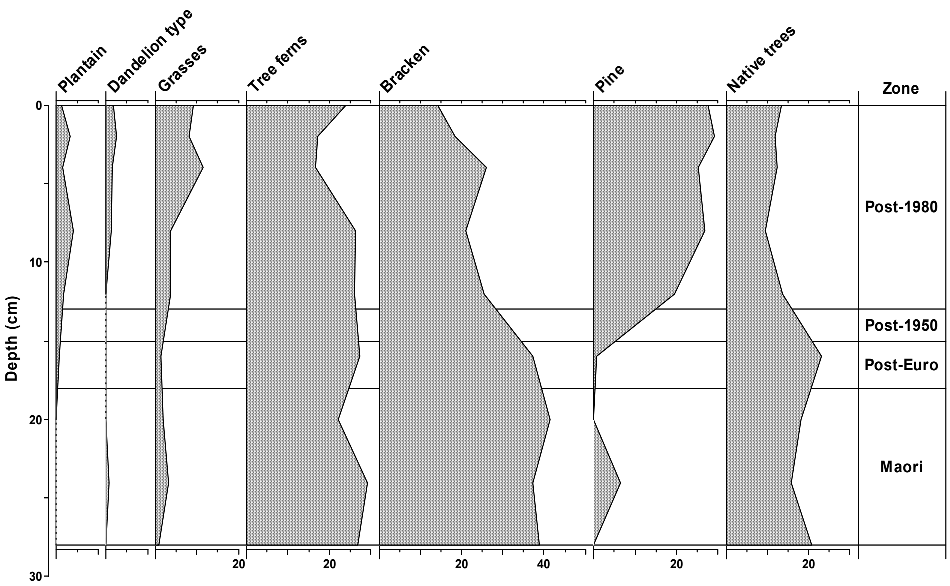

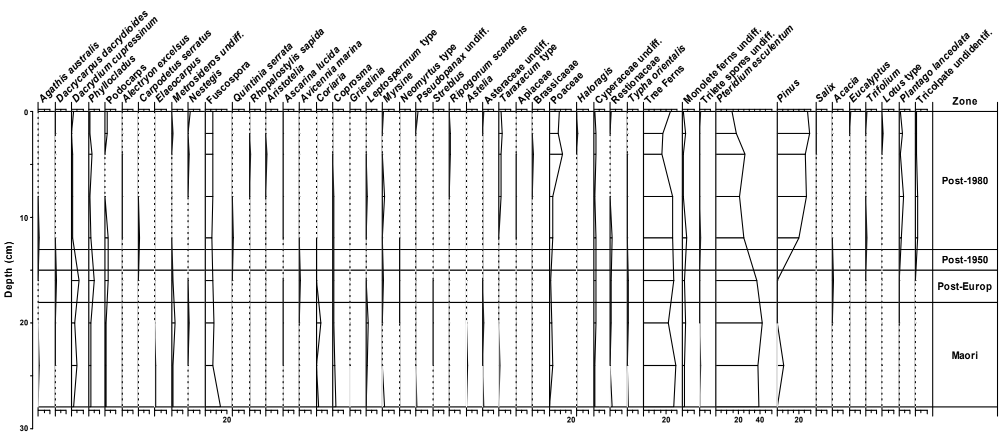

Core OK-I2

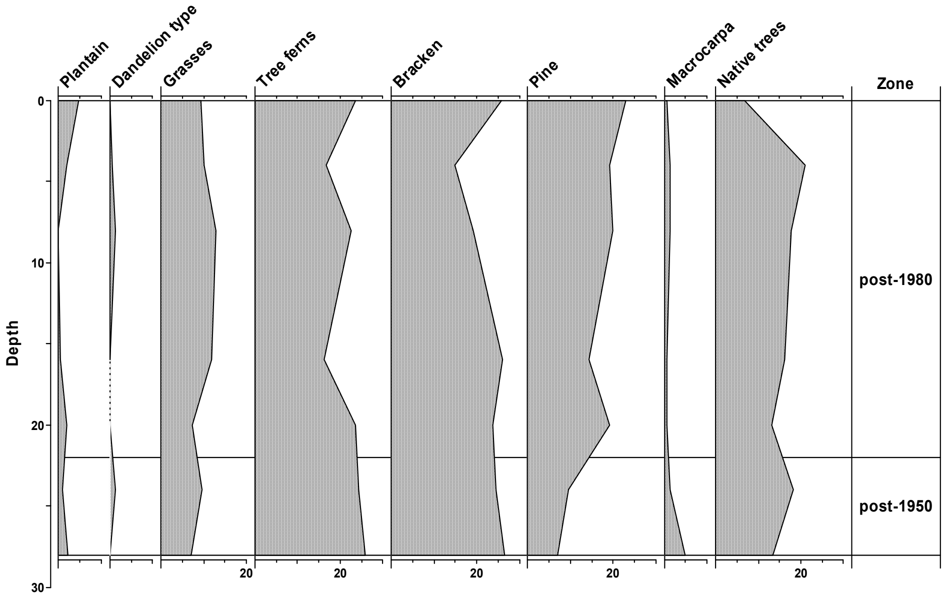

Plantain
Dandelion type
Grasses
Tree ferns
Bracken
Pine
Macrocarpa
Native trees
Zone
Depth
0
10
20
30
post-1980
post-1950
20
20
20
20
20

Core OK-I3

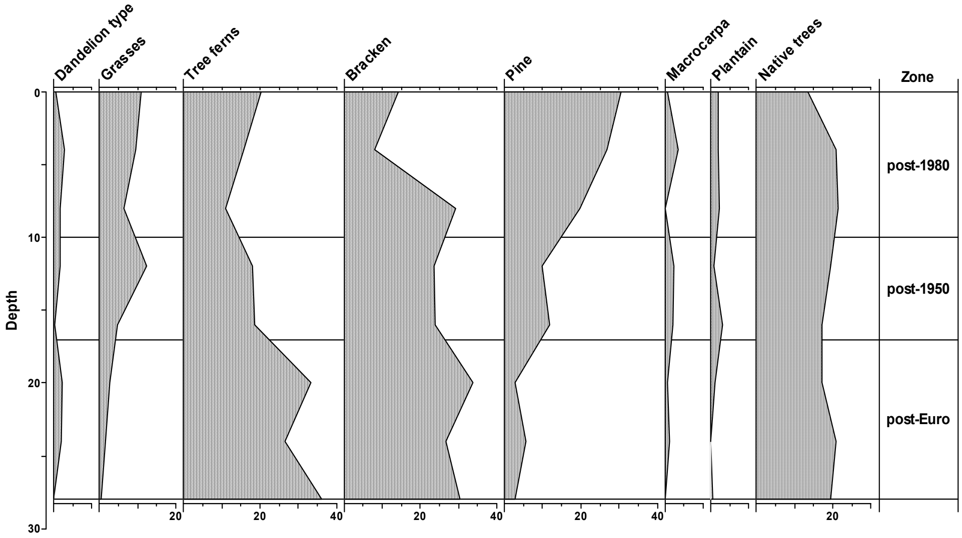
Dandelion type
Grasses
Tree ferns
Bracken
Pine
Macrocarpa
Plantain
Native trees
Zone
post-1980
post-1950
post-Euro
Depth
0
10
20
30
20
20
40
20
40
20
40
20

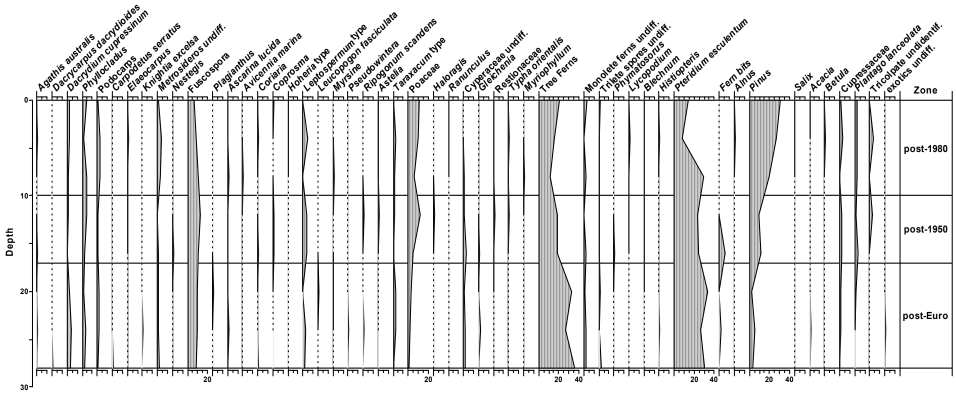
Agathis australis
Dacrycarpus dacrydioides
Dacrydium cupressinum
Phyllocladus
Podocarps
Carpodetus serratus
Elaeocarpus
Knightia excelsa
Metrosideros undiff.
Nestegis
Fuscospora
Plagianthus
Ascarina lucida
Avicennia marina
Coriaria
Coprosma
Hoheria type
Leptospermum type
Leucopogon fasciculata
Myrsine
Pseudowintera
Ripogonum scandens
Astelia
Taraxacum type
Poaceae
Haloragis
Ranunculus
Cyperaceae undiff.
Gleichenia
Restionaceae
Typha orientalis
Myriophyllum
Tree Ferns
Monolete ferns undiff.
Trilete spores undiff.
Phymatosorus
Lycopodium
Blechnum
Histiopteris
Pteridium esculentum
Fern bits
Alnus
Pinus
Salix
Acacia
Betula
Cupressaceae
Plantago lanceolata
Tricolpate unidentif.
exotics undiff.
Zone
post-1980
post-1950
post-Euro
Depth
0
10
20
30
20
20
20
40
20
40
20
40

9.4 Henderson Estuary

Core HN-I1

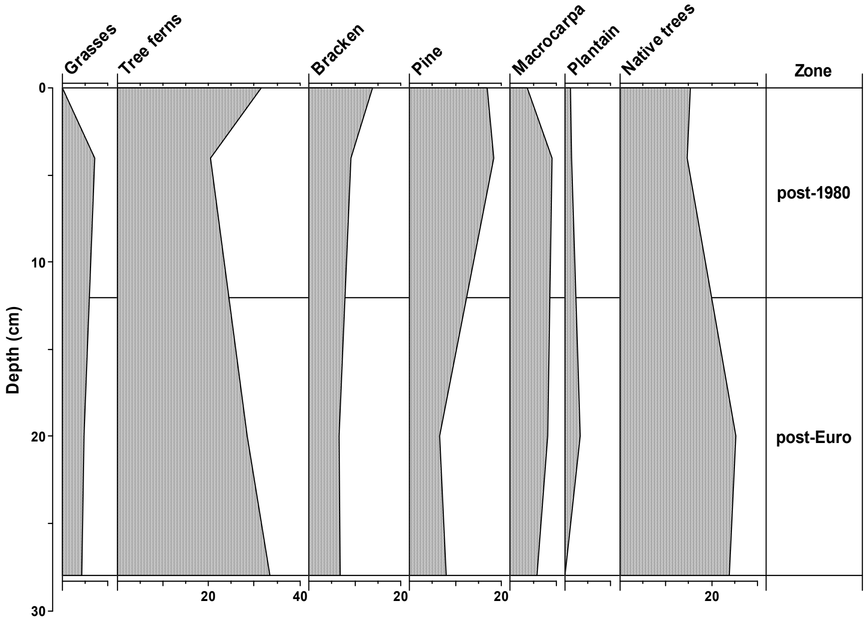

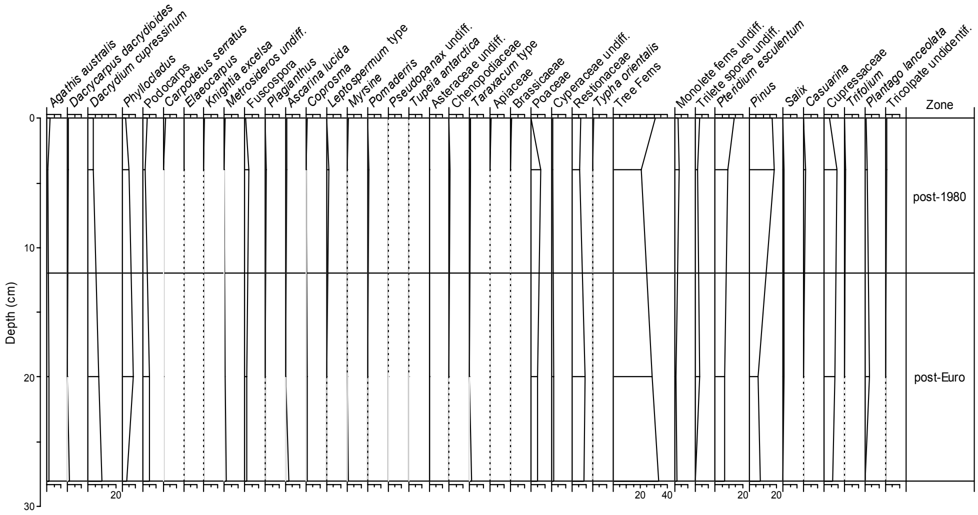

Core HN-I2

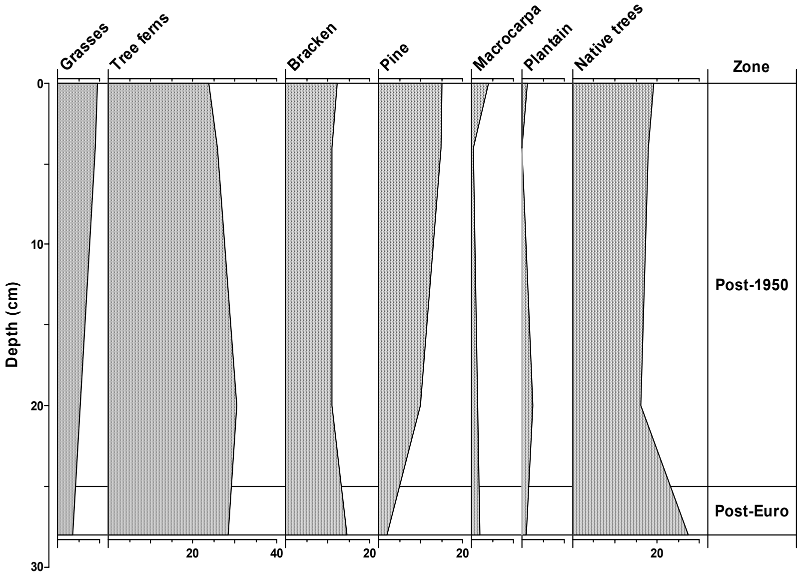
Grasses
Tree ferns
Bracken
Pine
Macrocarpa
Plantain
Native trees
Zone
Post-1950
Post-Euro
Depth (cm)
0
10
20
30
20
40
20
20
20

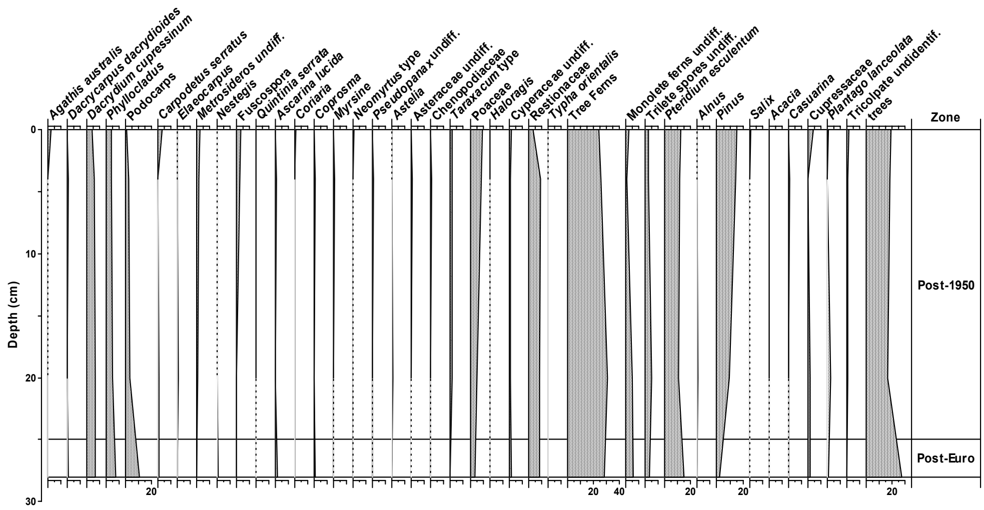
Agathis australis
Dacrycarpus dacrydioides
Dacrydium cupressinum
Phyllocladus
Podocarps
Carpodetus serratus
Elaeocarpus
Metrosideros undiff.
Nestegis
Fuscospora
Quintinia serrata
Ascarina lucida
Coriaria
Coprosma
Myrsine
Neomyrtus type
Pseudopanax undiff.
Astelia
Asteraceae undiff.
Chenopodiaceae
Taraxacum type
Poaceae
Haloragis
Cyperaceae undiff.
Restionaceae
Typha orientalis
Tree Ferns
Monolete ferns undiff.
Trilete spores undiff.
Pteridium esculentum
Alnus
Pinus
Salix
Acacia
Casuarina
Cupressaceae
Plantago lanceolata
Tricolpate undidentif. trees
Zone
Post-1950
Post-Euro
Depth (cm)
0
10
20
30
20
20
40
20
20
20

Core HN-I3

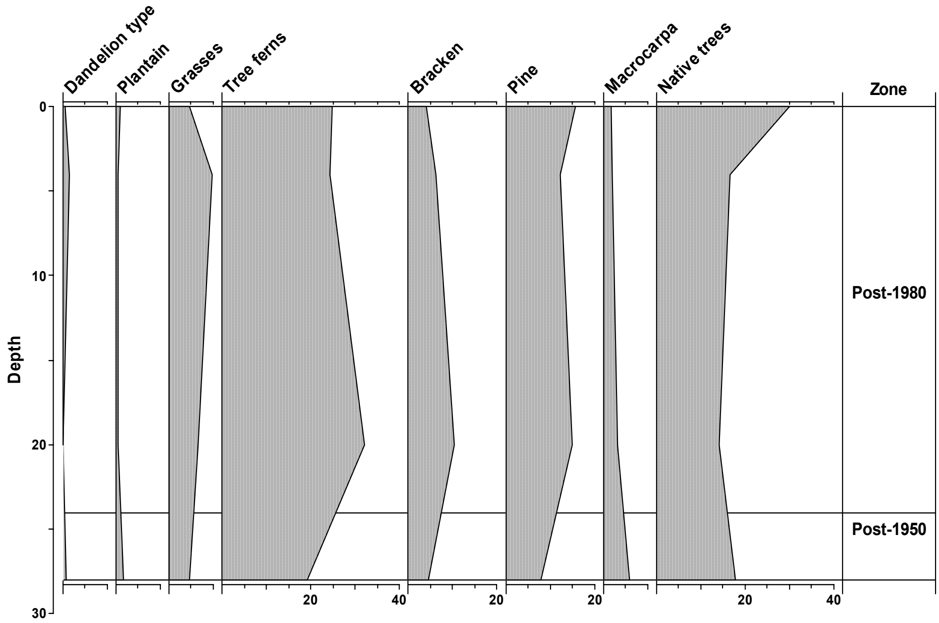
Dandelion type
Plantain
Grasses
Tree ferns
Bracken
Pine
Macrocarpa
Native trees
Zone
Depth
0
10
20
30
20
40
Post-1980
Post-1950

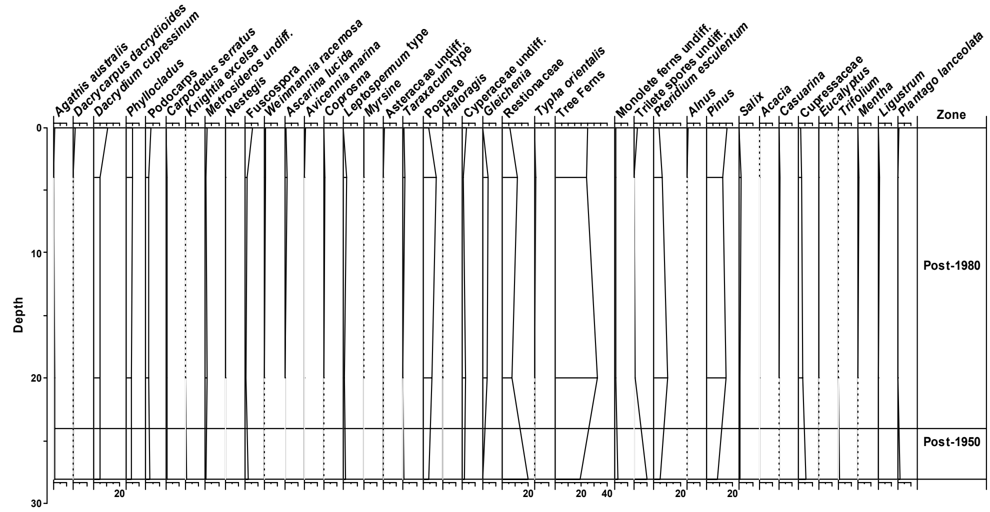
Agathis australis
Dacrycarpus dacrydioides
Dacrydium cupressinum
Phyllocladus
Podocarps
Carpodetus serratus
Knightia excelsa
Metrosideros undiff.
Nestegis
Fuscospora
Weinmannia racemosa
Ascarina lucida
Avicennia marina
Coprosma
Leptospermum type
Myrsine
Asteraceae undiff.
Taraxacum type
Poaceae
Haloragis
Cyperaceae undiff.
Gleichenia
Restionaceae
Typha orientalis
Tree Ferns
Monolete ferns undiff.
Trilete spores undiff.
Pteridium esculentum
Alnus
Pinus
Salix
Acacia
Casuarina
Cupressaceae
Eucalyptus
Trifolium
Mentha
Ligustrum
Plantago lanceolata
Zone
Depth
Post-1980
Post-1950

9.5 Waitemata (Te Atutu Subtidal)

Core WT-S1

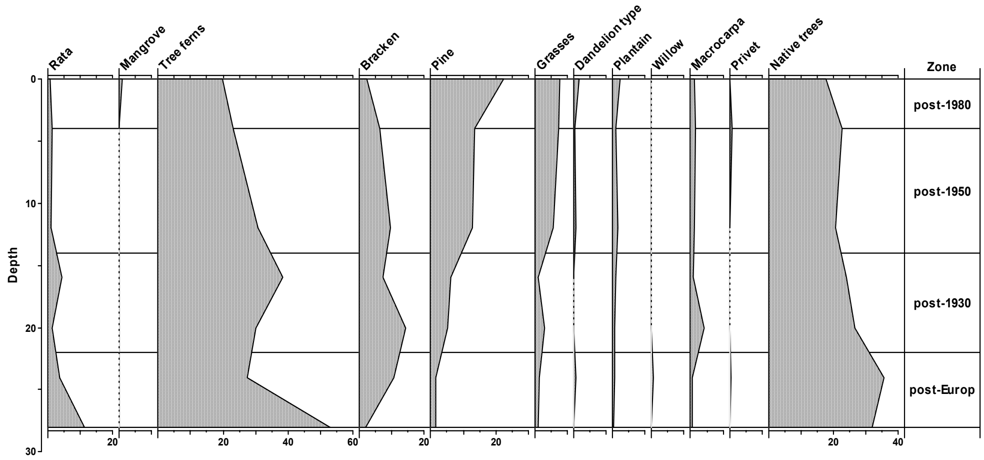

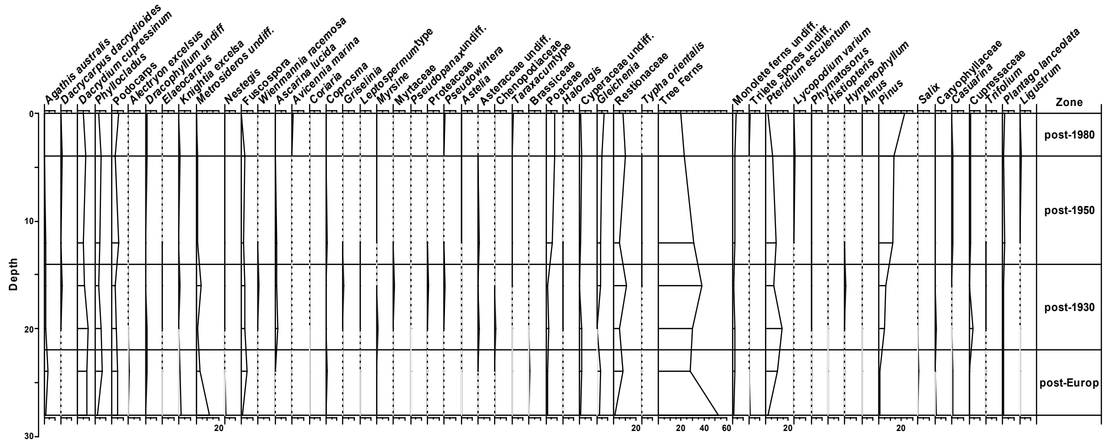

Core WT-S2

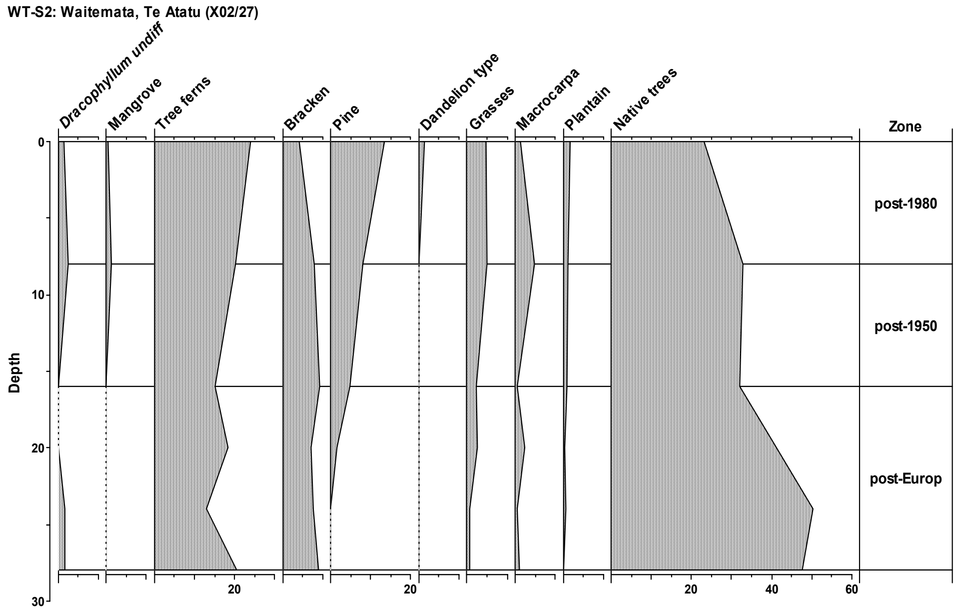

WT-S2: Waitemata, Te Atatu (X02/27)
Dracophyllum undiff
Mangrove
Tree ferns
Bracken
Pine
Dandelion type
Grasses
Macrocarpa
Plantain
Native trees
Zone
post-1980
post-1950
post-Europ
Depth

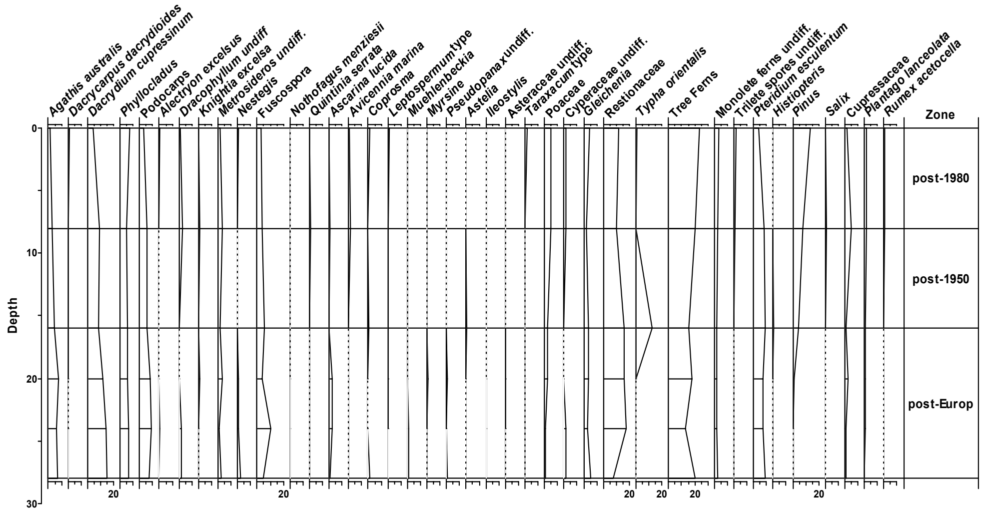

Agathis australis
Dacrycarpus dacrydioides
Dacrydium cupressinum
Phyllocladus
Podocarps
Alectryon excelsus
Dracophyllum undiff
Knightia excelsa
Metrosideros undiff.
Nestegis
Fuscospora
Nothofagus menziesii
Quintinia serrata
Ascarina lucida
Avicennia marina
Coprosma
Leptospermum type
Muehlenbeckia
Myrsine
Pseudopanax undiff.
Astelia
Ileostylis
Asteraceae undiff.
Taraxacum type
Poaceae
Cyperaceae undiff.
Gleichenia
Restionaceae
Typha orientalis
Tree Ferns
Monolete ferns undiff.
Trilete spores undiff.
Pteridium esculentum
Histiopteris
Pinus
Salix
Cupressaceae
Plantago lanceolata
Rumex acetocella
Zone
post-1980
post-1950
post-Europ
Depth

Core WT-S3

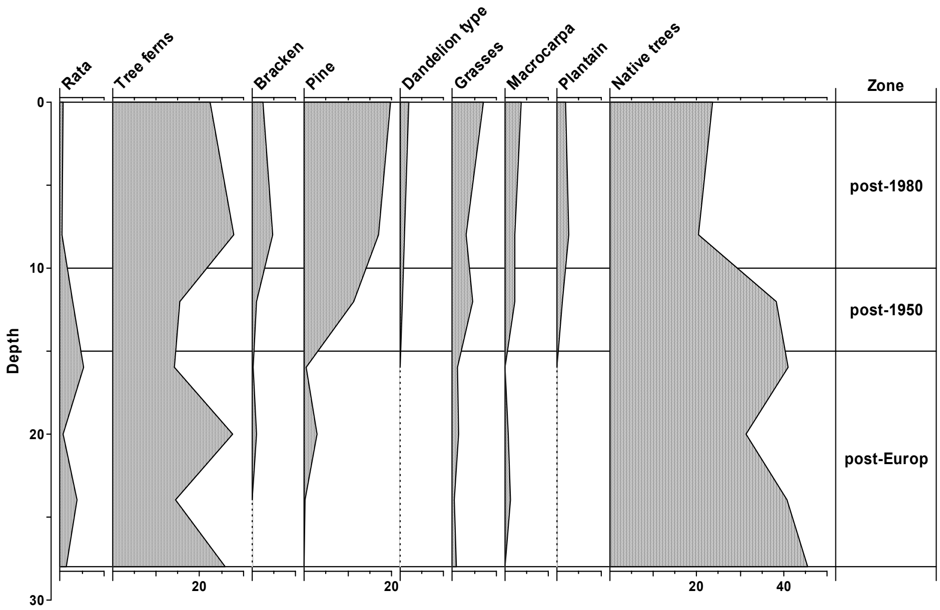

Rata
Tree ferns
Bracken
Pine
Dandelion type
Grasses
Macrocarpa
Plantain
Native trees
Zone
post-1980
post-1950
post-Europ
Depth
0
10
20
30
20
20
20
40

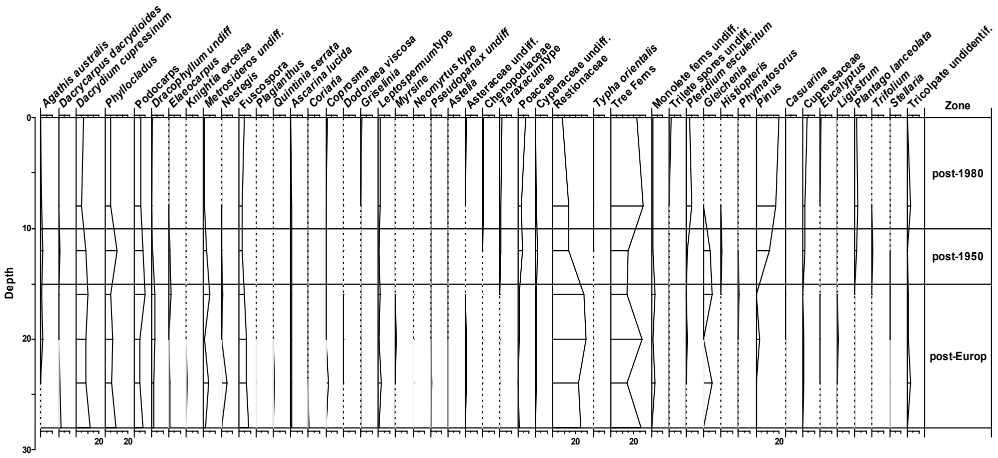

Agathis australis
Dacrycarpus dacrydioides
Dacrydium cupressinum
Phyllocladus
Podocarps
Dracophyllum undiff
Elaeocarpus
Knightia excelsa
Metrosideros undiff.
Nestegis
Fuscospora
Plagianthus
Quintinia serrata
Ascarina lucida
Coriaria
Coprosma
Dodonaea viscosa
Griselinia
Leptospermumtype
Myrsine
Neomyrtus type
Pseudopanax undiff
Astelia
Asteraceae undiff.
Chenopodiaceae
Taraxacumtype
Poaceae
Cyperaceae undiff.
Restionaceae
Typha orientalis
Tree Ferns
Monolete ferns undiff.
Trilete spores undiff.
Pteridium esculentum
Gleichenia
Histiopteris
Phymatosorus
Pinus
Casuarina
Cupressaceae
Eucalyptus
Ligustrum
Plantago lanceolata
Trifolium
Stellaria
Tricolpate undidentif.
Zone
post-1980
post-1950
post-Europ
Depth
0
10
20
30
20
20
20
20
20

9.6 Whitford Embayment (Sub-tidal)

Core WH-S1

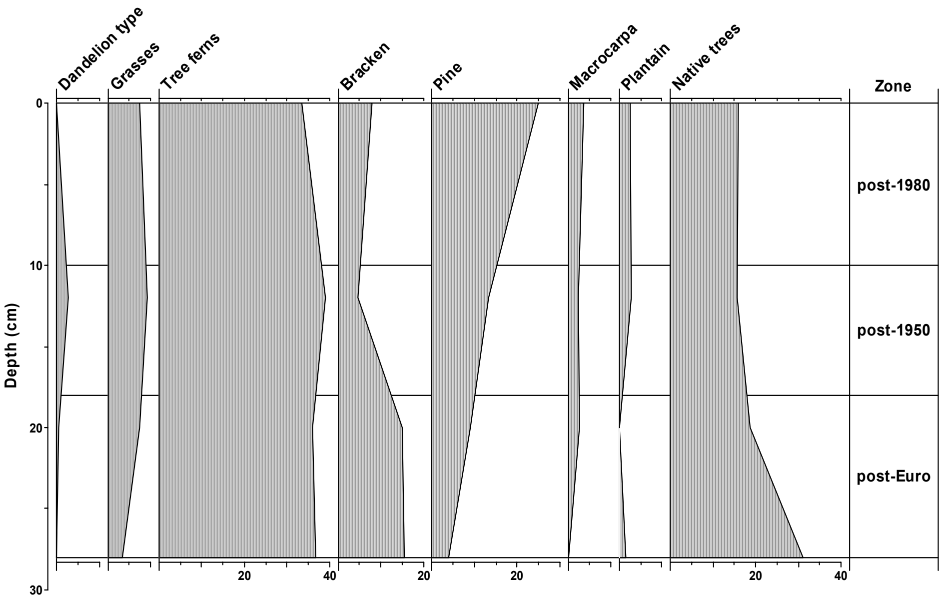

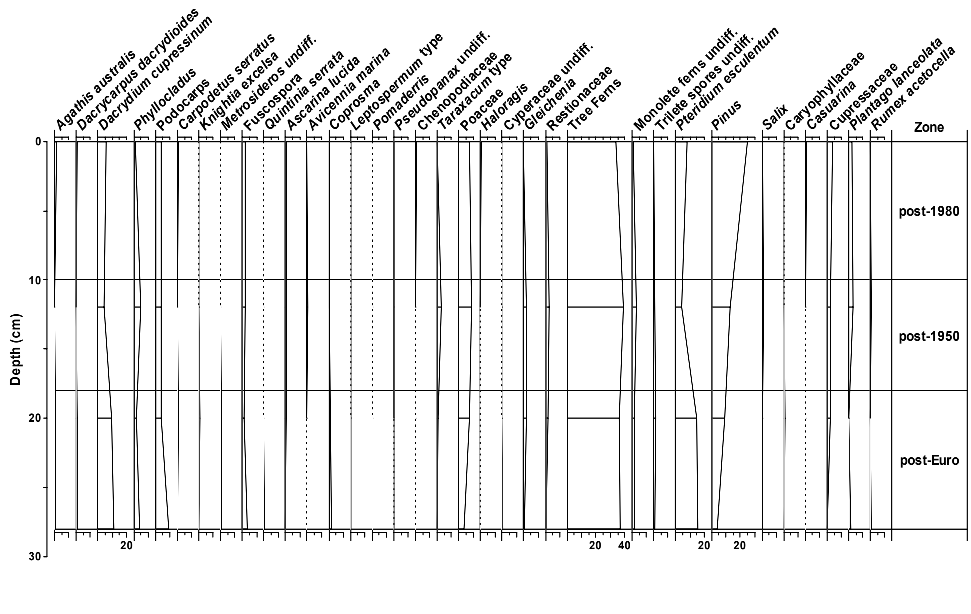

Core WH-S2

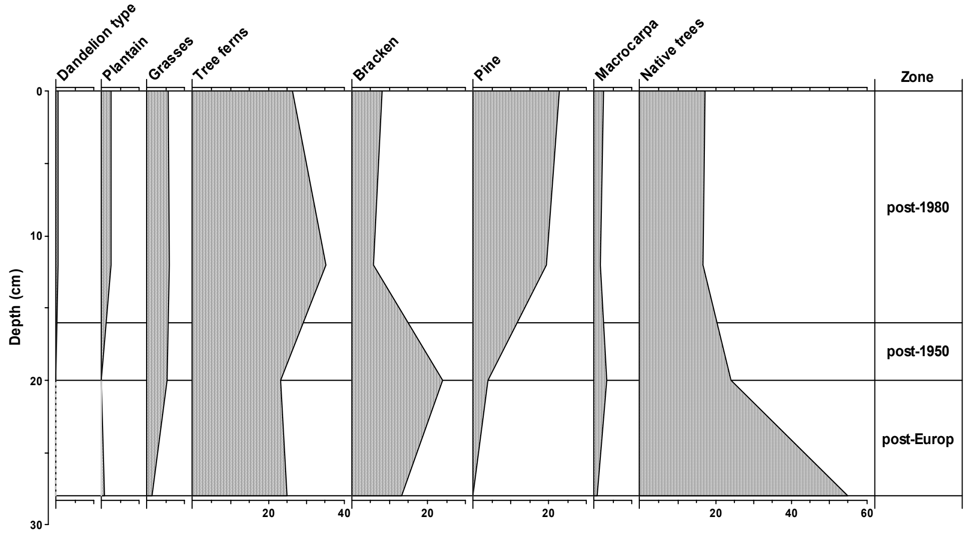

Dandelion type
Plantain
Grasses
Tree ferns
Bracken
Pine
Macrocarpa
Native trees
Zone
Depth (cm)
post-1980
post-1950
post-Europ

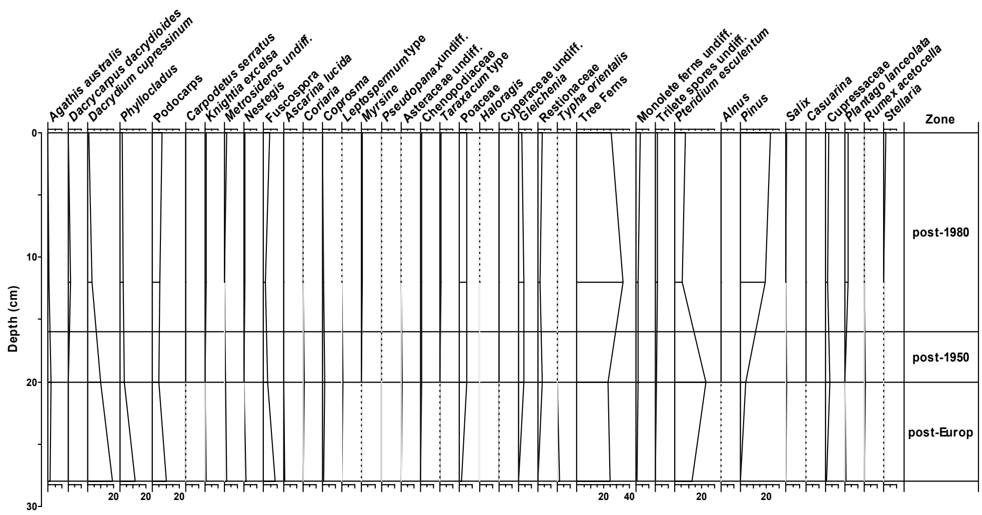

Agathis australis
Dacrycarpus dacrydioides
Dacrydium cupressinum
Phyllocladus
Podocarps
Carpodetus serratus
Knightia excelsa
Metrosideros undiff.
Nestegis
Fuscospora
Ascarina lucida
Coriaria
Coprosma
Leptospermum type
Myrsine
Pseudopanax undiff.
Asteraceae undiff.
Chenopodiaceae
Taraxacum type
Poaceae
Haloragis
Cyperaceae undiff.
Gleichenia
Restionaceae
Typha orientalis
Tree Ferns
Monolete ferns undiff.
Trilete spores undiff.
Pteridium esculentum
Alnus
Pinus
Salix
Casuarina
Cupressaceae
Plantago lanceolata
Rumex acetocella
Stellaria
Zone
Depth (cm)
post-1980
post-1950
post-Europ

Core WH-S3

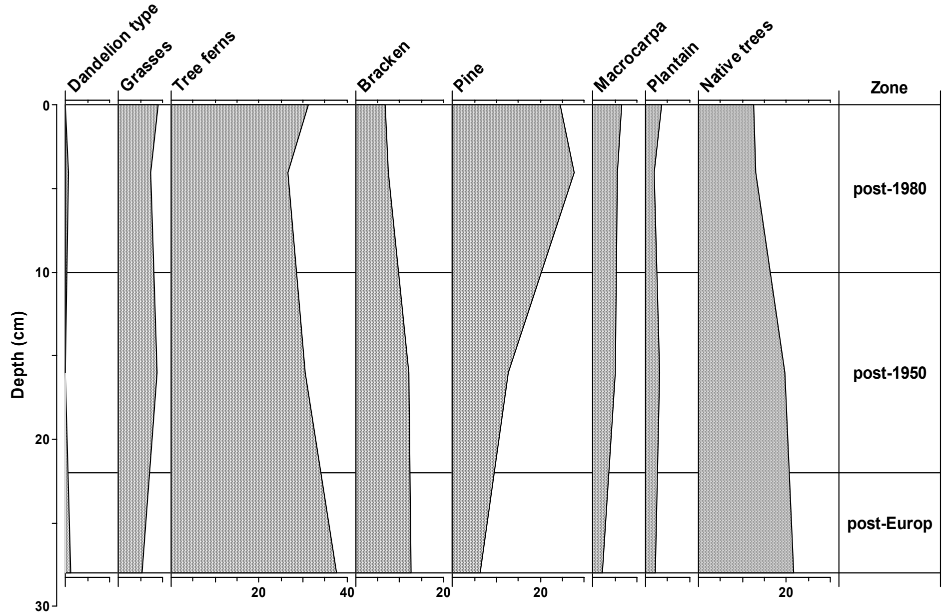

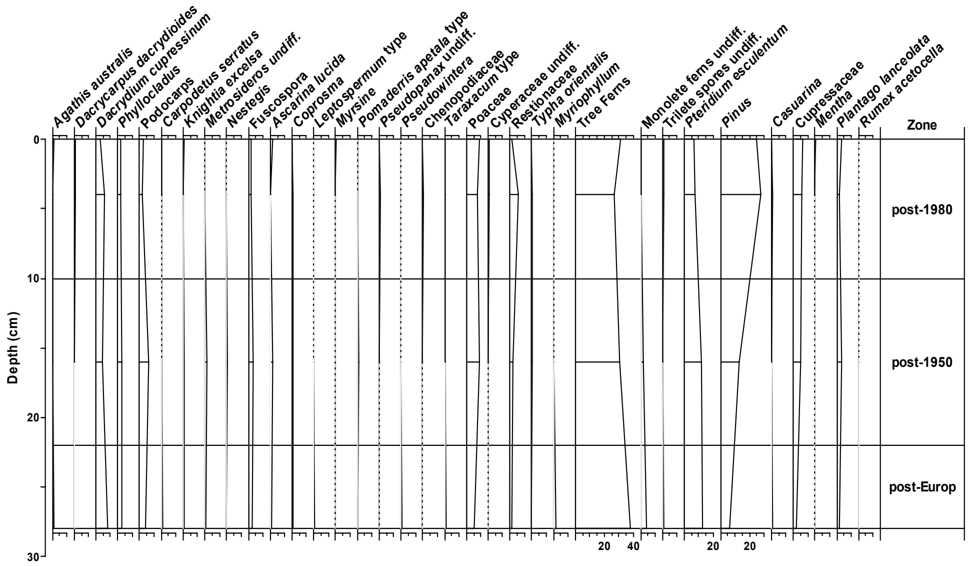

9.7 Wairoa Estuary

Intertidal Flats

Core WI-I1

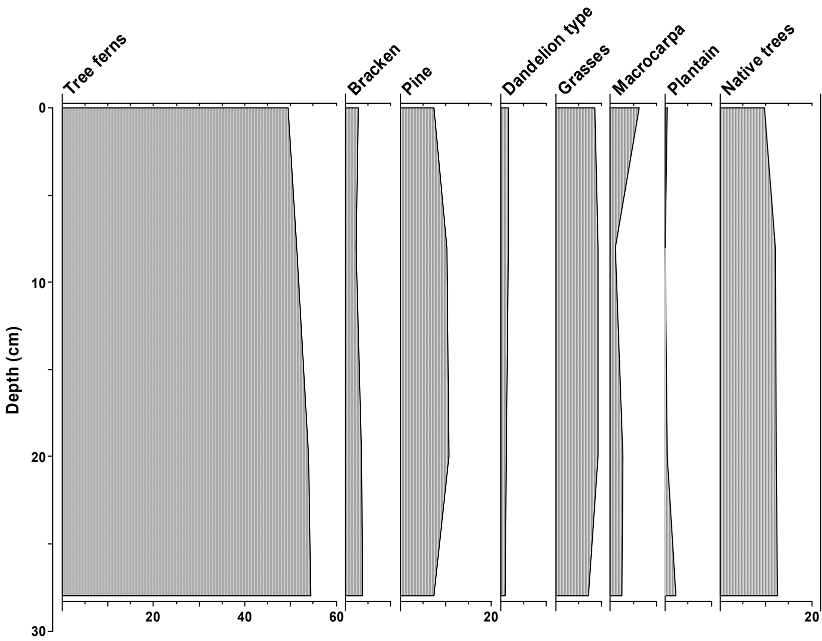

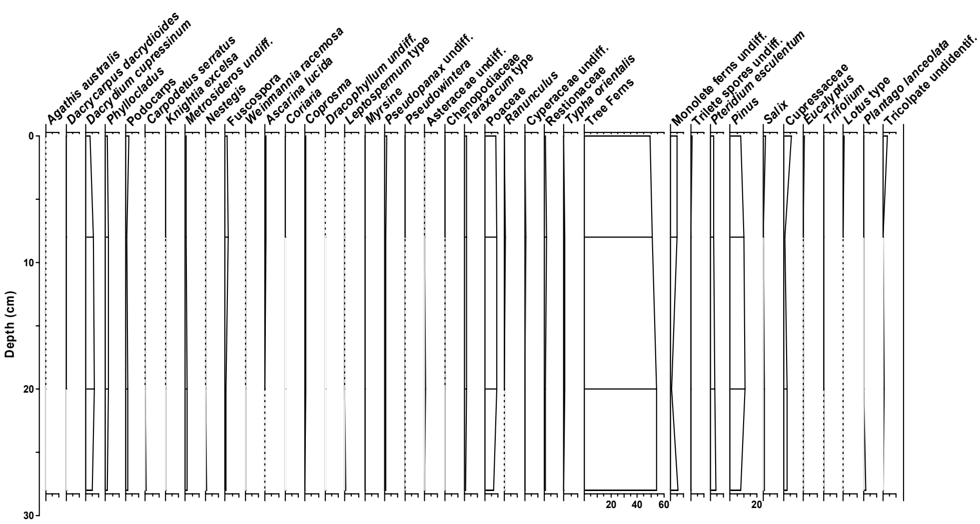

Core WI-I2

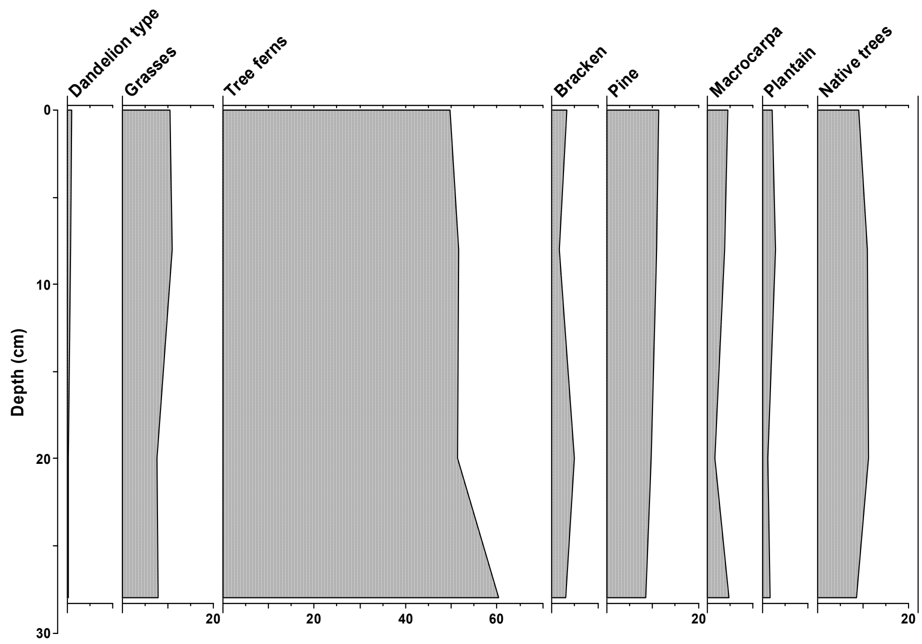
Dandelion type
Grasses
Tree ferns
Bracken
Pine
Macrocarpa
Plantain
Native trees
Depth (cm)

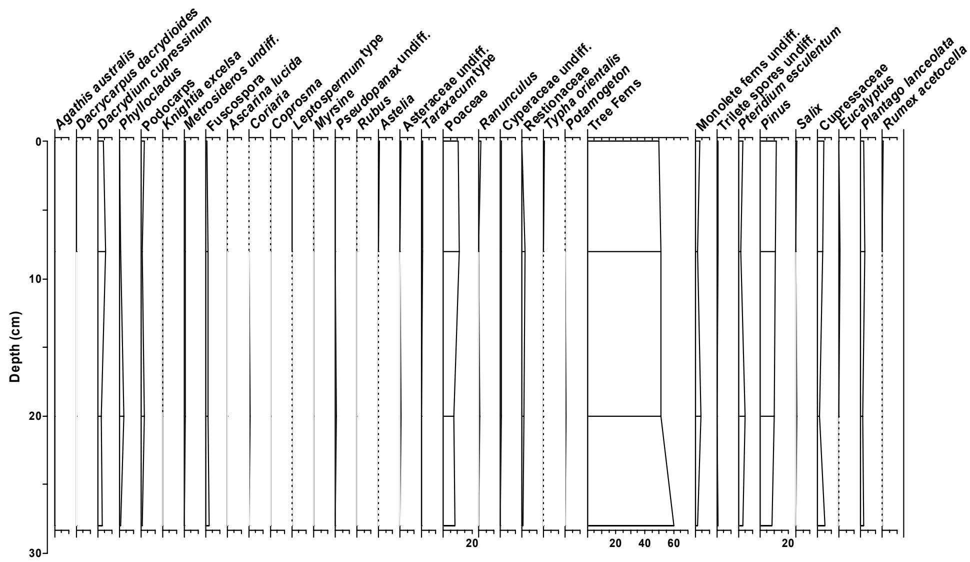
Agathis australis
Dacrycarpus dacrydioides
Dacrydium cupressinum
Phyllocladus
Podocarps
Knightia excelsa
Metrosideros undiff.
Fuscospora
Ascarina lucida
Coriaria
Coprosma
Leptospermum type
Myrsine
Pseudopanax undiff.
Rubus
Astelia
Asteraceae undiff.
Taraxacum type
Poaceae
Ranunculus
Cyperaceae undiff.
Restionaceae
Typha orientalis
Potamogeton
Tree Ferns
Monolete ferns undiff.
Trilete spores undiff.
Pteridium esculentum
Pinus
Salix
Cupressaceae
Eucalyptus
Plantago lanceolata
Rumex acetocella
Depth (cm)

Core WI-I3

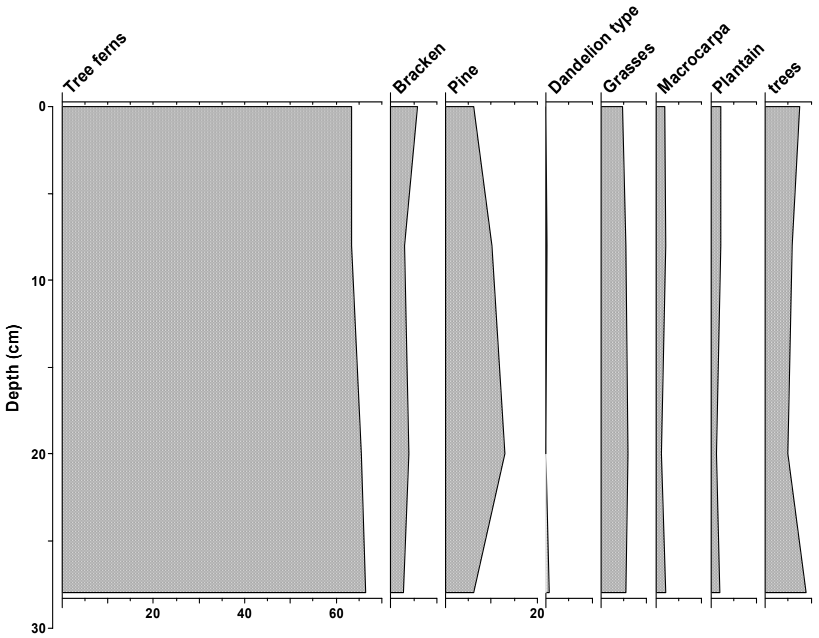
Tree ferns
Bracken
Pine
Dandelion type
Grasses
Macrocarpa
Plantain
trees
Depth (cm)
0
10
20
30
20
40
60
20

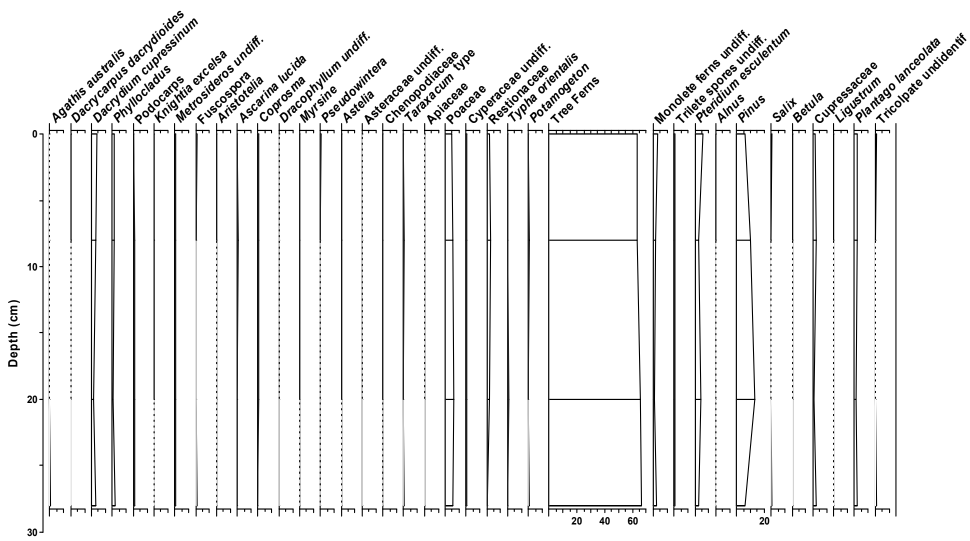
Agathis australis
Dacrycarpus dacrydioides
Dacrydium cupressinum
Phyllocladus
Podocarps
Knightia excelsa
Metrosideros undiff.
Fuscospora
Aristotelia
Ascarina lucida
Coprosma
Dracophyllum undiff.
Myrsine
Pseudowintera
Astelia
Asteraceae undiff.
Chenopodiaceae
Taraxacum type
Apiaceae
Poaceae
Cyperaceae undiff.
Restionaceae
Typha orientalis
Potamogeton
Tree Ferns
Monolete ferns undiff.
Trilete spores undiff.
Pteridium esculentum
Alnus
Pinus
Salix
Betula
Cupressaceae
Ligustrum
Plantago lanceolata
Tricolpate unidentif
Depth (cm)
0
10
20
30
20
40
60
20

Sub-tidal Flats

Core WA-S1

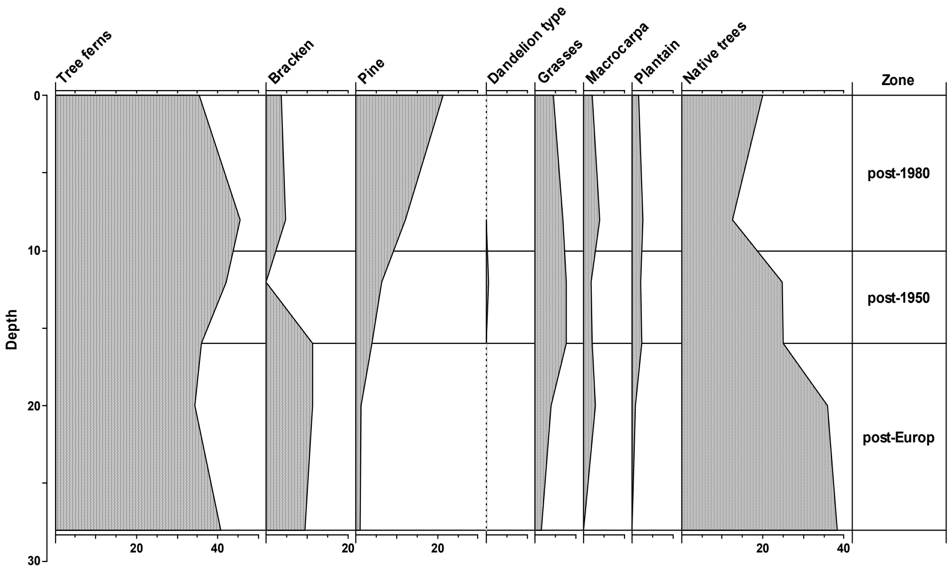

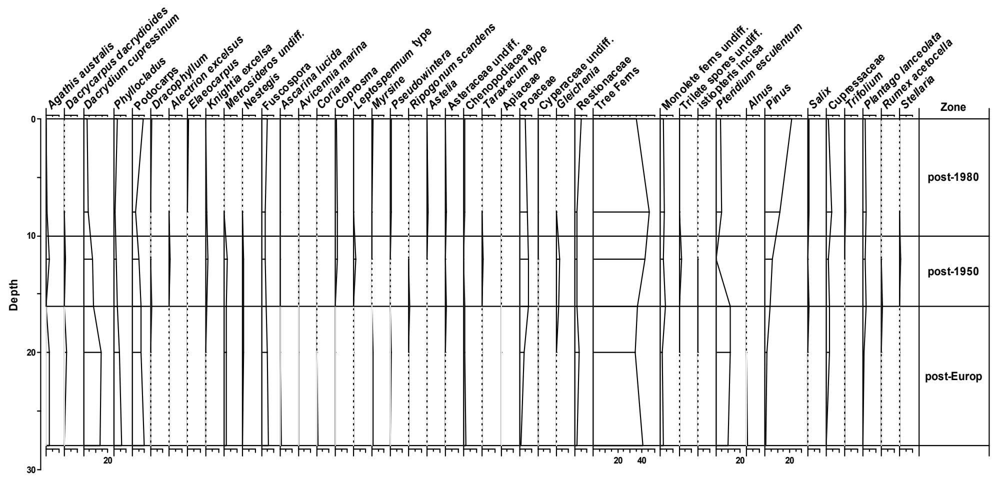

Core WA-S2

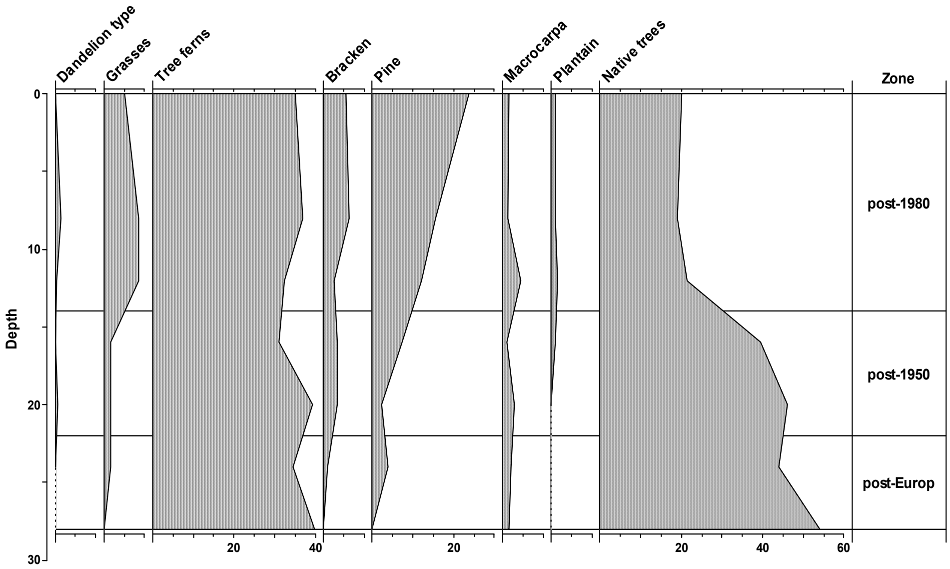
Dandelion type
Grasses
Tree ferns
Bracken
Pine
Macrocarpa
Plantain
Native trees
Zone
0
10
20
30
Depth
20
40
20
20
40
60
post-1980
post-1950
post-Europ

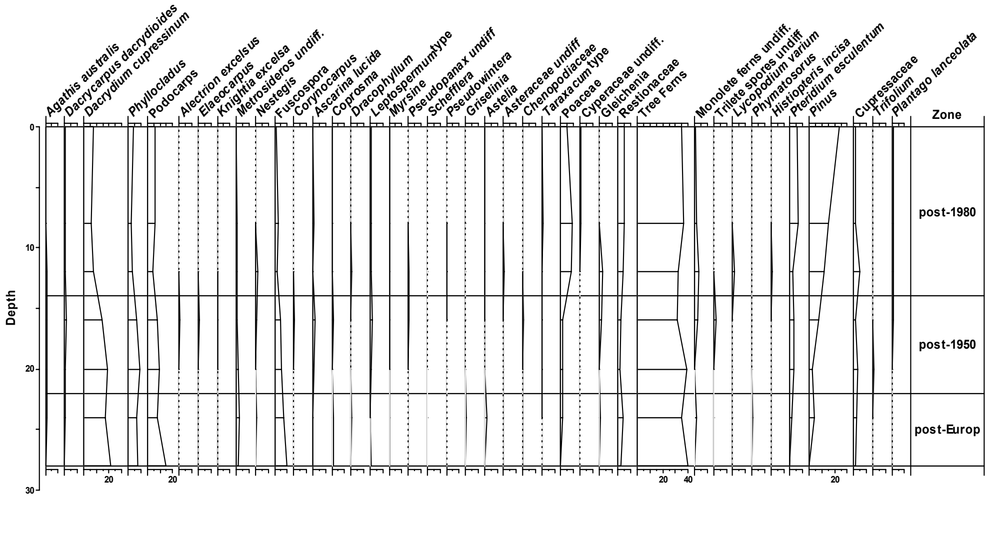
Agathis australis
Dacrycarpus dacrydioides
Dacrydium cupressinum
Phyllocladus
Podocarps
Alectrion excelsus
Elaeocarpus
Knightia excelsa
Metrosideros undiff.
Nestegis
Fuscospora
Corynocarpus
Ascarina lucida
Coprosma
Dracophyllum
Leptospermum type
Myrsine
Pseudopanax undiff
Schefflera
Pseudowintera
Griselinia
Astelia
Asteraceae undiff
Chenopodiaceae
Taraxacum type
Poaceae
Cyperaceae undiff.
Gleichenia
Restionaceae
Tree Ferns
Monolete ferns undiff.
Trilete spores undiff
Lycopodium varium
Phymatosorus
Histiopteris incisa
Pteridium esculentum
Pinus
Cupressaceae
Trifolium
Plantago lanceolata
Zone
0
10
20
30
Depth
20
20
20
40
20
post-1980
post-1950
post-Europ

Core WA-S3

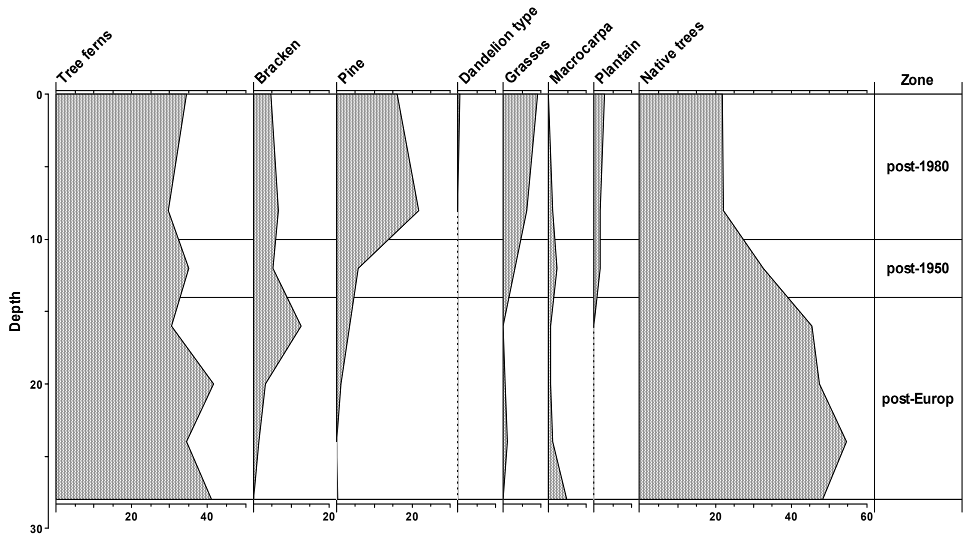

Tree ferns
Bracken
Pine
Dandelion type
Grasses
Macrocarpa
Plantain
Native trees
Zone
post-1980
post-1950
post-Europ
Depth
0
10
20
30
20
40
20
20
20
40
60

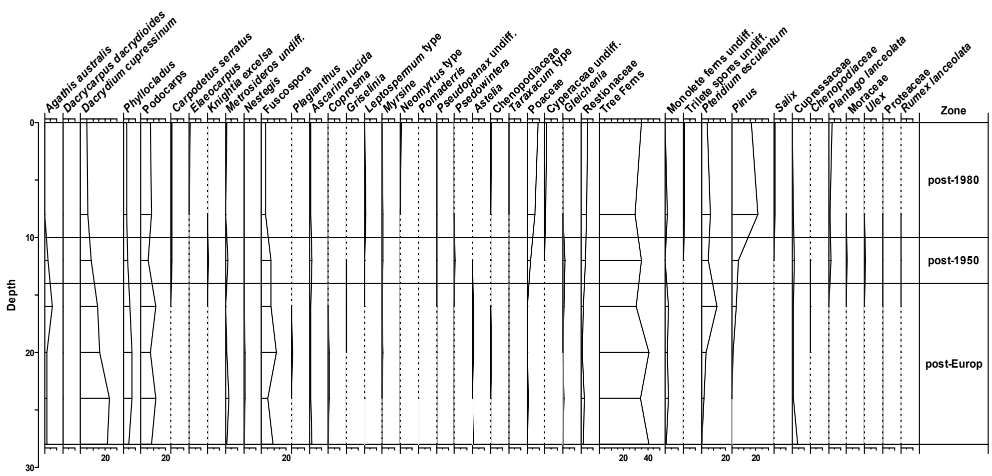

Agathis australis
Dacrycarpus dacrydioides
Dacrydium cupressinum
Phyllocladus
Podocarps
Carpodetus serratus
Elaeocarpus
Knightia excelsa
Metrosideros undiff.
Nestegis
Fuscospora
Plagianthus
Ascarina lucida
Coprosma
Griselinia
Leptospermum type
Myrsine
Neomyrtus type
Pomaderris
Pseudopanax undiff.
Psedowintera
Astelia
Chenopodiaceae
Taraxacum type
Poaceae
Cyperaceae undiff.
Gleichenia
Restionaceae
Tree Ferns
Monolete ferns undiff.
Trilete spores undiff.
Pteridium esculentum
Pinus
Salix
Cupressaceae
Chenopodiaceae
Plantago lanceolata
Moraceae
Ulex
Proteaceae
Rumex lanceolata
Zone
post-1980
post-1950
post-Europ
Depth
0
10
20
30
20
20
20
20
40
20
20

9.8 Te Matuku Bay (Waiheke Island)

Core TM-I1

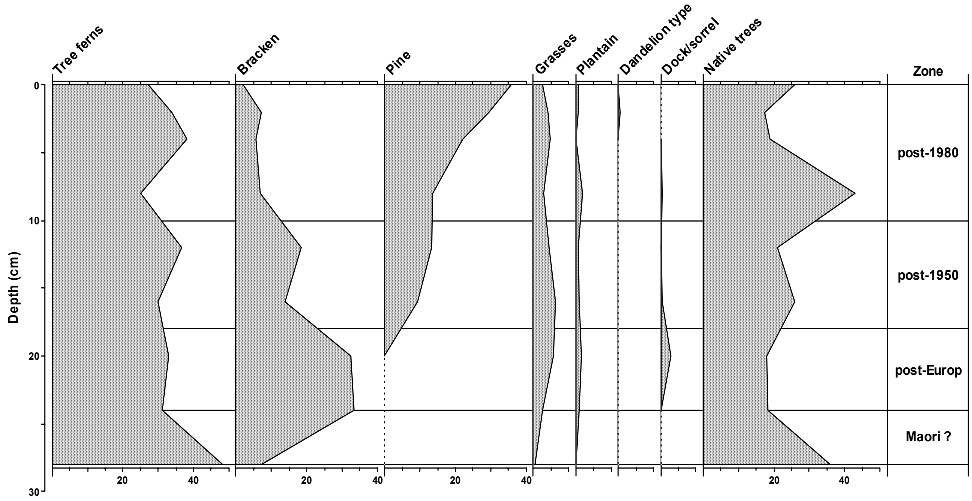

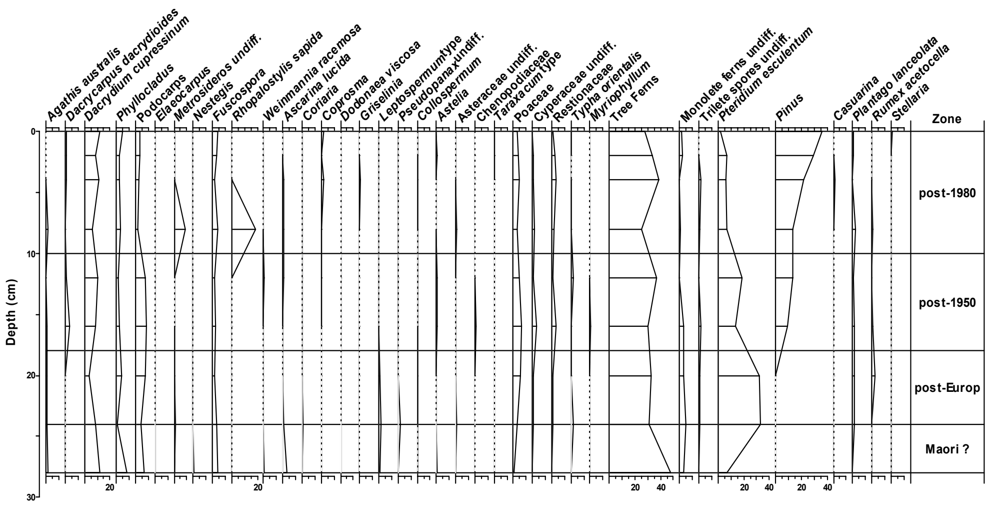

Core TM-I2

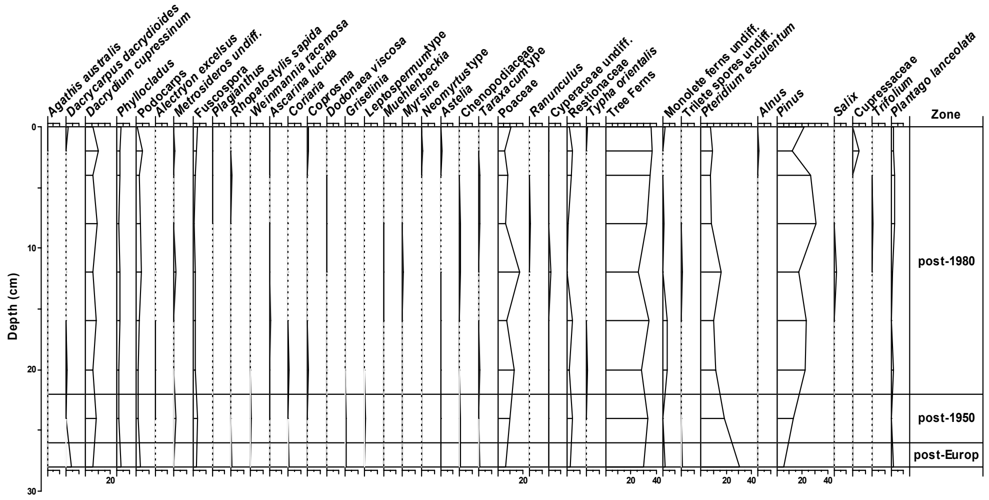

Core TM-I3

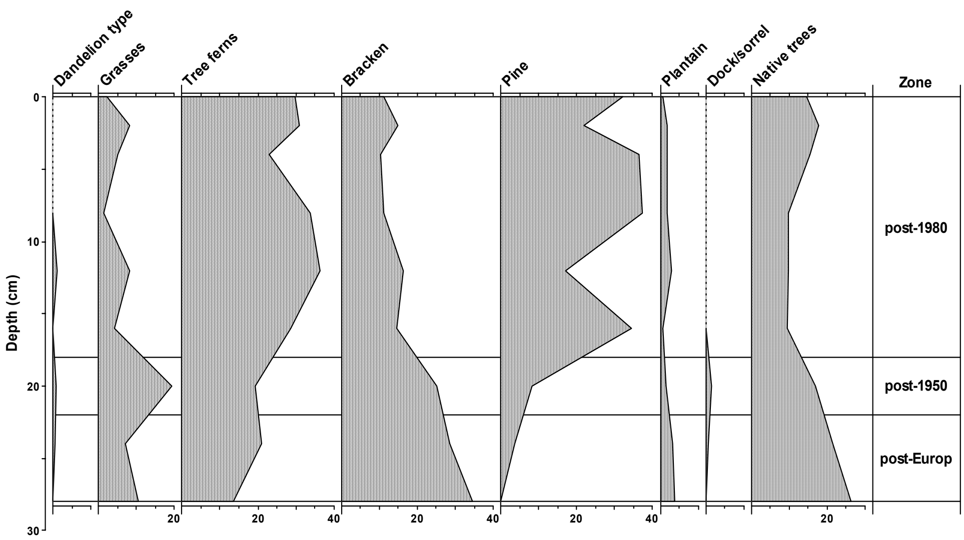

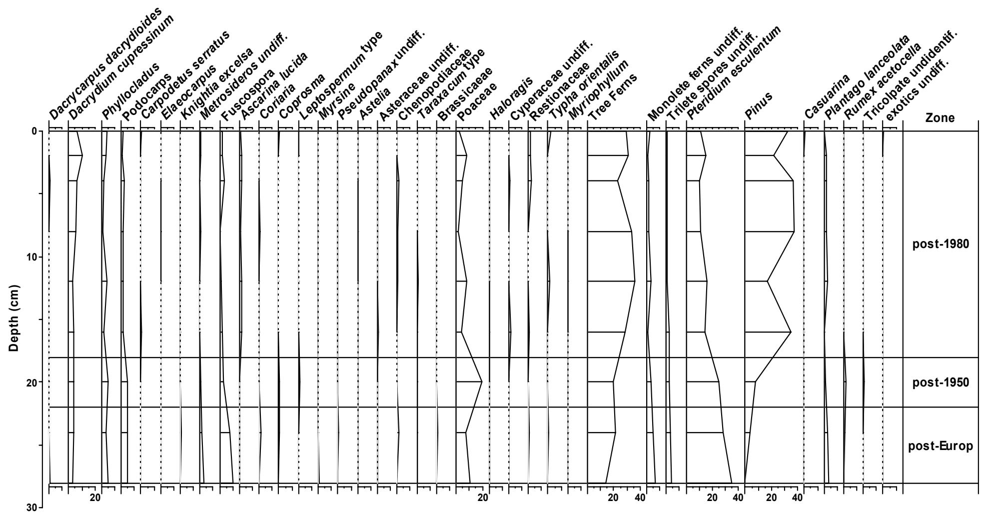
Dacrycarpus dacrydioides
Dacrydium cupressinum
Phyllocladus
Podocarps
Carpodetus serratus
Elaeocarpus
Knightia excelsa
Metrosideros undiff.
Fuscospora
Ascarina lucida
Coriaria
Coprosma
Leptospermum type
Myrsine
Pseudopanax undiff.
Astelia
Asteraceae undiff.
Chenopodiaceae
Taraxacum type
Brassicaceae
Poaceae
Haloragis
Cyperaceae undiff.
Restionaceae
Typha orientalis
Myriophyllum
Tree Ferns
Monolete ferns undiff.
Trilete spores undiff.
Pteridium esculentum
Pinus
Casuarina
Plantago lanceolata
Rumex acetocella
Tricolpate undidentif.
exotics undiff.
Zone
post-1980
post-1950
post-Europ
Depth (cm)

10. Appendix III: Estuary sediment cores: ^{226}Ra Concentration profiles

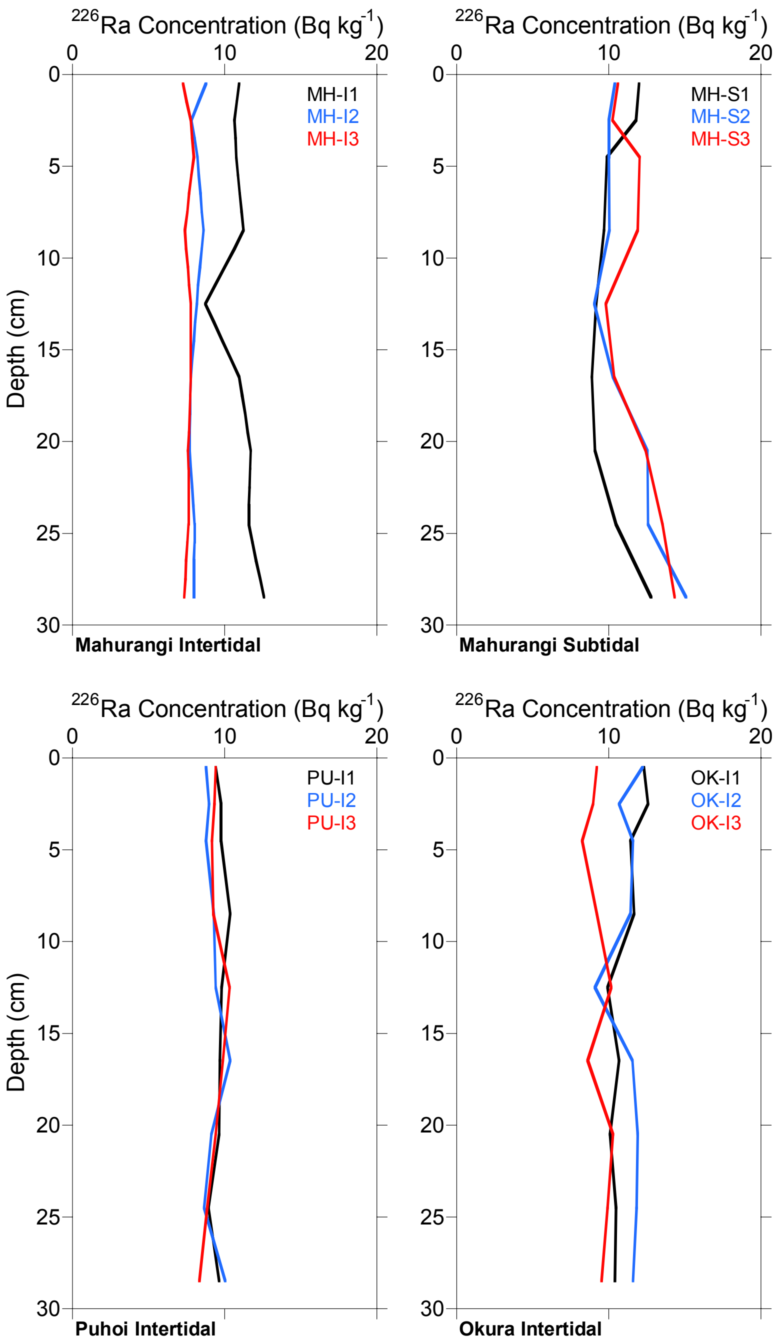

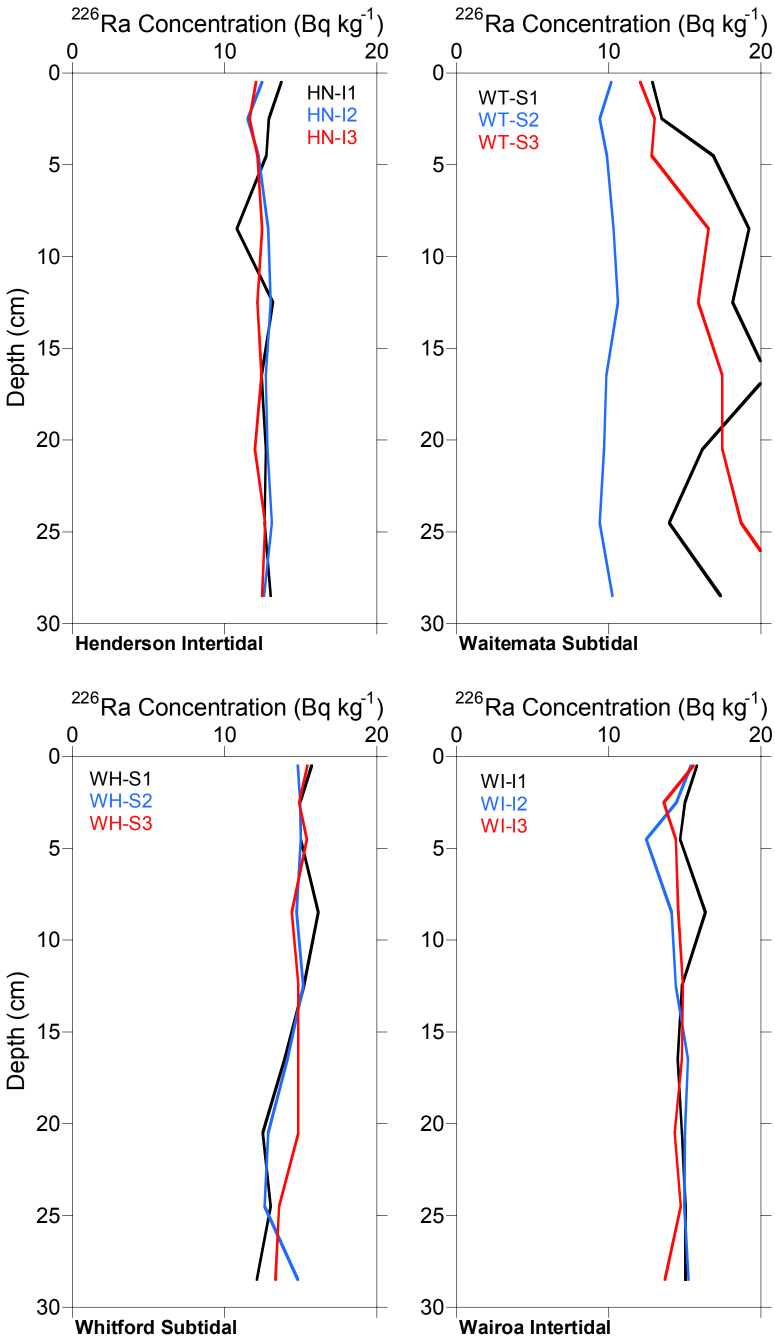
226Ra Concentration (Bq kg-1)
Depth (cm)
HN-I1
HN-I2
HN-I3
Henderson Intertidal
WT-S1
WT-S2
WT-S3
Waitemata Subtidal
WH-S1
WH-S2
WH-S3
Whitford Subtidal
WI-I1
WI-I2
WI-I3
Wairoa Intertidal

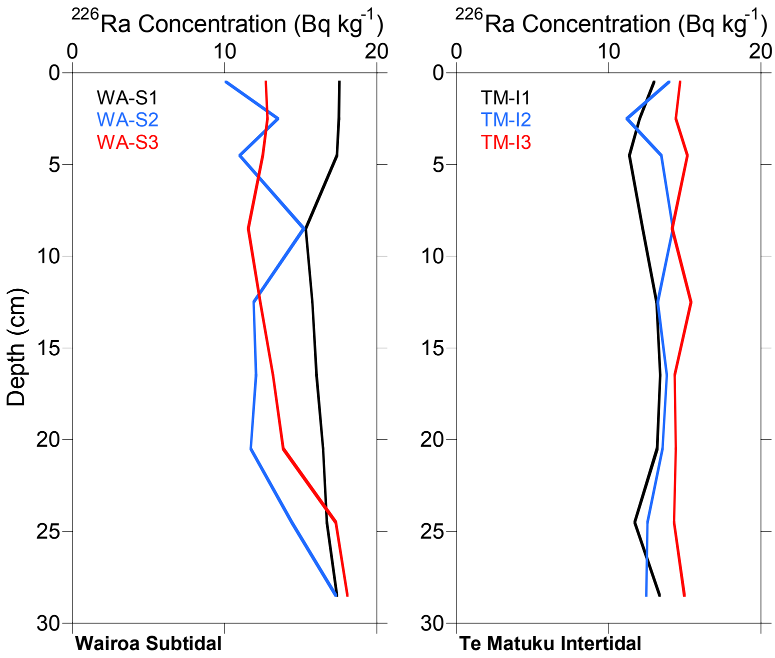

226Ra Concentration (Bq kg-1)
0
10
20
Depth (cm)
0
5
10
15
20
25
30
WA-S1
WA-S2
WA-S3
Wairoa Subtidal
226Ra Concentration (Bq kg-1)
TM-I1
TM-I2
TM-I3
Te Matuku Intertidal

11. Appendix IV: Estuary sediment cores: dry bulk sediment density (gcm^{-3}) profiles

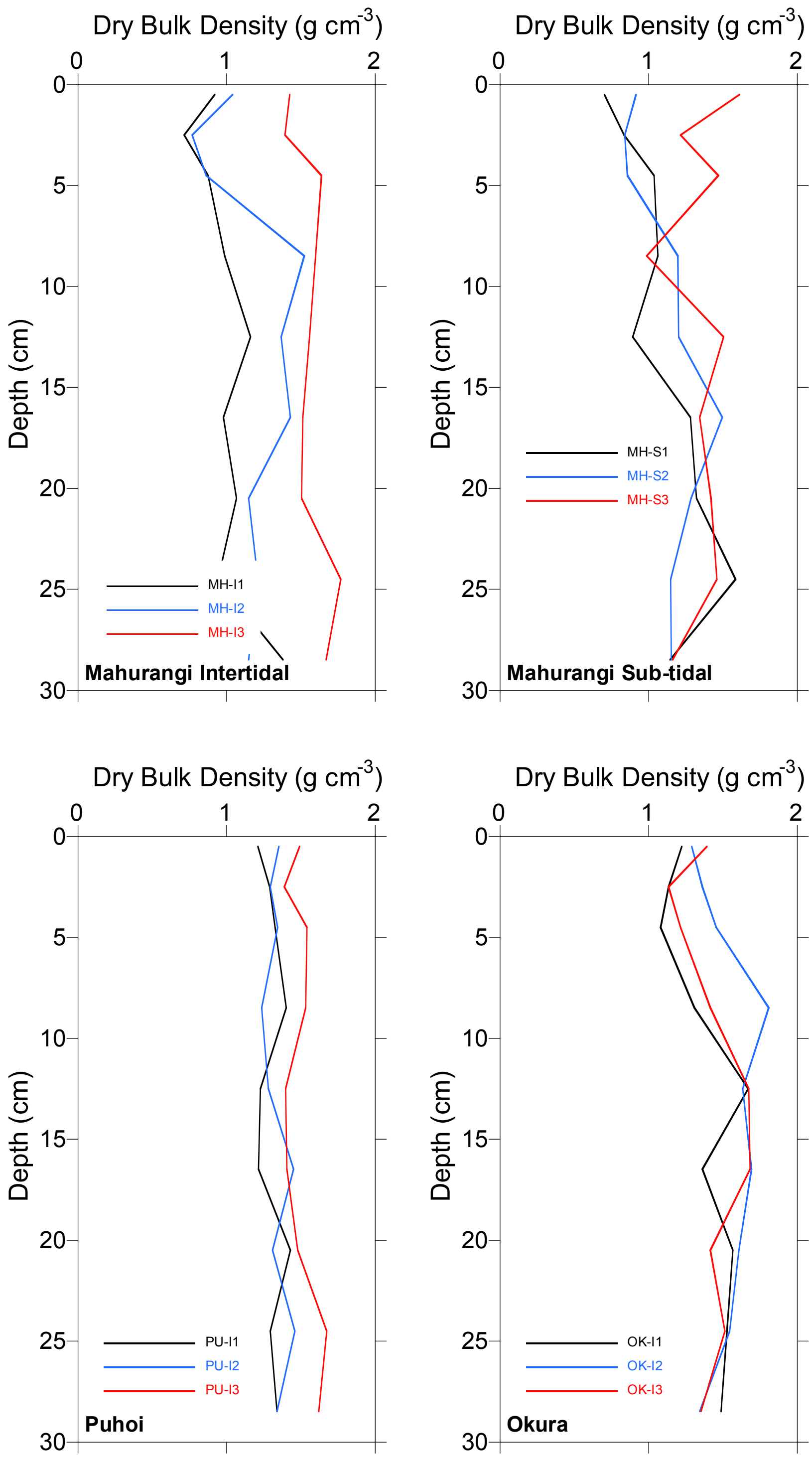

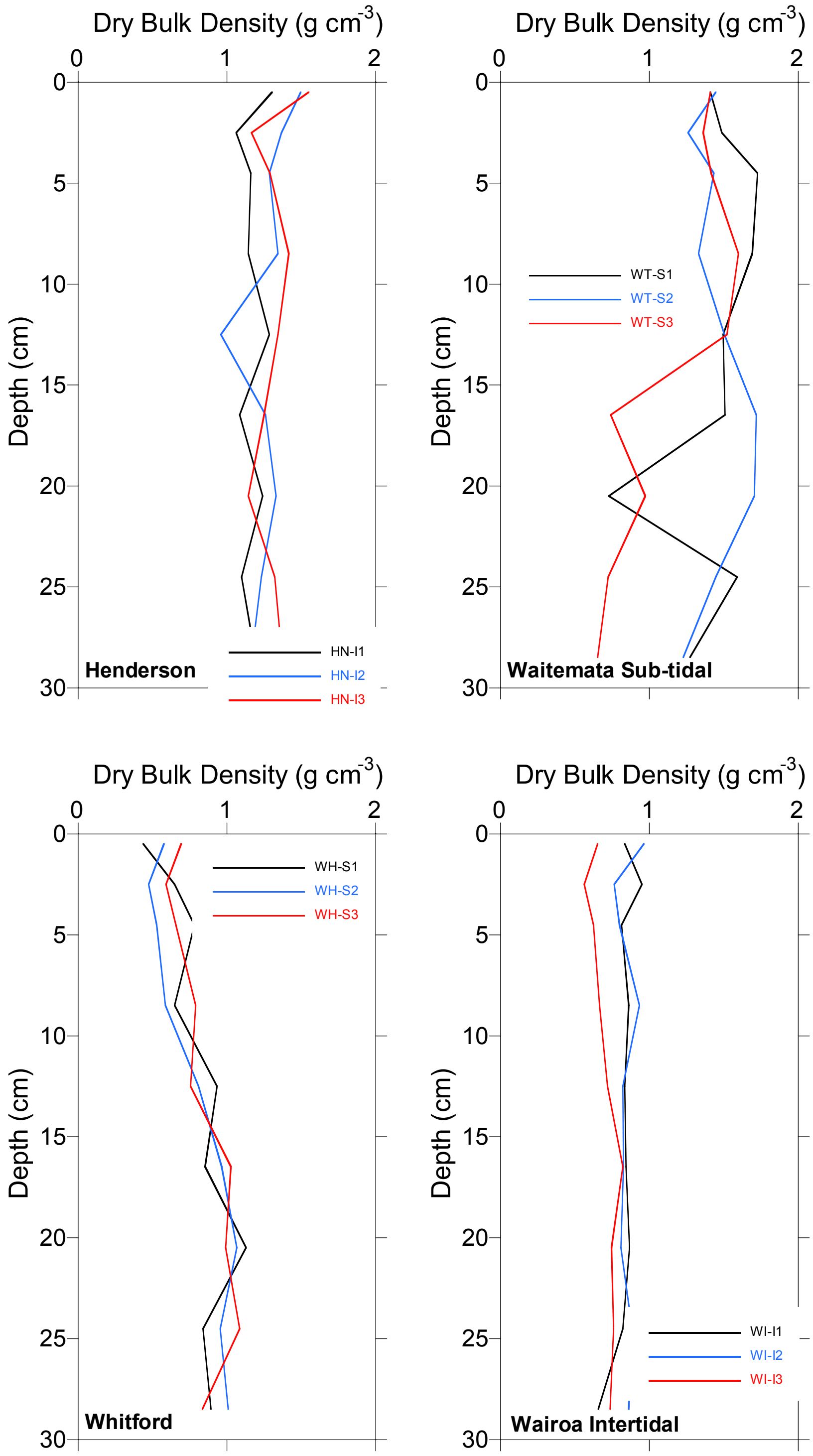
Dry Bulk Density (g cm-3)
Depth (cm)
HN-I1
HN-I2
HN-I3
Henderson
WT-S1
WT-S2
WT-S3
Waitemata Sub-tidal
WH-S1
WH-S2
WH-S3
Whitford
WI-I1
WI-I2
WI-I3
Wairoa Intertidal

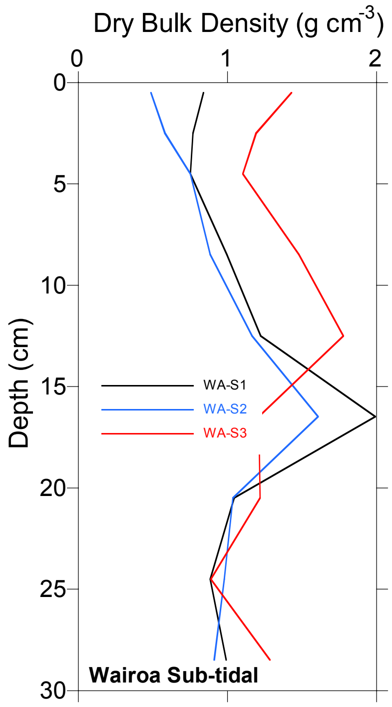
Dry Bulk Density (g cm-3)
0
1
2
Depth (cm)
0
5
10
15
20
25
30
WA-S1
WA-S2
WA-S3
Wairoa Sub-tidal

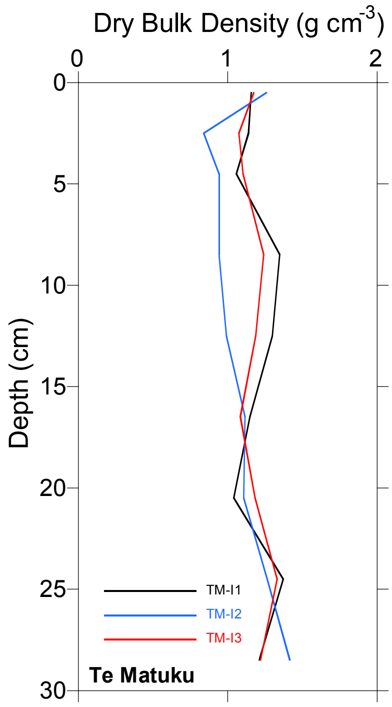
Dry Bulk Density (g cm-3)
0
1
2
Depth (cm)
0
5
10
15
20
25
30
TM-I1
TM-I2
TM-I3
Te Matuku